HHS Public Access

Author manuscript

J Med Chem. Author manuscript; available in PMC 2024 August 05.

Published in final edited form as:

J Med Chem. 2023 July 27; 66(14): 9466–9494. doi:10.1021/acs.jmedchem.3c00061.

Structure–Activity Relationship Study of Cannabidiol-Based Analogs as Negative Allosteric Modulators of the μ-Opioid Receptor

Taryn Bosquez-Berger[§],
Gill Center for Biomolecular Science, Department of Psychological and Brain Sciences, Program in Neuroscience, Indiana University, Bloomington, Indiana 47405, United States

Jessica A. Gudorf[§],
Department of Chemistry, Indiana University, Bloomington, Indiana 47405, United States

Charles P. Kuntz,
Department of Chemistry, Indiana University, Bloomington, Indiana 47405, United States

Jacob A. Desmond,
Department of Chemistry, Indiana University, Bloomington, Indiana 47405, United States

Jonathan P. Schlebach,
Department of Chemistry, Indiana University, Bloomington, Indiana 47405, United States

Michael S. VanNieuwenhze,
Department of Chemistry, Indiana University, Bloomington, Indiana 47405, United

Alex Straiker
Gill Center for Biomolecular Science, Department of Psychological and Brain Sciences, Program in Neuroscience, Indiana University, Bloomington, Indiana

Abstract

The US faces an unprecedented surge in fatal drug overdoses. Naloxone, the only antidote for opiate overdose, competes at the mu opioid receptor (μOR) orthosteric site. Naloxone struggles

Corresponding Authors Michael S. VanNieuwenhze – *Department of Chemistry, Indiana University, Bloomington, Indiana 47405, United States*, mvannieu@iu.edu.

[§]T.B.-B. and J.A.G. contributed equally to this work.

Author Contributions

All authors contributed equally to the experimental design and execution, statistical analysis, and composition of this manuscript.

ASSOCIATED CONTENT

Supporting Information

The Supporting Information is available free of charge at https://pubs.acs.org/doi/10.1021/acs.jmedchem.3c00061.

Supporting figures and tables from cellular experimentation, representative HPLC traces for all synthesized compounds, and NMR data for all synthesized compounds (PDF)

Molecular formula strings (CSV)

The authors declare the following competing financial interest(s): T.B.B, J.A.G, M.S.V., and A.S. are inventors in a patent application filed by Indiana UniversityBloomington, that entails the CBD analogs described in the present article. Data for the homology models have been deposited in the Mendeley Data repository and can be accessed at the following URL: https://data.mendeley.com/datasets/9df5yp88ck/draft?a=fb5a2795-ed9f-4165-9ed5-98eb39a25a0c.

T.B.B, J.A.G, M.S.V., and A.S. are inventors in a patent application filed by Indiana University—Bloomington, that entails the CBD analogs described in the present article.

Complete contact information is available at: https://pubs.acs.org/10.1021/acs.jmedchem.3c00061

against fentanyl-class synthetic opioids that now cause ~80% of deaths. Negative allosteric modulators (NAMs) targeting secondary sites may noncompetitively downregulate μOR activation. (–)-Cannabidiol ((–)-CBD) is a candidate μOR NAM. To explore its therapeutic potential, we evaluated the structure–activity relationships among CBD analogs to identify NAMs with increased potency. Using a cyclic AMP assay, we characterize reversal of μOR activation by 15 CBD analogs, several of which proved more potent than (–)-CBD. Comparative docking investigations suggest that potent compounds interact with a putative allosteric pocket to stabilize the inactive μOR conformation. Finally, these compounds enhance naloxone displacement of fentanyl from the orthosteric site. Our results suggest that CBD analogs offer considerable potential for the development of next-generation antidotes for opioid overdose.

Graphical Abstract

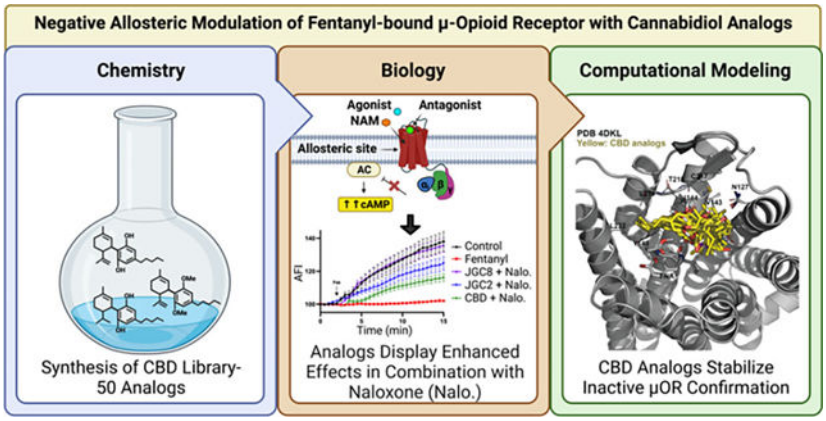

INTRODUCTION

Medications targeting the opioid signaling system remain the most common in clinical practice for the management of acute and chronic pain. The opioid signaling system includes several endogenous receptors (μ, δ, and κ) that are located throughout the central and peripheral nervous system. Most opioid analgesics target the μ opioid receptor (μOR)[1,2] that, upon activation, lead to effective analgesia. μOR effects on analgesia, mood, and the body's reward circuitry have resulted in strong abuse liability.[3,4] This largely underlies the steady rise in opioid overdose deaths since 1999, but the progression of the opioid crisis is more complex, having evolved in several "waves".[5] The first wave of the opioid epidemic consisted largely of deaths due to prescription opiates. As prescription guidelines became more tightly regulated, use shifted toward plant-based opiates such as heroin. This second wave caused an alarming increase in overdose deaths but was within a few years superseded by a still more-deadly development. A third wave resulted from increased use of synthetic opioids typified by the drug fentanyl but including other related compounds such as carfentanyl.[5] These fentanyl-class drugs are generally quite potent and are highly lipophilic, enabling them to rapidly diffuse through the blood brain barrier[6,7] and elicit an analgesic effect within minutes.[8–10] Fentanyl itself was developed to treat chronic pain due to cancer. Some derivatives of fentanyl, such as carfentanyl, exhibit an extraordinary potency

and, while useful for sedation of large animals such as moose or elephants,[9,11] present an extraordinary risk to humans who may encounter them.

The frontline treatment for opioid-related overdoses is naloxone, a competitive μOR antagonist. Naloxone has many attractive qualities and is an effective antidote against prescription (morphine and oxycodone) and illegal (heroin) opiates.[12] However, the increased lethality of fentanyl-class synthetic opioids can be attributed, in part, to their extremely high binding affinity for the orthosteric site of the μOR,[4,13] presenting a formidable challenge to a competitive antagonist such as naloxone.[14,15] Case in point, CDC guidelines indicate that multiple doses of naloxone may be required to combat overdoses due to fentanyl-class opiates.[16] Thus, there is a need for the development of an antidote effective at reversing synthetic opioid overdoses.

One strategy would be to identify classical antagonists with still-higher binding affinity for the μOR, but the morphinan scaffold, on which naloxone is based, has been exhaustively explored. An alternative strategy is to avoid direct competition at the orthosteric site and instead target allosteric sites at the μOR. It is well-known that receptors have secondary or allosteric sites, which upon binding, can modulate the affinity and signaling of orthosteric-bound ligands.[17–20] Specifically, negative allosteric modulation at the μOR[21] has the potential to noncompetitively decrease the signaling intensity of fentanyl-class synthetics. Most studies of μOR allosteric sites have focused on positive allosteric modulation,[2] but a few studies have identified candidate negative allosteric modulators, or NAMs, at the μOR. In particular, (–)-cannabidiol ((–)-CBD) was shown to have potential as a NAM at the μOR.[22,23] We and others have shown that (–)-CBD, best known as a principle compound of cannabis that is used as therapeutics for several forms of childhood epilepsy, also has NAM-like properties at cannabinoid CB_1 receptors.[24,25]

In this work, we synthesized and characterized a series of CBD analogs to explore the structure–activity relationship for this scaffold and improve its negative allosteric potency. The activity of our most promising analogs was evaluated using an *in vitro* hμOR-mediated cAMP signaling assay. Finally, we utilized computational docking to evaluate how these compounds potentially interact with the various conformational states of the μOR and propose a speculative energetic model to account for the observed allosteric modulation of this receptor. Our results point to promising new lead compounds for the development of antidotes for fentanyl class opioid overdoses.

RESULTS

Investigation of (–)-CBD and Synthetic CBD Analogs at the μOR.

Naturally occurring (–)-cannabidiol ((–)-CBD) has many postulated molecular targets with varying characteristics at each.[26] One interesting aspect of (–)-CBD, which could have advantageous implications for the clinical/emergency fields, is that it may behave as a negative allosteric modulator (NAM) at the μOR. Ligand binding studies have shown that, while naloxone, a classic μOR antagonist, promotes the dissociation of DAMGO from μORs, adding (–)-CBD rapidly accelerates this dissociation.[23] This finding indicates that (–)-CBD could modulate the opioid receptor via an allosteric mechanism that modulates the

dissociation kinetics of orthosteric ligands. Although the study of allostery at the μOR is still in its infancy, it is important to investigate the structural elements of (–)-CBD that are essential for the inhibition of μOR ligand binding and subsequent μOR activation.

Structure–Activity Relationship Study.

The initial hit compound (–)-CBD was reported to display negative allosteric potency for the μ-opioid receptor; however, high concentrations were necessary (EC_{50} = 41.7 μM[23]). To improve the therapeutic effect of (–)-CBD, we modified four distinct regions of the CBD scaffold (Figure 1). Utilizing (–)-CBD isolate, we first modified the limonene moiety (Figure 1, blue) to examine both the necessity of its rigidity and whether or not introduction of hydrogen bond donors and acceptors would vary its activity (JGC4–16,48–50).[27–29] We also altered the lipid tail of both (+/−)-CBD (Figure 1, green) via total synthesis utilizing commercially available starting materials and late-stage diversification (JGC23–47).[30–34] We modified the resorcinol ring (Figure 1, red) to examine the necessity of the phenolic groups (JGC2,3). Finally, we synthesized four diastereomer analogs of CBD (Figure 1, asterisk) to evaluate the geometric constraints of its binding pockets (JGC17–22).[35] These structural changes led to a library of 49 CBD (JGC*x*) analogs that possess singular and collective modifications (Table SI–1). See the Experimental Section for synthesis and characterization.

(–)-CBD Reverses hμOR-Mediated cAMP Inhibition Induced by μOR Agonist DAMGO.

As a $G\alpha_{i/o}$-coupled GPCR, the activation of the μOR inhibits the synthetic pathway involving adenylyl cyclase and subsequently decreases the accumulation of the secondary messenger cAMP.[36,37] We therefore used cyclic AMP (cAMP) levels as a cellular indicator of μOR activity to test whether (–)-CBD modulates μOR-mediated cAMP inhibition in human μOR (hμOR)-transfected HEK293 cells. We tracked changes in cellular cAMP levels by measuring changes in the fluorescence emission of Pink Flamindo following the addition of various combinations of agonists, antagonists, and NAMs. Pink Flamindo intensity increases in response to treatment with the adenylyl cyclase activator forskolin (Fsk; 100 μM), which confirms this readout reliably detects changes in the cellular cAMP pool. Using this assay, we evaluated the effects of various CBD analogs on μOR signaling when in the presence of DAMGO, a pentapeptide μOR agonist.[38] Following the coapplication of (–)-CBD and DAMGO, we found that (–)-CBD attenuates μOR signaling in a concentration dependent manner (Figure 2A), as it incrementally increased cAMP accumulation in our hμOR-HEK293 cells, with an IC_{50} of 311 nM (Figure 2B).

Library Screening of CBD (JGC*x*) Analogs against DAMGO in the Pink Flamindo cAMP Assay.

Each of our library of 50 CBD analogs (JGC1 through JGC2–50, Table SI–1) were coapplied with DAMGO in our Pink Flamindo assay. The signaling responses for each CBD analog varied across the analog library (Figure SI–1). (–)-CBD appeared to reduce DAMGO-induced signaling by ~53%. We selected 15 of the most promising candidates that also substantially attenuated DAMGO-induced μOR signaling (i.e. increasing cAMP accumulation) for further examination against fentanyl (Table SI–2; Figure 3).

μOR-Mediated cAMP Inhibition Induced by Fentanyl Is Reversed by (–)-CBD.

We continued our investigations on the modulatory properties of (–)-CBD at the μOR and tested its ability to interfere with agonist-induced signaling of fentanyl (Figure 4). Using the same experimental design, we find that (–)-CBD had similar effects against fentanyl-induced μOR signaling as DAMGO-induced signaling, meaning fentanyl signaling was also perturbed in a concentration-dependent manner (Figure 4A). (–)-CBD interfered with μOR-mediated inhibition of cAMP accumulation, by fentanyl, at moderate nanomolar concentrations, and had an IC_{50} of 1.8 μM (Figure 4B).

CBD Analogs Inhibit μOR-Mediated Effects in cAMP Accumulation, in the Presence of Fentanyl.

An overarching goal of this work was to identify the key structural components of the CBD analogs that enable them to attenuate μOR signaling and to identify whether there were compounds that appeared superior to (–)-CBD (JGC1) in curbing μOR signaling. Since we have shown (–)-CBD to modestly interfere with fentanyl-induced signaling, we expected our synthetic analogs to behave similarly.

First, as a control, we tested these same 15 analogs in our cAMP assay in the absence of either fentanyl or μOR (Figure 5) to examine whether the mechanism of the observed effects depends on the receptor. In the absence of fentanyl, the analogs had no effect on cAMP accumulation (Figure 5A), which suggests that the analogs are not activating or functioning as an agonist for the μOR. Furthermore, the CBD analogs did not inhibit cAMP accumulation when tested against wild-type HEK293 cells lacking μORs (Figure 5B). These results confirm that the CBD analogs are targeting the μOR to elicit their activity.

Next, using our cAMP assay, the 15 chosen CBD analogs were tested against fentanyl. Our results demonstrated that all 15 analogs interfere with fentanyl-induced μOR-mediated cAMP inhibition in a concentration-dependent manner (Figures SI–3 and SI–4; Figures SI–8 through SI–15). The inhibition of cAMP accumulation was reversed at varying degrees with CBD analogs JGC8 and JGC37 being the most and least effective compounds, respectively, at mitigating μOR signaling when applied to our hμOR-HEK293 cells (Table 1). When comparing the IC_{50} values of each CBD analog to their natural counterpart, 9 out of the 15 appeared to be more potent than (–)-CBD (Figure SI–5). Whereas six had a similar or reduced potency when compared to (–)-CBD (Figure SI–6). The diverse potency of these compounds could indicate that certain structural modifications were more favorable than others, when targeting the allosteric site of the μOR.

Naloxone Inhibits μOR-Mediated cAMP Accumulation, When Coapplied with Fentanyl.

The μOR antagonist naloxone is a highly effective antidote used to reverse an opioid overdose; however, due to fentanyl's exceptionally high binding affinity for the orthosteric site on μOR, the effectiveness of naloxone can be reduced.[4,13–15] Therefore, we sought to investigate the ability of naloxone to competitively antagonize fentanyl effects using our Pink Flamindo cAMP assay. We then compared the effectiveness of naloxone as a competitive antagonist to the allosteric 15 CBD analogs.

As with (–)-CBD and the CBD analogs, naloxone application also resulted in the inhibition of fentanyl-induced signaling in a concentration dependent manner, increasing cAMP accumulation with an IC_{50} value of 722 nM (Figure 6A,B). Naloxone had no effect on cAMP signaling in the absence of either fentanyl or μORs, confirming its known mechanism of action as an μOR antagonist (Figure 6C,D).

Although the μOR antagonist naloxone had a higher potency than that of (–)-CBD, this difference failed to reach statistical significance (IC_{50} for naloxone (95% CI): 722 nM (367 nM–1.5 μM); (–)-CBD: 1.8 μM (1.4 μM–2.2 μM) overlapping 95% confidence intervals). In contrast, three of our CBD analogs (JGC2, JGC8, and JGC13) had a higher potency than naloxone (IC_{50} for naloxone (95% CI): 722 nM (367 nM–1.5 μM); JGC2: 90 nM (48 nM–155 nM); JGC8: 21 nM (2.1 nM–111 nM); JGC13: 137 nM (106 nM–175 nM) nonoverlapping 95% confidence intervals). The enhanced potency of our CBD analogs for cAMP signaling could indicate that noncompetitive antagonism may be superior to competitive antagonism when attenuating potent synthetic opioid signaling of the μOR.

Coapplication of Naloxone and CBD Analogs Synergistically Reverse Fentanyl-Induced cAMP Inhibition.

Allosteric modulators can act via several mechanisms, including the induction of steric changes to the orthosteric binding site[17–20] as Kathmann et al.[23] suggested is the case for (–)-CBD. In this case, we may expect CBD analogs to synergistically enhance the effects of an antagonist like naloxone. To explore the potential synergistic effect(s), we measured the effects of two potent CBD analogs, along with (–)-CBD, in combination with naloxone on cellular cAMP levels following preapplication of fentanyl. (–)-CBD, JGC2, JGC8, and naloxone all interfered with μOR-induced inhibition of cAMP accumulation 2 min post-fentanyl application (Figure 7). Combining each compound with naloxone enhanced this accumulation of cellular cAMP in our hμOR-HEK293 cells with the combination of JGC8 and naloxone completely abolishing the effect of fentanyl on cAMP inhibition (Figure 7). The overall augmented cAMP accumulation following the combination of a μOR antagonist and postulated negative allosteric modulator (NAM) confirm that these two classes of ligands can synergistically block synthetic opioid-induced signaling.

Structural Aspects of the Allosteric Modulation of μOR by (–)-CBD.

To rationalize the structural basis for variations in the activity of these analogs, we compared their propensity to interact favorably with allosteric sites found in the active and inactive conformations of μOR. Given that (–)-CBD does not competitively displace opioids, we made the simplifying assumption that the allosteric effects of these compounds arise from their selective stabilization of the opioid-bound inactive conformation over the opioid-bound active conformation (Figure 8A,B). We first utilized Autosite[39] to identify putative allosteric binding sites within a structure of the inactive μOR bound to the irreversible antagonist β-funaltrexamine (β-FNA, PDB 4DKL).[40] The top scoring site (Autosite score 51.09) consists of a prominent cavity situated above the orthosteric site within the extracellular vestibule (Figure 8B). Although it is partially occluded by the N-terminal loop, we find that a more constricted version of this cavity is also present in the structure of the active μOR bound to the morphinan agonist BU72 (PDB 5C1ML, Figure 8A).[41] For the sake of comparison, we

used Autodock Vina[42] to dock (–)-CBD within this pocket in the context of both the inactive and active structures. The top scoring poses for the inactive conformation are relatively similar and feature extensive van der Walls contacts between the limonene moiety and transmembrane helices (TMs) 1, 2, and 3 within the deepest portion of the pocket (Figure 8F). As a result of the steric occlusion of the allosteric pocket in the active conformation, the top active-state poses for (–)-CBD are considerably more diverse across the collection of the 15 experimentally characterized CBD analogs described above (Figure 8D,E). We identified a consensus low-energy pose that is similar in both conformations in which the limonene moiety is nested within the cavity and the alkyl chain is projected toward TM5 (Figure 8D–F). To assess whether these compounds exhibit preferential binding to either conformation, we compared the predicted binding energies of this consensus pose in the active and inactive state for each compound using a convolutional neural network known as K_{DEEP}.[43] Across our collection of 15 experimentally characterized CBD analogs, we find the difference in the predicted binding energy in the inactive and active conformations ($\Delta\Delta G_{I-A}$) to be statistically correlated with log IC_{50} values (Pearson's $R = 0.64$, $p = 4.5 \times 10^{-4}$, Figure 8C). Consistent with our hypothesis, these observations suggest that the most potent compounds bind a secondary allosteric pocket and stabilize the inactive conformation relative to the active conformation. Although speculative, we note that this energetic interpretation is consistent with the observed synergistic interactions, as it does not require direct interactions between (–)-CBD analogs and any specific agonists/antagonists. Their selective stabilization of the inactive conformation of the allosteric pocket can potentially shift the conformational equilibrium of μOR toward its inactive conformation regardless of the occupancy of the orthosteric site. This proposed energetic coupling between binding and inactivation would lower the effective binding affinity of agonists without any direct interactions.

DISCUSSION

The last 10 years have seen a spike in synthetic opioid use with overdose deaths in the United States increasing almost exponentially.[44] The lethality of fentanyl-class opioids is due, in no small part, to their potency and binding affinity for the μOR, which renders competitive antagonists like naloxone (Narcan) ineffective.[13–15] There is an urgency to explore alternative mechanisms to curb μOR signaling. A promising strategy is to avoid direct competition with these synthetic agonists using NAMs. (–)-CBD was proposed to function as a NAM;[23] however, our current understanding of this interaction, as well as the μOR allosteric site itself, is still very limited.[21] In this work, we assessed whether (–)-CBD was capable of interfering with μOR signaling and performed a structure–activity relationship study that probed this scaffold to determine the minimal pharmacophore. Using an *in vitro* cAMP assay, we identified several CBD analogs that proved to be more potent than the natural cannabinoid and show that these enhance the activity of the μOR antagonist naloxone.

Initial assay analyses of (–)-CBD and the synthesized CBD library were conducted against the μOR agonist DAMGO using an *in vitro* cAMP signaling assay. We find that (–)-CBD curbs DAMGO signaling in this context, confirming the findings of Kathmann et al.[23] However, we also found that several CBD analogs reversed μOR-mediated cAMP inhibition. We chose 15 promising compounds that substantially inhibited DAMGO signaling in this

assay that were then selected for testing against fentanyl. All of the CBD compounds tested attenuated fentanyl-induced μOR-mediated cAMP inhibition, and more than half of our CBD analogs performed significantly better than the lead compound (–)-CBD. The reduced potency of (–)-CBD in the presence of fentanyl relative to DAMGO constitutes an example of probe dependence—a feature seen for other allosteric modulators where protein signaling can diverge for an allosteric modulator when a different orthosteric agonist is bound.[19,20] These observations are also consistent with expectations of our proposed thermodynamic model for negative allosteric modulation. Fentanyl binds with a higher affinity and should therefore stabilize the inactive conformation to a greater extent than DAMGO, which should generally render (–)-CBD binding less effective at shifting the equilibrium toward the inactive conformation. Nevertheless, we identified NAMs that were selective for both DAMGO and fentanyl. For instance, JGC8 had similar NAM activity to (–)-CBD vs DAMGO, but much greater potency (~86x) against fentanyl. The reverse was true for JGC37, which proved ~3.6x less potent than (–)-CBD vs fentanyl. Given our putative docking poses, these deviations could potentially arise as a result of direct, differential interactions between (–)-CBD analogs and the agonists themselves (Figure 8E). Additional investigations are needed to gain mechanistic insights into the agonist-specific NAM activity of certain (–)-CBD analogs.

One important question involves the mechanistic basis for the effects of these compounds relative to the effects of naloxone. Naloxone is a potent μOR antagonist and for decades has served as the gold-standard antidote for opiate overdose.[4] In our cAMP signaling assay, the three most promising compounds all proved to be 5- to 34-fold more potent than naloxone. Allosteric modulators like (–)-CBD can act via several potential mechanisms, including the induction of conformational changes to the orthosteric binding site[17–19] as is suggested to be the case for (–)-CBD by Kathmann et al.[23] Interestingly, we find that the coapplication of naloxone with certain CBD analogs (e.g. JGC2 and JGC8) enhances μOR inhibition in the presence of fentanyl, which implies that naloxone and (–)-CBD occupy distinct binding sites. In the simplest allosteric case, we can assume that allosteric modulators selectively stabilize either the active or inactive conformation of the μOR (Figure 8A,B). We have explored such a possibility through our speculative docking studies, which presuppose that these NAMs bind to an allosteric pocket within the extracellular vestibule of receptors bearing an occupied orthosteric site. According to this model, NAMs would associate with a liganded receptor and bias it toward its inactive conformation (Figure 8A,B). Although the putative allosteric pocket we have analyzed in this investigation is lined by the same residues within the agonist-bound active (PDB 5C1ML) and antagonist-bound inactive (PDB 4DKL) conformations, our docking results suggest the distinct geometric constraints of these two conformation results in the preferential binding of NAMs to the inactive conformation (Figure 8C). The association of a NAM to the liganded receptor should bias the receptor toward the inactive conformation, which should in turn decrease the net affinity for agonists and increase the affinity for antagonists by virtue of the thermodynamic coupling of the binding equilibria. Although additional experimental evidence is needed to confirm this hypothesis, we note that the degree to which these NAMs exhibit preferential binding to the inactive conformation is well correlated with Log(IC_{50}) values (Figure 8C). Furthermore, this interpretation potentially explains how candidate NAMs (–)-CBD, JGC2, and JGC8

reduce μOR-mediated cAMP inhibition on their own as they can stabilize the inactive state even without naloxone. Furthermore, the additivity of the binding energy within the orthosteric and allosteric sites can potentially explain the synergistic antagonism achieved by our candidate μOR NAMs and naloxone, they each stabilize the same inactive conformation in different ways. Although using cellular cAMP accumulation as an endpoint restricts our ability to distinguish modes of inactivation or inhibition, this model provides a new mechanistic interpretation for the synergistic interactions of these two classes of ligands.

A systematic interrogation of the putative allosteric site at the μOR provides important insights into the pharmacophore necessary for allosteric modulation at the opioid receptor. The limonene region was probed by eliminating its rigidity and extending oxidation (JGC4–16,48–50). The necessity of the hydrogen-bond acceptor resorcinol ring was examined by addition of functional groups to the phenolic hydroxyl groups of (–)-CBD (JGC2,3). Additionally, (+/−)-CBD (JGC17,18) along with analogs having varied lipid tail lengths and/or other modifications (JGC23–47) were synthesized to investigate whether stereochemical configuration and/or lipid tail modification of the (–)-CBD scaffold affected NAM activity. Our computational models of the CBD-bound conformations rationalized some of the observed trends and have provided insight regarding modifications that may be made to the CBD core structure that may enhance stability of the inactive receptor confirmation. To stabilize the inactive conformation of the receptor, our models suggest that the hydrophobic limonene substituent of (–)-CBD must insert within a prominent pocket found within the allosteric site (Figure 8B). This pocket has nonpolar residues Val 143 and Ile 144 in transmembrane helix 3 that may form favorable van der Waals interactions with the limonene group (Figure 8F). Replacing the ^{i}propenyl group with an ^{i}propyl group in JGC8 appears to strengthen potency, indicating that the enhanced rigidity compromises the association of the limonene within this site. The more polar resorcinol ring may form polar contacts with adjacent residues such as Thr 218 in extracellular loop 2 and Asp 147 in transmembrane helix 3 (Figure 8F). Our docked models also suggest that Tyr 148 could potentially form pi–pi contacts with the aromatic ring in certain conformations (Figure 8F). Hydrogen bond donors do not appear particularly important for these interactions, as the substitution of the phenolic hydroxyl groups with methoxy groups in JGC2 had higher affinity than (–)-CBD. However, the analog JGC11 features acetylated phenolic hydroxyl groups, which resulted in lower affinity analogs that may instead reflect the costs of installing bulky less-polar groups at these positions. Finally, we note that the lipid tail in these compounds appears to extend toward a hydrophobic subpocket situated between transmembrane helix 4 and transmembrane helix 5 while making contacts with nonpolar residues in extracellular loop 2 (Figure 8F). Leu 219 on extracellular loop 2, valine 202 on transmembrane helix 4, and leucine 232 on transmembrane helix 5 may play a role in the formation of this hydrophobic subpocket (Figure 8F). Decreasing the length of this alkyl chain from an ^{n}butyl (JGC39) group to an ^{n}propyl group (JGC38) seemed to diminish potency, which may reflect the loss of nonpolar van der Waals contacts. In addition, an ^{i}butyl substituent did not have as much potency as an ^{n}butyl group, indicating that the geometry of the site is optimized to accommodate a linear chain. Together, these observations provide hypotheses that merit future efforts to map the structure–activity relationships for these compounds.

Mascal, et al.[45] recently reported that JGC8 has similar effects to (–)-CBD *in vivo* in a rodent model of epilepsy. As noted above, (–)-CBD is an approved therapy for two forms of childhood epilepsy but the mechanism of action for this effect remains a subject of debate. Candidate receptors include CB_1 and GPR55,[46] but (–)-CBD is also known to act on an array of other targets, including sodium channels (e.g. Sait et al.[47]). Therefore, it is difficult to interpret their findings until more is known about the receptor(s) that mediate the antispasmodic effects of (–)-CBD, but their work does highlight the challenges of developing target-specific compounds especially where the starting compound is known to act on multiple endogenous targets.

Additionally, recent discoveries concerning the structural aspects of μOR pharmacology have provided new insights into the structural basis for the distinct pharmacological properties of fentanyl relative to other opioids. Recent experimental structures demonstrate that naloxone and morphine occupy distinct subpockets within the orthosteric site in relation to larger, more potent agonists such as lofentanil (LFT) and fentanyl.[48,49] Two recent structural studies show that the hydrophobic phenethyl moieties of LFT and fentanyl extend into a subpocket that is not occupied by morphine or, presumably, naloxone.[48,49] The occupation of this subpocket may account for the enhanced affinity of these compounds and appears to coincide with β-arrestin recruitment.[49] Notably, the subpocket occupied by the phenethyl moieties within LFT and fentanyl corresponds to the limonene pocket identified in our docking studies. The partial overlap between these sites potentially accounts for our observation that fentanyl can be displaced through coadministration of naloxone and our candidate μOR NAMs. Additional investigations are needed to assess this hypothesis.

CONCLUSIONS

In summary, we have conducted a structure–activity relationship study of a library of synthetic cannabidiol analogs that were tested in a cAMP assay to measure their inhibition of μOR signaling. We found structural alterations to the (–)-CBD scaffold that enhanced the potency of the lead compound. Docking investigations suggest this enhanced potency arises from modifications that heighten the selective binding of these compounds to the opioid-bound inactive conformation. This emerging understanding of the role that structural modifications to the CBD scaffold play in allosteric modulation, along with further elucidation of the allosteric site at the μOR, will pave the way for developing a novel class of compounds that noncompetitively curb opioid signaling. This novel strategy may offer several therapeutic advantages over available competitive antagonists.

EXPERIMENTAL SECTION

Chemistry.

General Information.—Unless otherwise indicated, all reactions were carried out at 25 °C in flame-dried glassware, and all nonaqueous reactions were conducted in an atmosphere of argon using standard Schlenk techniques for the exclusion of moisture and air. All reagents were purchased from commercial suppliers: Sigma-Aldrich, Strem Chemical, Inc., Alfa Aesar, and Oakwood Chemical and used without purification. (–)-Cannabidiol isolate [(–)-CBD, JGC1] and cannabigerol (CBG, JGC16) was acquired from Jacob Desmond.

Analytical thin-layer chromatography (TLC) was performed on Silica Gel 60, 250 μm plates with an F-254 indicator and visualized using UV light. Column chromatography was performed using Silicycle SiliaFlash F60, 40–63 μm (230–400 Mesh). Analytical reverse-phase high-pressure liquid chromatography (HPLC) was collected using Hewlett Packard Series 1100 utilizing an Agilent-C18 (250 × 4.6 mm, 5 μm) column with the method of 10–90% MeCN/H_2O (v/v) over 10 min, 0.1% TFA (v/v). Compounds were dissolved in acetone or tetrahydrofuran (THF) and monitored via UV detection (217 nm, 254 nm, and 280 nm) and an Evaporative Light Scattering Detector (Agilent 1200 Series ELSD). All compounds are >95% pure by analytical HPLC. Optical rotations were measured on a Mandel Rudolph Research Analytical Automatic Polarimeter at 589 nm with a cell length of 50 mm. ^{1}H NMR spectra were recorded at room temperature on a Varian 500 MHz Inova spectrometer. All chemical shifts are referenced to residual nondeuterated solvent ($CHCl_3$: δ 7.26 ppm). Data for ^{1}H spectra are reported as follows: chemical shift, multiplicity, [singlet (s), doublet (d), triplet (t), quartet (q), and multiplet (m)], coupling constant(s) [Hz], integration. ^{13}C spectra were recorded on a Varian 500 MHz Inova spectrometer with complete proton decoupling. Chemical shifts are reported in ppm relative to solvent resonance ($CDCl_3$: δ 77.16). Low-resolution mass spectra were recorded on an Agilent 6130 mass selective detector connected to an Agilent 1200 HPLC (loop injection). High-resolution mass spectra (HRMS) were obtained by the Mass Spectrometry Facility at Indiana University-Bloomington on a Thermo Finnigan LTQ Orbitrap XL Mass Spectrometer connected to an Agilent 1100 HPLC.

(1′R,2′R)-5′-Methyl-4-pentyl-2′-(prop-1-en-2-yl)-1′,2′,3′,4′-tetrahydro-[1,1′-biphenyl]-2,6-diol (JGC1 or (–)-CBD Isolate).—

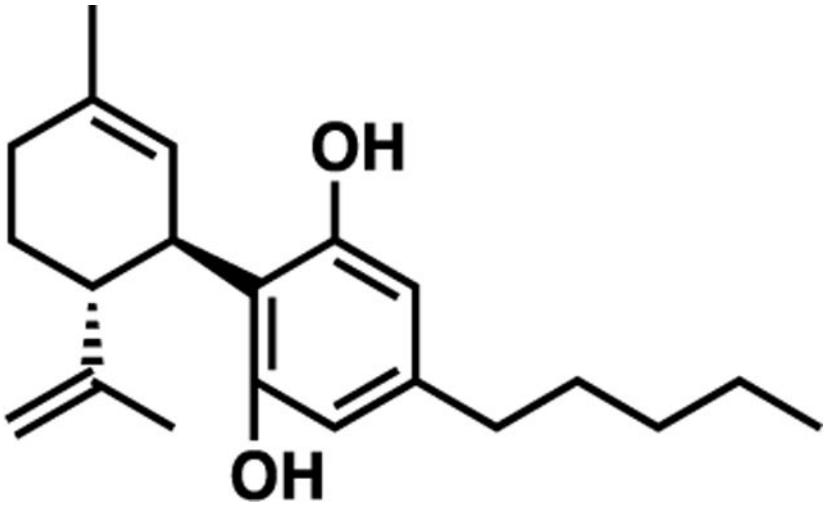

R_f = 0.46 [hexanes:ethyl acetate (9:1)]; Matched literature data.[50] mp 66–67 °C (pentanes); $[A]_D^{20}$ −127.6 (*c* 1.326, abs. EtOH) [literature: $[A]_D^{20}$ −127.2 (*c* 1.32, $CHCl_3$)] and $[A]_D^{20}$ −76.5 (*c* 0.790, $CHCl_3$) ^{1}H NMR (500 MHz, chloroform-*d*) δ 6.34–5.83 (m, 3H), 5.57 (d, *J* = 2.6 Hz, 1H), 4.61 (dt, *J* = 50.5, 1.6 Hz, 2H), 3.84 (ddd, *J* = 10.4, 4.2, 2.3 Hz, 1H), 2.54–2.32 (m, 4H), 2.31–2.16 (m, 1H), 2.09 (dd, *J* = 17.8, 4.0 Hz, 1H), 1.88–1.72 (m, 5H), 1.65 (dd, *J* = 1.5, 0.9 Hz, 3H), 1.61–1.49 (m, 4H), 1.38–1.20 (m, 4H), 0.88 (t, *J* = 7.0 Hz, 3H). ^{13}C NMR (126 MHz, chloroform-*d*) δ 153.9, 149.3, 143.0, 140.0, 124.2, 113.8, 110.9, 108.0,

46.2, 37.2, 35.5, 31.5, 30.6, 30.4, 28.4, 23.7, 22.5, 20.5, 14.0; TOF-MS (ES+) *m*/*z* $(M+H)^+$ calculated for $C_{21}H_{31}O_2$ $(M+H)^+$ 315.4, found 315.1.

Limonene and Resorcinol Cannabidiol Derivatives. (1R,2R)-2′,6′-Dimethoxy-5-methyl-4′-pentyl-2-(prop-1-en-2-yl)-1,2,3,4-tetrahydro-1,1′-biphenyl (JGC2).

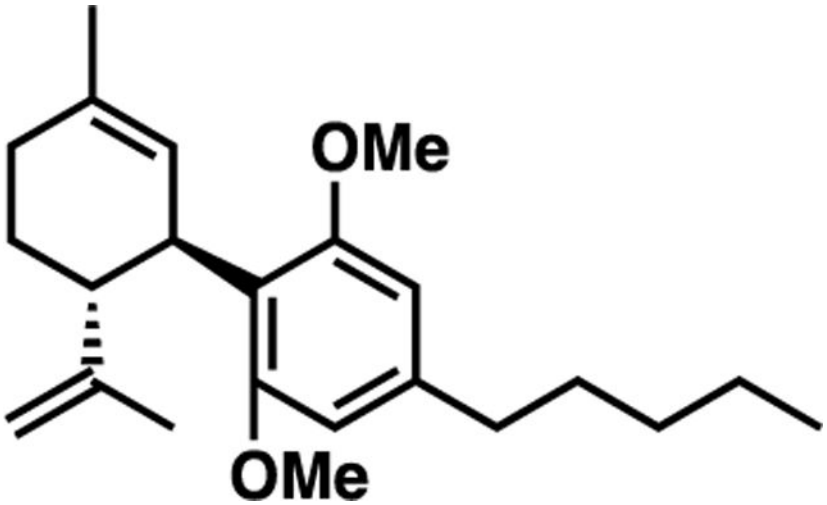

(–)-CBD (1.0 g, 3.2 mmol) was dissolved in acetone (25 mL), and then K_2CO_3 (1.8 g, 12.8 mmol) was added to the stirring solution. Me_2SO_4 (1.21 mL, 12.8 mmol) was added to the solution dropwise and allowed to stir for 10 min after the complete addition of Me_2SO_4. The reaction was then heated to reflux and stirred for 24 h. Upon completion, a solution of H_2O, EtOH, and NH_4OH (1:1:1) was added to the reaction flask, and the solution was allowed to stir for 30 min at room temperature before the addition of 1 M HCl (50 mL). The quench solution was then extracted with Et_2O (3 × 20 mL), and the organic layer was washed with brine (20 mL), dried over $MgSO_4$, and concentrated *in vacuo* to produce a clear, colorless oil (1.0 g, 2.9 mmol, 92%).

R_f = 0.429 [5% Et_2O in petroleum ether]; ^1H NMR (500 MHz, chloroform-*d*) δ 6.41 (s, 2H), 5.29 (s, 1H), 4.57–4.43 (m, 2H), 4.14–4.00 (m, 1H), 3.79 (s, 6H), 2.99 (td, *J* = 10.9, 4.0 Hz, 1H), 2.69–2.53 (m, 2H), 2.27 (qd, *J* = 9.7, 4.4 Hz, 1H), 2.13–1.99 (m, 1H), 1.91–1.75 (m, 2H), 1.74 (s, 3H), 1.68 (s, 5H), 1.41 (tq, *J* = 7.3, 4.1, 2.7 Hz, 4H), 0.98 (q, *J* = 6.2 Hz, 3H). ^{13}C NMR (126 MHz, chloroform-*d*) δ 158.9, 149.5, 141.9, 131.1, 126.1, 119.1, 109.7, 105.0, 55.9, 45.3, 36.5, 36.2, 31.8, 31.1, 30.9, 29.8, 23.5, 22.7, 19.2, 14.2; TOF-MS (ESI+) *m*/*z* $(M+H)^+$ calculated for $C_{23}H_{35}O_2$ $(M+H)^+$ 343.2, found 343.2.

(1′R,2′R)-5′-Methyl-4-pentyl-2′-(prop-1-en-2-yl)-1′,2′,3′,4′-tetrahydro-[1,1′-biphenyl]-2,6-diyl Diacetate (JGC3).

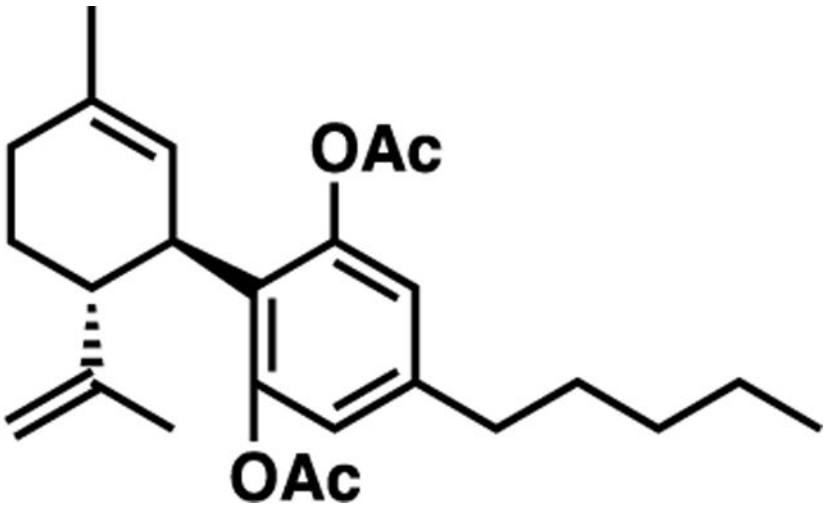

(–)-CBD (2.0 g, 6.36 mmol) was dissolved in pyridine (11.8 mL, 146 mmol) and acetic anhydride (12 mL, 127 mmol). The solution was aged overnight at room temperature. Upon completion, cold water (200 mL) was added to the solution, which was then extracted with Et_2O (3 × 50 mL). The organic layer was washed with 1 M HCl (50 mL), saturated aqueous Na_2CO_3 (50 mL), and brine (50 mL), consecutively. The solution was dried over $MgSO_4$ and concentrated *in vacuo* to afford a translucent, pale yellow oil (2.5 g, 6.3 mmol, 99%), which was carried to the next step without further purification.

Characterization matched literature data.[28] R_f = 0.32 [hexanes:ethyl acetate (7:1)]; ^{1}H NMR (500 MHz, chloroform-*d*) δ 6.71 (s, 2H), 5.24 (s, 1H), 4.66–4.38 (m, 1H), 3.58–3.40 (m, 1H), 2.65 (ddd, J = 13.3, 10.6, 3.1 Hz, 1H), 2.55 (dd, J = 8.9, 6.8 Hz, 1H), 2.32–1.93 (m, 5H), 1.87–1.48 (m, 6H), 1.45–1.18 (m, 2H), 0.88 (t, J = 6.8 Hz, 2H). ^{13}C NMR (101 MHz, chloroform-*d*) δ 168.7, 149.6, 147.6, 141.7, 132.6, 125.9, 124.6, 121.0, 119.7, 110.9, 53.5, 45.6, 38.4, 35.1, 31.4, 30.4, 30.3, 28.7, 23.3, 22.4, 20.7, 19.5, 13.9; TOF-MS (ES+) *m*/*z* $[M+Na]^+$ calculated for $C_{25}H_{34}O_4Na$ $(M+Na)^+$ 421.2, found 421.1.

(1′R,2′R)-2′-(3-Hydroxyprop-1-en-2-yl)-5′-methyl-4-pentyl-1′,2′,3′,4′-tetrahydro-[1,1′-biphenyl]-2,6-diyl Diacetate (JGC4).

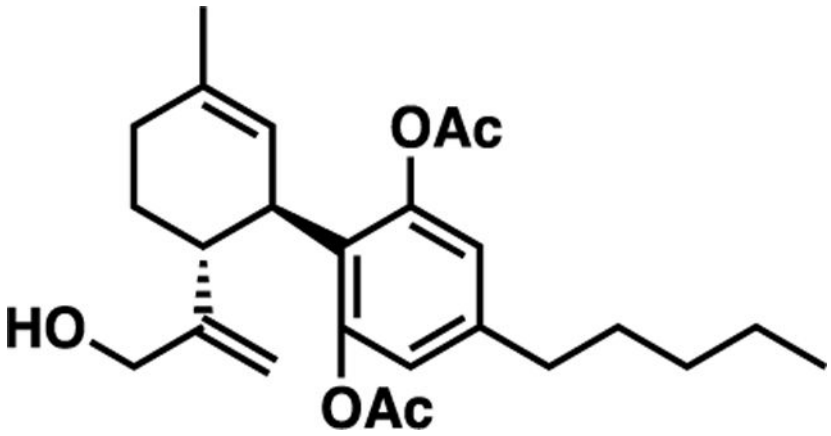

To a suspension at 0 °C of SeO_2 (104 mg, 0.94 mmol) and salicylic acid (152 mg, 1.1 mmol) in DCM (40 mL) under an inert atmosphere, a solution of JGC3 (2.5 g, 6.3 mmol) and ^{t}BuOOH (6 M in decane, 2.8 mL, 25 mmol) in dry DCM (40 mL) was added. The solution was stirred and allowed to warm to room temperature for 40 h. Upon completion, water (120 mL) was added to the reaction flask, and the golden solution was extracted with DCM (3 × 20 mL). The organic layer was washed with saturated aqueous Na_2CO_3 (20 mL) and brine (20 mL), dried over $MgSO_4$, and concentrated *in vacuo* to produce an orange oil. The oil was purified via flash chromatography [hexanes:Et_2O (7:1 → 2:1)] to produce a translucent oil (1.0 g, 2.4 mmol, 38%).

R_f = 0.27 [hexanes:Et_2O (1:1)]; ^{1}H NMR (500 MHz, chloroform-*d*) δ 6.71 (s, 2H), 5.18 (d, J = 2.3 Hz, 1H), 5.00 (d, J = 1.7 Hz, 1H), 4.87 (d, J = 1.5 Hz, 1H), 3.85–3.68 (m, 1H), 3.64–3.53 (m, 1H), 3.49 (ddt, J = 15.1, 5.7, 1.6 Hz, 1H), 2.56 (td, J = 7.6, 3.9 Hz, 2H), 2.46 (td, J = 11.0, 3.9 Hz, 1H), 2.19 (s, 7H), 2.09–1.98 (m, 1H), 1.90–1.73 (m, 2H), 1.69 (dt, J = 2.4, 1.2 Hz, 3H), 1.66–1.49 (m, 4H), 1.30 (qd, J = 7.9, 7.1, 4.4 Hz, 4H), 0.88 (t, J = 6.9 Hz, 3H). ^{13}C NMR (126 MHz, chloroform-*d*) δ 154.0, 142.4, 132.9, 125.7, 124.5, 108.3, 65.4, 41.2, 40.8, 35.2, 31.4, 30.6, 30.3, 29.3, 23.4, 22.4, 14.0; TOF-MS (ESI+) m/z $[M+Na]^+$ calculated for $C_{25}H_{34}O_5Na$ $(M+Na)^+$ 437.2, found 437.2.

(1′R,2′R)-2′-(3-Acetoxyprop-1-en-2-yl)-5′-methyl-4-pentyl-1′,2′,3′,4′-tetrahydro-[1,1′-biphenyl]-2,6-diyl Diacetate (JGC5).

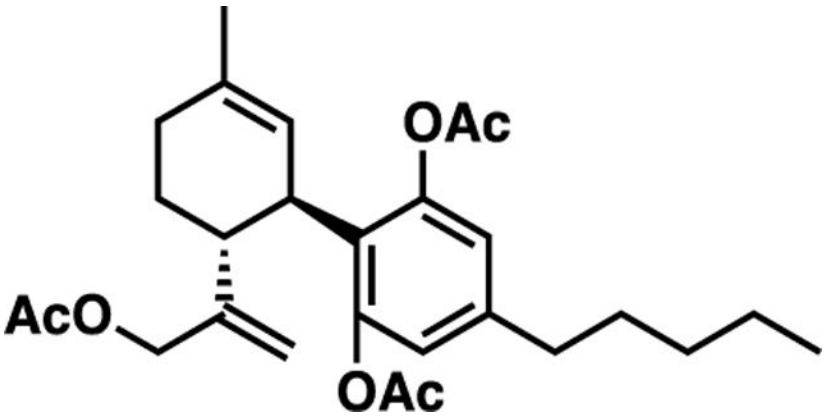

JGC4 (0.6 g, 1.5 mmol) was dissolved in pyridine (2.5 mL, 29 mmol), and acetic anhydride (2.7 mL, 29 mmol) was added to the solution. The solution was aged for 1.5 h, which was confirmed by TLC. Cold water (80 mL) was added to the reaction flask, and the solution was extracted with Et_2O (3 × 50 mL). The organic layer was washed with 1 M HCl (50 mL), saturated aqueous Na_2CO_3 (50 mL), and brine (50 mL), dried over $MgSO_4$, and concentrated *in vacuo* to produce a clear yellow oil (0.66 g, 1.4 mmol, 99%). The product was carried on to the next step without further purification.

R_f = 0.4 [hexanes:Et_2O (2:1)]; ^{1}H NMR (500 MHz, chloroform-*d*) δ 6.66 (s, 2H), 5.19 (s, 1H), 5.12 (d, J = 1.8 Hz, 1H), 4.94–4.78 (m, 2H), 4.34–4.16 (m, 2H), 2.65 (ddd, J = 12.9, 10.4, 2.7 Hz, 1H), 2.56–2.40 (m, 3H), 2.33–1.72 (m, 14H), 1.61 (t, J = 1.8 Hz, 4H), 1.25 (q, J = 3.5, 2.7 Hz, 3H), 0.82 (t, J = 6.8 Hz, 3H). ^{13}C NMR (126 MHz, chloroform-*d*) δ 174.7, 170.5, 168.9, 166.3, 149.5, 146.8, 142.2, 132.8, 125.4, 124.4, 112.4, 53.5, 41.8, 39.3, 35.1, 31.4, 30.5, 30.3, 29.5, 23.3, 22.4, 21.9, 20.8, 13.9; TOF-MS (ESI+) m/z $[M+Na]^+$ calculated for $C_{27}H_{36}O_6Na$ $(M+Na)^+$ 479.3, found 479.2.

2-((1R,2R)-2′,6′-Dihydroxy-5-methyl-4′-pentyl-1,2,3,4-tetrahydro-[1,1′-biphenyl]-2-yl)allyl Acetate (JGC6).

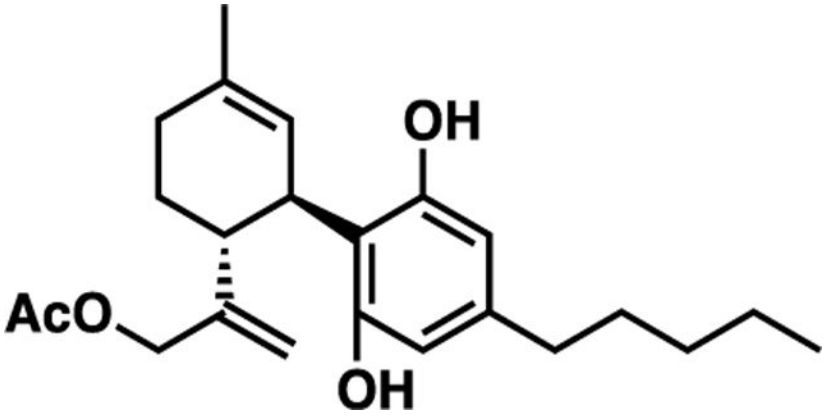

Phenylhydrazine (0.75 mL, 7.6 mmol) and aqueous sodium hydroxide (15%, 1 mL) were added to a stirred suspension of JGC5 (174 mg, 3.8 mmol) in ethanol (20 mL) under an inert atmosphere. TLC confirmed that the reaction was complete after stirring at room temperature for 0.5 h. To the reaction flask, 1 M HCl (10 mL) was added, and the solution was extracted with Et_2O (3 × 20 mL). The organic layer was washed with brine (20 mL) and concentrated *in vacuo* to produce a clear golden oil. The oil was purified by flash column chromatography [hexanes:Et_2O (1:1)] to afford a translucent oil (0.12 g, 0.32 mmol, 84.5%).

R_f = 0.11 [hexanes:Et_2O (2:1)]; ^{1}H NMR (500 MHz, chloroform-*d*) δ 6.24 (s, 1H), 6.23 (s, 1H), 5.97 (s, 1H), 5.57 (d, J = 2.7 Hz, 1H), 4.89 (d, J = 1.6 Hz, 1H), 4.60 (d, J = 1.6 Hz, 1H), 4.28 (dd, J = 12.4, 1.1 Hz, 1H), 3.99 (dd, J = 12.4, 3.7 Hz, 2H), 2.51 (td, J = 11.2, 3.3 Hz, 1H), 2.47–2.38 (m, 2H), 2.32–2.06 (m, 2H), 1.99–1.83 (m, 2H), 1.79 (t, J = 1.6 Hz, 3H), 1.54 (p, J = 7.4 Hz, 2H), 1.29 (ddq, J = 15.1, 7.3, 4.7, 3.2 Hz, 4H), 0.88 (t, J = 6.9 Hz, 3H). ^{13}C NMR (126 MHz, chloroform-*d*) δ 153.9, 148.6, 143.2, 139.9, 124.1, 120.8, 115.5, 113.4, 108.5, 64.6, 44.7, 37.9, 35.5, 31.5, 30.7, 30.4, 29.7, 27.3, 23.7, 22.5, 14.1; TOF-MS (ESI−) m/z $[M-H]^-$ calculated for $C_{23}H_{31}O_4$ $(M-H)^-$ 371.2, found 371.2.

(1′R,2′R)-2′-(3-Hydroxyprop-1-en-2-yl)-5′-methyl-4-pentyl-1′,2′,3′,4′-tetrahydro-[1,1′-biphenyl]-2,6-diol (JGC7).

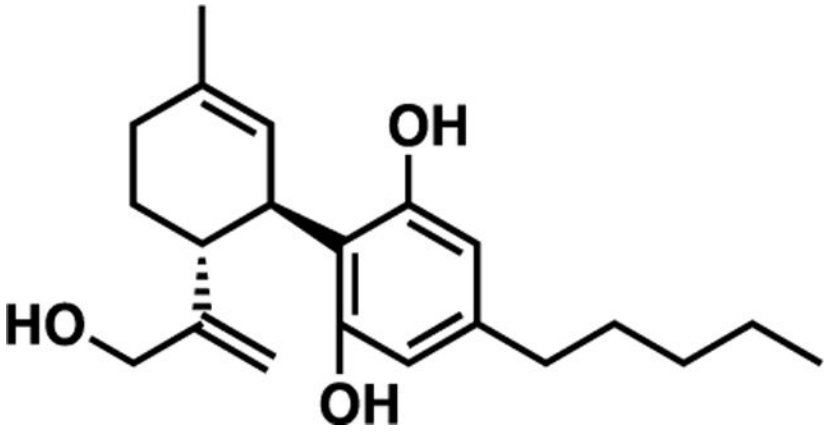

JGC4 (1.0 g, 2.4 mmol) was dissolved in ethanol (375 mL), and $NaBH_4$ (154 mg, 4.1 mmol) was added to the solution. The solution was heated to reflux for 3 h, and TLC confirmed that the reaction was complete. The ethanol was removed under reduced pressure, and water (500 mL) was used to dilute the resulting residue. The solution was extracted several times with Et_2O (3 × 50 mL), and the combined organic layers were washed with brine (50 mL), dried over $MgSO_4$, and concentrated *in vacuo* to produce a clear oil (0.7 g, 2.1 mmol, 88%).

R_f = 0.5 [hexanes:Et_2O (1:1)]; ^{1}H NMR (400 MHz, chloroform-*d*) δ 6.74 (s, 1H), 6.23 (s, 1H), 6.22 (s, 1H), 5.92 (s, 1H), 5.56 (d, J = 2.5 Hz, 1H), 4.89 (d, J = 1.5 Hz, 1H), 4.60 (d, J = 1.6 Hz, 1H), 4.27 (d, J = 12.2 Hz, 1H), 3.97 (dd, J = 14.5, 10.4 Hz, 2H), 2.74 (s, 1H), 2.49 (td, J = 11.1, 3.6 Hz, 1H), 2.44–2.36 (m, 2H), 2.23 (dd, J = 12.6, 5.6 Hz, 1H), 2.16–1.99 (m, 1H), 1.98–1.80 (m, 2H), 1.78 (d, J = 2.1 Hz, 3H), 1.52 (q, J = 7.4 Hz, 2H), 1.27 (qt, J = 6.3, 4.0 Hz, 5H), 0.85 (t, J = 6.9 Hz, 3H). ^{13}C NMR (101 MHz, chloroform-*d*) δ 153.9, 148.5, 143.1, 139.7, 124.1, 115.2, 113.5, 108.4, 77.1, 64.3, 53.4, 44.7, 37.7, 35.5, 31.5, 30.6, 30.3,

27.3, 23.7, 22.5, 14.0; TOF-MS (ES+) *m*/*z* $[M+Na]^+$ calculated for $C_{21}H_{30}O_3Na$ $(M+Na)^+$ 353.2, found 353.2.

(1′*S*,2′*S*)-2′-Isopropyl-5′-methyl-4-pentyl-1′,2′,3′,4′-tetrahydro-[1,1′-biphenyl]-2,6-diol (JGC8).

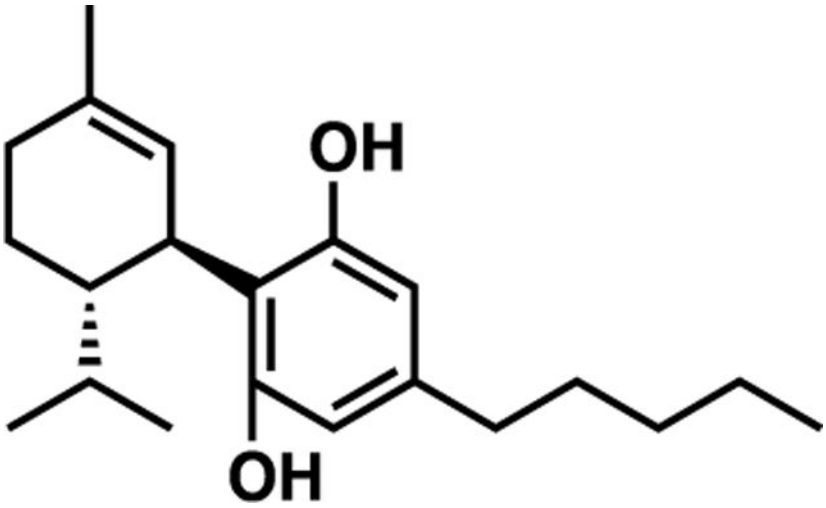

Synthesized as previously published.[28]

(–)-CBD (2.0 g, 6.36 mmol) and PtO_2 (77 mg, 0.34 mmol) were placed under an argon atmosphere, and then ethyl acetate (37 mL) was added to the reaction flask. The solution was vigorously stirred, while the head space was evacuated and back filled with hydrogen gas (3 cycles). A hydrogen balloon was added to the reaction to exert 1 atm of pressure. The reaction was aged for 40 min at room temperature, and completion of the reaction was confirmed via mass spectrometry. The solution was filtered through Celite and washed with ethyl acetate (100 mL). The organic layer was concentrated *in vacuo* to produce a clear colorless oil (2.0 g, 6.3 mmol, 99.5%).

Matched literature data.[28] R_f = 0.71 [10% Et_2O in petroleum ether]; ^{1}H NMR (400 MHz, chloroform-*d*) δ 6.46–5.62 (m, 4H), 5.54 (s, 1H), 3.91 (d, J = 9.9 Hz, 1H), 2.45 (t, J = 7.8 Hz, 2H), 2.25–2.07 (m, 2H), 1.89–1.81 (m, 1H), 1.79 (s, 3H), 1.74–1.63 (m, 2H), 1.58 (t, J = 7.6 Hz, 2H), 1.45 (td, J = 12.1, 5.6 Hz, 1H), 1.34 (dq, J = 9.0, 4.7 Hz, 4H), 0.92 (d, J = 7.1 Hz, 6H), 0.88 (d, J = 6.8 Hz, 3H). ^{13}C NMR (126 MHz, chloroform-*d*) δ 154.3, 142.9, 140.1, 125.0, 114.3, 108.1, 43.8, 35.6, 35.6, 31.7, 30.8, 30.7, 27.9, 23.6, 22.6, 22.2, 21.7, 16.5, 14.1; TOF-MS (ESI+) *m*/*z* $[M+H]^+$ calculated for $C_{21}H_{33}O_2$ $(M+H)^+$ 317.2, found 317.2.

2-((1R,2S,5S)-2-Isopropyl-5-methylcyclohexyl)-5-pentylbenzene-1,3-diol (JGC9).

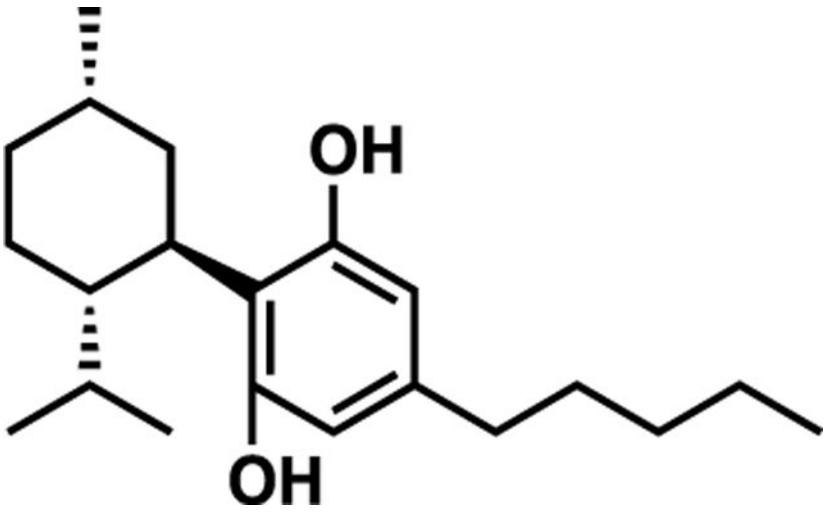

Synthesis was done as previously published with modifications to procedure.[51]

(–)-CBD (0.5 g, 1.6 mmol) and Pt_2O (18 mg, 0.08 mmol) were placed under argon, and then acetic acid (15 mL) was added to the reaction flask. The head space was exchanged with hydrogen gas (3 cycles) and maintained at 11 atm. The reaction was vigorously stirred overnight at room temperature. After 12 h, mass spectrometry confirmed full conversion. The solution was filtered through Celite and washed with ethyl acetate (100 mL). The filtrate was concentrated *in vacuo* to produce a translucent, burnt orange oil (0.5 g, 1.57 mmol, 98.8%). Stereochemistry was proved via 2D-NMR.

Matched literature data.[51] R_f = 0.82 [hexanes:Et_2O (1:1)]; ^{1}H NMR (400 MHz, chloroform-*d*) δ 6.13 (s, 1H), 6.12 (s, 1H), 5.28 (s, 3H), 2.99 (td, J = 11.4, 3.8 Hz, 1H), 2.40 (t, J = 7.8 Hz, 2H), 2.05 (d, J = 31.6 Hz, 2H), 1.89–0.94 (m, 11H), 0.94–0.75 (m, 10H), 0.70 (d, J = 6.9 Hz, 3H). ^{13}C NMR (126 MHz, chloroform-*d*) δ 155.5, 154.1, 141.9, 115.3, 109.1, 108.2, 53.4, 44.7, 40.3, 38.2, 35.5, 35.3, 33.6, 31.6, 30.6, 28.7, 25.5, 22.6, 21.7, 15.8, 14.0; TOF-MS (ESI+) m/z $[M+H]^+$ calculated for $C_{21}H_{35}O_2$ $(M+H)^+$ 319.2, found 319.2.

(1′S,2′S)-5′-(Hydroxymethyl)-2′-isopropyl-4-pentyl-1′,2′,3′,4′-tetrahydro-[1,1′-biphenyl]-2,6-diol (JGC10).

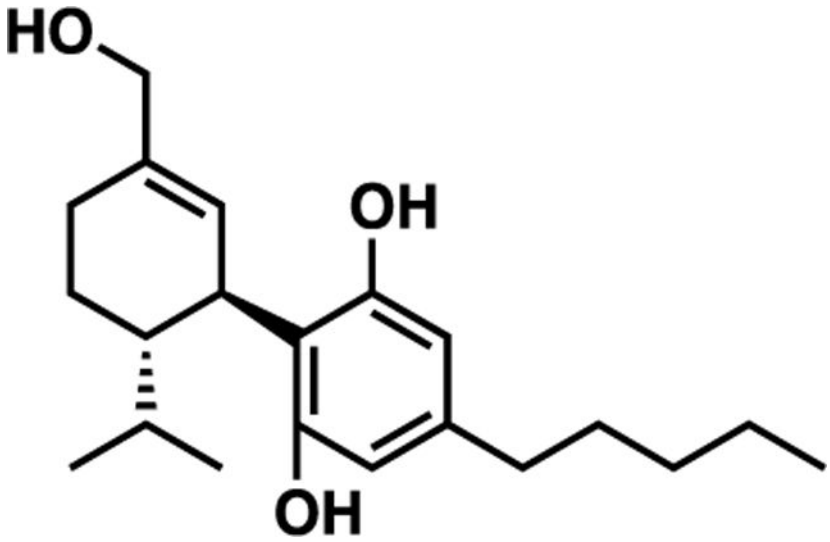

JGC12 (0.8 g, 1.9 mmol) was dissolved in ethanol (375 mL), and then $NaBH_4$ (144 mg, 3.8 mmol) was added to the reaction flask. The solution was heated to reflux for 4.5 h, and was monitored by TLC. Water (500 mL) was added, and the solution was extracted with Et_2O (6 × 100 mL). The organic layer was washed with brine (100 mL), dried over $MgSO_4$, and concentrated *in vacuo* to produce a white powder. The crude product was purified via flash chromatography [hexanes:Et_2O (4:1)] to produce a white powder (0.2 g, 0.602 mmol, 31%).

R_f = 0.17 [hexanes:Et_2O (1:1)]; ^{1}H NMR (400 MHz, chloroform-*d*) δ 6.19 (s, 1H), 6.17 (s, 1H), 5.69–5.19 (m, 3H), 4.36 (d, J = 5.6 Hz, 1H), 3.87 (dd, J = 10.8, 3.0 Hz, 1H), 2.52–2.31 (m, 2H), 2.12 (ddd, J = 12.1, 5.5, 2.3 Hz, 1H), 1.97–1.76 (m, 6H), 1.55 (q, J = 7.4 Hz, 4H), 1.46–1.19 (m, 5H), 0.84 (dd, J = 17.0, 6.9 Hz, 11H). ^{13}C NMR (126 MHz, chloroform-*d*) δ 154.4, 143.3, 141.2, 128.1, 113.2, 107.5, 71.2, 43.3, 35.8, 35.5, 33.1, 31.6, 30.7, 27.8, 22.6, 21.6, 18.8, 16.1, 14.0; TOF-MS (ESI−) m/z $[M-H]^-$ calculated for $C_{21}H_{31}O_3$ $[M-H]^-$ 331.2, found 331.2.

(1′S,2′S)-2′-Isopropyl-5′-methyl-4-pentyl-1′,2′,3′,4′-tetrahydro-[1,1′-biphenyl]-2,6-diyl Diacetate (JGC11).

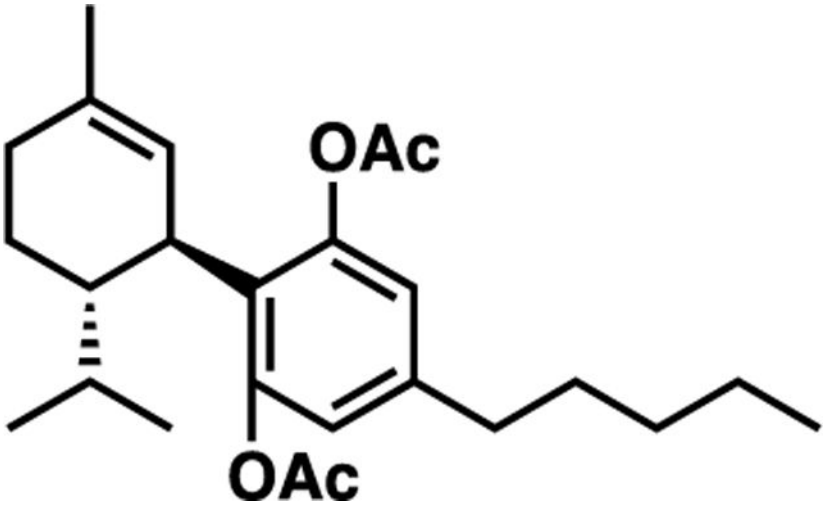

JGC8 (2.0 g, 6.3 mmol) was dissolved in pyridine (11.7 mL, 145 mmol), and acetic anhydride (12 mL, 126 mmol) was added. The solution was aged for 12 h at room temperature. TLC confirmed the reaction was complete, and cold water (120 mL) was added to the reaction flask. The solution was extracted with Et_2O (3 × 50 mL). The organic layer was washed with 1 M HCl (50 mL), saturated aqueous Na_2CO_3 (50 mL), and brine (50 mL), dried over $MgSO_4$, and concentrated *in vacuo* to produce a translucent oil (2.3 g,5.74 mmol, 92%) that was carried to the next step without further purification.

R_f = 0.77 [hexanes:Et_2O (1:1)]; ^{1}H NMR (400 MHz, chloroform-*d*) δ 6.70 (s, 2H), 5.11 (d, J = 2.6 Hz, 1H), 3.54–3.33 (m, 1H), 2.53 (dd, J = 9.0, 6.8 Hz, 2H), 2.38–1.92 (m, 10H), 1.92–1.68 (m, 1H), 1.67–1.50 (m, 6H), 1.50–1.22 (m, 6H), 1.18 (t, J = 7.0 Hz, 1H), 0.93–0.83 (m, 4H), 0.81 (d, J = 6.9 Hz, 4H), 0.74 (d, J = 6.9 Hz, 3H). ^{13}C NMR (101 MHz, chloroform-*d*) δ 175.9, 169.1, 149.9, 142.0, 133.1, 126.3, 124.9, 124.0, 121.5, 119.9, 65.8, 42.7, 37.4, 35.2, 31.5, 30.7, 30.3, 27.9, 23.4, 22.4, 21.5, 20.9, 16.0, 15.2, 13.9; TOF-MS (ESI+) m/z $[M+Na]^+$ calculated for $C_{25}H_{36}O_4Na$ $(M+Na)^+$ 423.3, found 423.2.

(1′S,2′S)-5′-(Hydroxymethyl)-2′-isopropyl-4-pentyl-1′,2′,3′,4′-tetrahydro-[1,1′-biphenyl]-2,6-diyl Diacetate (JGC12).

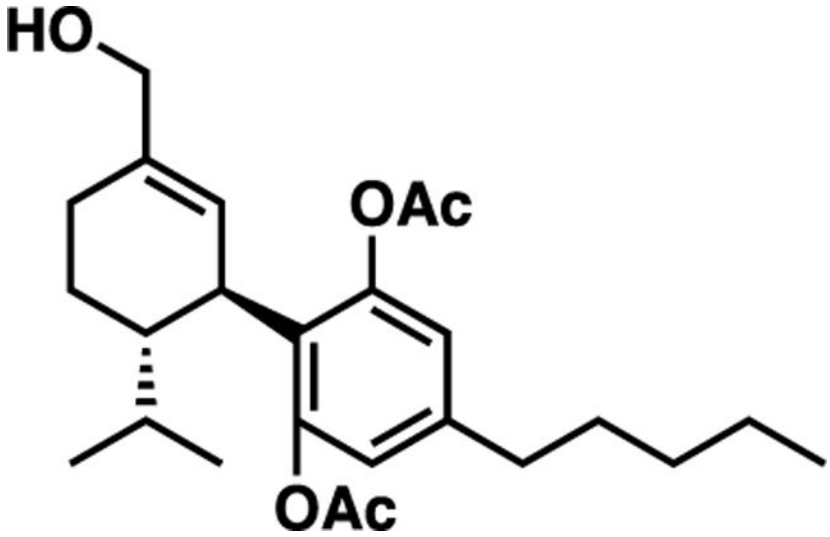

To a solution at 0 °C under argon of SeO_2 (95 mg, 0.86 mmol), salicylic acid (135 mg, 0.98 mmol), and dry DCM (40 mL), a solution of JGC11 (2.3 g, 5.8 mmol), ^{t}BuOOH (6 M in decane, 2.6 mL, 23 mmol), and dry DCM (40 mL) were added. The reaction was allowed to warm to room temperature and was vigorously stirred for 48 h. Water (120 mL) was added to the reaction flask, and the solution was extracted with DCM (3 × 40 mL). The organic layer was washed with saturated aqueous Na_2CO_3 (40 mL) and brine (40 mL), dried over $MgSO_4$, and concentrated *in vacuo* to produce a yellow oil. The oil was purified by flash column chromatography [hexanes:Et_2O (4:1 → 1:1)] to produce a clear oil (1.1 g, 2.64 mmol, 46%).

R_f = 0.13 [hexanes:Et_2O (1:1)]; ^{1}H NMR (400 MHz, chloroform-*d*) δ 6.71 (s, 2H), 5.47–5.14 (m, 1H), 4.12 (d, J = 125.0 Hz, 1H), 3.53–3.33 (m, 1H), 2.54 (dd, J = 9.0, 6.8 Hz, 2H), 2.21 (s, 2H), 1.74 (p, J = 1.2 Hz, 3H), 1.65–1.35 (m, 3H), 1.35–1.20 (m, 6H), 0.97–0.66 (m, 12H). ^{13}C NMR (126 MHz, chloroform-*d*) δ 169.0, 149.8, 142.5, 136.8, 135.6, 128.0, 126.3, 125.9, 125.3, 71.3, 66.8, 42.8, 37.7, 35.2, 33.2, 31.5, 30.4, 27.8, 22.5, 21.4, 20.9, 18.6, 15.9, 13.9; TOF-MS (ESI+) m/z $[M+Na]^+$ calculated for $C_{25}H_{36}O_5Na$ $(M+Na)^+$ 439.2, found 439.2.

2-((1R,2S,5S)-5-(Hydroxymethyl)-2-isopropylcyclohexyl)-5-pentylbenzene-1,3-diol (JGC13).

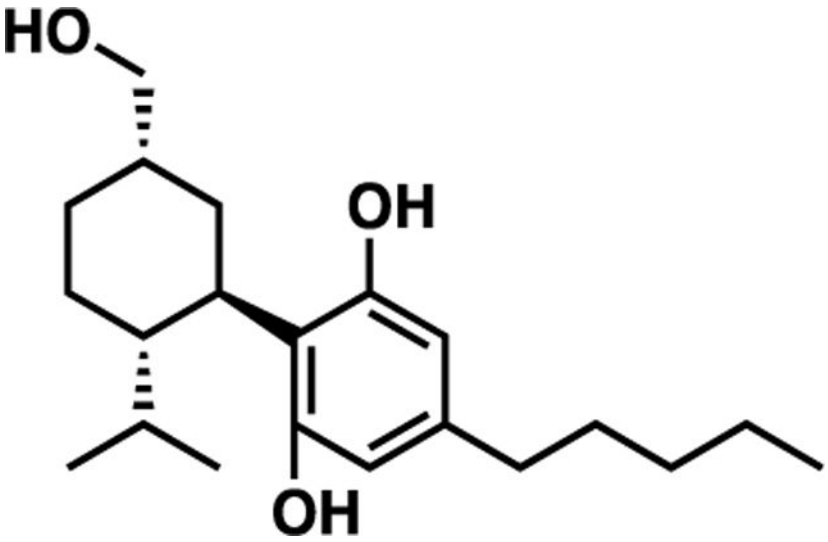

JGC10 (65 mg, 0.2 mmol) and PtO_2 (2.3 mg, 0.01 mmol) were placed under argon, and acetic acid (10 mL) was added to the reaction flask. The solution was placed inside a high-pressure vessel, and the head space was replaced with hydrogen gas (3 cycles). The reaction was stirred for 4 h at a maintained pressure of 11 atm. Mass spectrometry confirmed full conversion; thus, the solution was filtered through Celite and washed with ethyl acetate (100 mL). The filtrate was concentrated *in vacuo* to afford a brown, powdery solid (0.066 g, 0.197 mmol, 99%). Stereochemistry was proved via NMR.

R_f = 0.242 [hexanes:Et_2O (1:1)]; ^{1}H NMR (500 MHz, chloroform-*d*) δ 6.14 (s, 1H), 6.12 (s, 1H), 5.97–5.11 (m, 2H), 3.63–3.29 (m, 2H), 3.06 (t, J = 11.9 Hz, 1H), 2.38 (dt, J = 40.3, 10.1 Hz, 3H), 1.99 (d, J = 11.5 Hz, 1H), 1.82 (q, J = 12.5 Hz, 1H), 1.74–1.41 (m, 6H), 1.41–1.11 (m, 6H), 1.03 (d, J = 6.3 Hz, 3H), 0.96–0.54 (m, 10H). ^{13}C NMR (126 MHz, chloroform-*d*) δ 155.7, 154.7, 141.9, 114.4, 108.7, 107.9, 65.9, 42.8, 40.7, 37.7, 37.5, 35.4, 34.8, 31.7, 30.7, 28.5, 22.6, 21.7, 18.3, 15.8, 15.1, 14.1; TOF-MS (ESI−) m/z $[M-H]^-$ calculated for $C_{21}H_{33}O_3$ $[M-H]^-$ 333.2, found 333.2.

5-Pentylbenzene-1,3-diol (JGC14 or Olivetol).

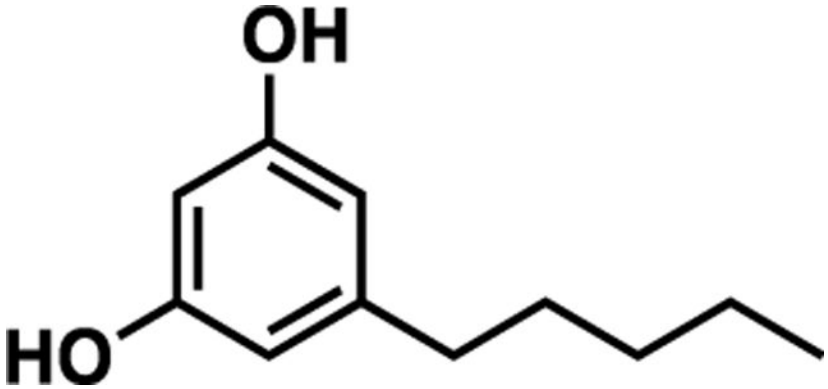

Synthesis was done as previously published.[52]

Methyl 2-hydroxy-4-oxo-6-pentylcyclohex-2-ene-1-carboxylate (23.5 g, 98 mmol) was dissolved in DMF (47 mL), and the reaction flask was cooled to 0 °C. A solution of Br_2 (4.0 mL, 78.1 mmol) in DMF (25 mL) was charged to an addition funnel and added dropwise over the course of an hour. Upon complete addition, the reaction was slowly heated to 80 °C to expel carbon dioxide from the reaction, and then heated further to reflux (160 ° C) for 12 h. The reaction flask was then cooled to room temperature, and water (750 mL) was added. The resulting solution was extracted with Et_2O (4 × 100 mL), and the combined organic layers were washed with 10% sodium bisulfate (100 mL), 10% acetic acid (100 mL), water (100 mL), and brine (100 mL). The organic layer was dried over $MgSO_4$ and concentrated *in vacuo* to produce a brown oil, which was purified via distillation (2 mmHg, 160–170 °C) to yield an off-white solid (10.2 g, 56.6 mmol, 57%).

Matched literature data.[52] R_f = 0.286 [hexanes:ethyl acetate (2:1)]; ^{1}H NMR (500 MHz, chloroform-*d*) δ 6.30 (d, J = 2.1 Hz, 2H), 6.21 (t, J = 2.2 Hz, 1H), 2.54–2.29 (m, 2H), 1.52 (t, J = 7.6 Hz, 2H), 1.38–1.15 (m, 4H), 0.88 (t, J = 6.9 Hz, 3H). ^{13}C NMR (126 MHz, chloroform-*d*) δ 156.1, 146.5, 108.4, 100.4, 35.8, 31.5, 30.7, 22.5, 14.0; TOF-MS (ESI+) m/z $[M+H]^+$ calculated for $C_{11}H_{17}O_2$ $(M+H)^+$ 181.1, found 181.1.

(1S,2S)-2-Isopropyl-2′,6′-dimethoxy-5-methyl-4′-pentyl-1,2,3,4-tetrahydro-1,1′-biphenyl (JGC15).

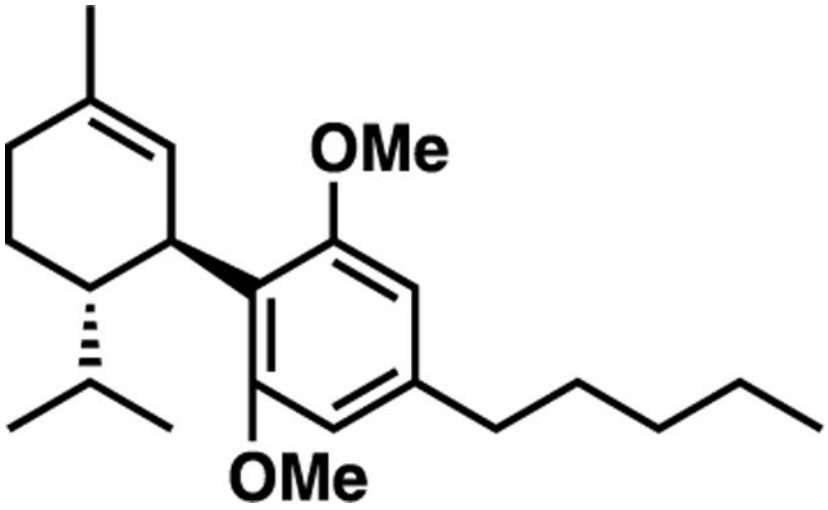

JGC2 (1.1 g, 3.26 mmol) and PtO_2 (37 mg, 0.163 mmol) were placed under an argon atmosphere, and then ethyl acetate (16 mL) was added to the reaction flask. The solution was vigorously stirred, while the head space was evacuated and back filled with hydrogen gas (3 cycles). A hydrogen balloon was added to the reaction to exert 1 atm of pressure. The reaction was aged overnight at room temperature. The solution was filtered through Celite and washed with ethyl acetate (100 mL). The organic layer was concentrated *in vacuo* to produce a clear colorless oil (1.06 g, 3.08 mmol, 94%).

R_f = 0.429 [5% Et_2O in petroleum ether]; ^{1}H NMR (500 MHz, chloroform-*d*) δ 6.36 (s, 2H), 5.21–5.10 (m, 1H), 3.86 (dh, J = 8.8, 2.3 Hz, 1H), 3.73 (s, 6H), 2.63–2.40 (m, 2H), 2.18–1.91 (m, 3H), 1.73 (ddt, J = 12.6, 4.9, 2.3 Hz, 1H), 1.68–1.57 (m, 5H), 1.47–1.27 (m, 6H),

0.96–0.88 (m, 3H), 0.78 (dd, J = 21.5, 6.9 Hz, 6H). ^{13}C NMR (126 MHz, chloroform-d) δ 159.1, 141.9, 131.5, 126.3, 119.6, 104.9, 56.0, 42.1, 36.4, 35.9, 31.8, 31.1, 31.0, 28.4, 23.5, 23.0, 22.6, 21.7, 16.2, 14.1; TOF-MS (ESI+) m/z $[M+H]^+$ calculated for $C_{23}H_{35}O_2$ $(M+H)^+$ 345.3, found 345.4.

2-((1R,2S,5S)-2-Isopropyl-5-methylcyclohexyl)-1,3-dimethoxy-5-pentylbenzene (JGC48).

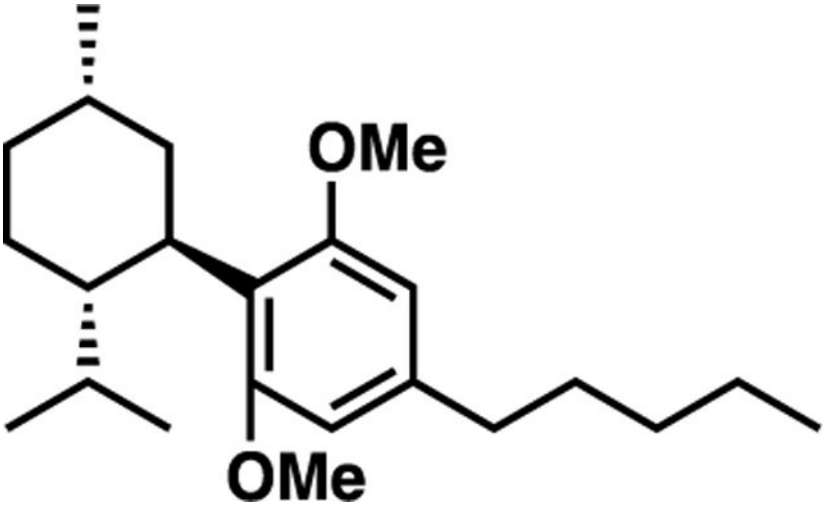

JGC15 (700 mg, 2.03 mmol) and PtO_2 (23 mg, 0.102 mmol) were placed under an argon atmosphere, and then acetic acid (20 mL) was added to the reaction flask. The head space was exchanged with hydrogen gas (3 cycles) and maintained at 100 atm. The reaction was vigorously stirred for 5 h at room temperature. The solution was filtered through Celite and washed with ethyl acetate (100 mL). The filtrate was concentrated *in vacuo* and purified via flash column chromatography (hexanes → 2% Et_2O in hexanes) to produce a clear, colorless oil (0.480 g, 1.39 mmol, 68%). Stereochemistry was proved via 2D-NMR.

R_f = 0.411 [2% Et_2O in hexanes]; ^{1}H NMR (500 MHz, chloroform-d) δ 6.39–6.31 (m, 2H), 3.77 (d, J = 5.0 Hz, 6H), 3.14 (td, J = 11.5, 3.4 Hz, 1H), 2.60–2.51 (m, 2H), 2.07 (tt, J = 11.6, 2.9 Hz, 1H), 1.75 (dq, J = 12.2, 3.0 Hz, 1H), 1.70–1.55 (m, 4H), 1.55–1.41 (m, 2H), 1.35 (dt, J = 8.9, 3.2 Hz, 4H), 1.13–0.94 (m, 2H), 0.95–0.87 (m, 3H), 0.87 (d, J = 6.4 Hz, 3H), 0.79 (d, J = 7.0 Hz, 3H), 0.63 (d, J = 6.9 Hz, 3H). ^{13}C NMR (126 MHz, chloroform-d) δ 159.6, 158.0, 141.6, 119.5, 105.1, 104.6, 56.2, 55.5, 44.1, 40.3, 38.0, 36.6, 35.8, 33.8, 31.9, 31.2, 28.7, 25.6, 22.8, 22.7, 21.9 15.7, 14.2; TOF-MS (ESI+) m/z [M+H] + calculated for $C_{23}H_{39}O_2$ (M+H) +346.3, found 347.3.

((1S,6S)-6-Isopropyl-2′,6′-dimethoxy-4′-pentyl-1,4,5,6-tetrahydro-[1,1′-biphenyl]-3-yl)methanol (JGC49).

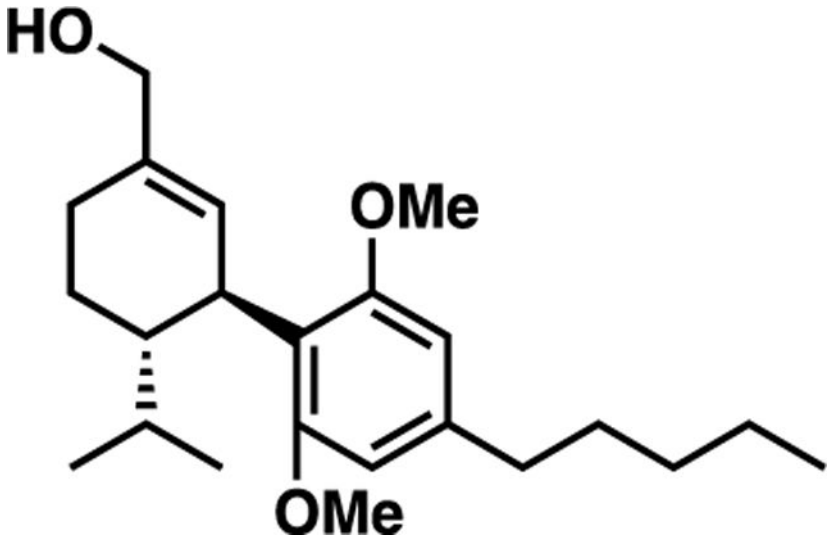

To a solution of SeO_2 (68 mg, 0.616 mmol) and salicylic acid (106 mg, 0.770 mmol) in DCM (31 mL) at 0 °C under argon, a solution of JGC48 (1.06 g, 3.08 mmol) in ^{t}BuOOH (6 M in decane, 1.37 mL, 12.3 mmol) was added. The reaction was allowed to warm to room temperature and was vigorously stirred for 24 h. Water (60 mL) was added to the reaction flask, and the solution was extracted with DCM (3 × 40 mL). The organic layer was washed with saturated aqueous Na_2CO_3 (40 mL) and brine (40 mL), dried over $MgSO_4$, and concentrated *in vacuo*. The oil was purified by flash column chromatography [hexanes:Et_2O (4:1 → 1:1)] to produce a clear oil (832 mg, 2.31 mmol, 75%).

R_f = 0.23 [hexanes:Et_2O (2:1)]; ^{1}H NMR (500 MHz, chloroform-*d*) δ 6.35 (s, 2H), 5.25 (q, J = 1.7 Hz, 1H), 4.31 (h, J = 4.8 Hz, 1H), 3.90 (dh, J = 10.8, 2.5 Hz, 1H), 3.73 (s, 7H), 2.61–2.49 (m, 2H), 2.25–2.15 (m, 1H), 2.09 (ddd, J = 11.9, 5.6, 2.5 Hz, 1H), 1.75 (d, J = 1.3 Hz, 2H), 1.62 (dq, J = 11.8, 7.5 Hz, 2H), 1.38–1.28 (m, 6H), 0.95–0.88 (m, 3H), 0.79 (dd, J = 6.9, 5.2 Hz, 6H). ^{13}C NMR (126 MHz, chloroform-*d*) δ 142.5, 133.7, 130.1, 118.4, 72.2, 56.0, 42.4, 36.6, 36.2, 34.1, 31.9, 31.2, 28.4, 22.7, 21.7, 18.8, 16.2, 14.2; TOF-MS (ESI+) m/z $[M–OH]^+$ calculated for $C_{23}H_{35}O_2$ $[M–OH]^+$ 343.3, found 343.4.

((1S, 3R, 4S) - 3 - (2, 6 - Dimethoxy - 4 - pentylphenyl) - 4 isopropylcyclohexyl)methanol (JGC50).

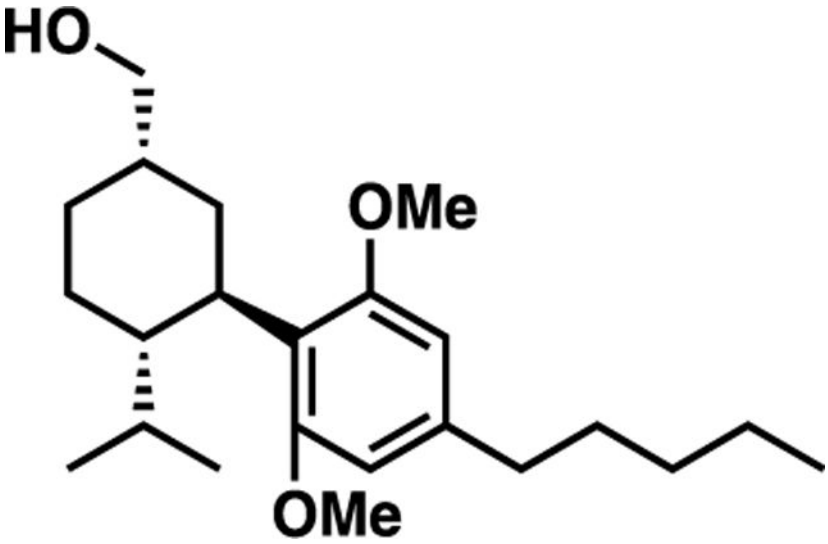

JGC49 (350 mg, 0.971 mmol) and PtO_2 (11 mg, 0.049 mmol) were placed under argon, and acetic acid (10 mL) was added to the reaction flask. The solution was placed inside a high-pressure vessel, and the head space was replaced with hydrogen gas (3 cycles). The reaction was stirred for 5 h at a maintained pressure of 100 psi. The solution was filtered through Celite and washed with ethyl acetate (100 mL). The filtrate was concentrated *in vacuo* to afford a clear, colorless oil (340 mg, 0.942 mmol, 97%). Stereochemistry was proved via NMR.

R_f = 0.23 [hexanes:Et_2O (2:1)]; ^{1}H NMR (500 MHz, chloroform-*d*) δ 7.19 (s, 2H), 6.27 (dd, J = 13.0, 1.4 Hz, 3H), 4.05 (q, J = 7.1 Hz, 0H), 3.69 (d, J = 11.1 Hz, 9H), 3.21 (td, J = 10.8, 4.2 Hz, 1H), 3.08 (td, J = 11.7, 3.5 Hz, 1H), 2.55–2.36 (m, 3H), 2.18 (tq, J = 13.9, 2.8 Hz, 2H), 1.85 (ddd, J = 12.0, 4.2, 3.1 Hz, 1H), 1.75–1.60 (m, 1H), 1.55 (p, J = 7.4 Hz, 3H), 1.47 (dt, J = 13.2, 3.7 Hz, 2H), 1.37 (tdd, J = 9.8, 6.2, 3.2 Hz, 1H), 1.27 (hept, J = 4.1, 3.4 Hz, 7H), 1.19 (t, J = 7.1 Hz, 1H), 0.93 (d, J = 6.4 Hz, 4H), 0.88–0.78 (m, 3H), 0.73 (d, J = 7.0 Hz, 4H), 0.58 (d, J = 6.9 Hz, 4H). ^{13}C NMR (126 MHz, chloroform-*d*) δ 159.4, 158.1, 141.9, 118.1, 104.9, 104.5, 56.1, 55.4, 42.9, 41.1, 37.9, 37.3, 36.6, 35.1, 31.9, 31.2, 28.6, 22.7, 21.8, 18.4, 15.7, 14.3; TOF-MS (ESI+) m/z $[M–OH]^+$ calculated for $C_{23}H_{37}O_2$ $[M–OH]^+$ 345.3, found 345.4.

Diastereomers of Cannabidiol.

Starting materials were synthesized as previously published with modifications.[52–56]

General Procedure for Chiral Iridium and Amine Dual Catalyst Coupling.

Synthesis was done as previously published.[35]

To a flame-dried flack equipped with a stir bar and argon inlet, $[Ir(cod)Cl]_2$ (136 mg, 0.203 mmol, 3 mol %) and 5-((11b*S*/*R*)-dinaphtho[2,1-*d*:1′,2′-*f*][1,3,2]dioxaphosphepin-4-yl)-5*H*-dibenzo[*b*,*f*]azepine (411 mg, 0.81 mmol, 12 mol %) were dissolved in DCE (13.5

mL). The reaction was vigorously stirred for 15 min. To the deep red solution, 1-(2,6-dimethoxy-4-pentylphenyl)prop-2-en-1-ol (1.78 g, 6.75 mmol) and 5-methylhex-5-enal (2.27 g, 20.3 mmol) were added. Then, (*S*/*R*)-α,α-bis[3,5-bis(trifluoromethyl)phenyl]-2-pyrrolidinemethanol trimethylsilyl ether (605 mg, 1.01 mmol, 15 mol %) and $Zn(OTf)_2$ (123 mg, 0.338 mmol, 5 mol %) were added, and the reaction flask was purged with argon and allowed to stir at room temperature for 24 h. The orange solution was directly added to a silica column and purified (toluene to 4:1 toluene:DCM).

(R)-2-((R)-1-(2,6-Dimethoxy-4-pentylphenyl)allyl)-5-methylhex-5-enal.

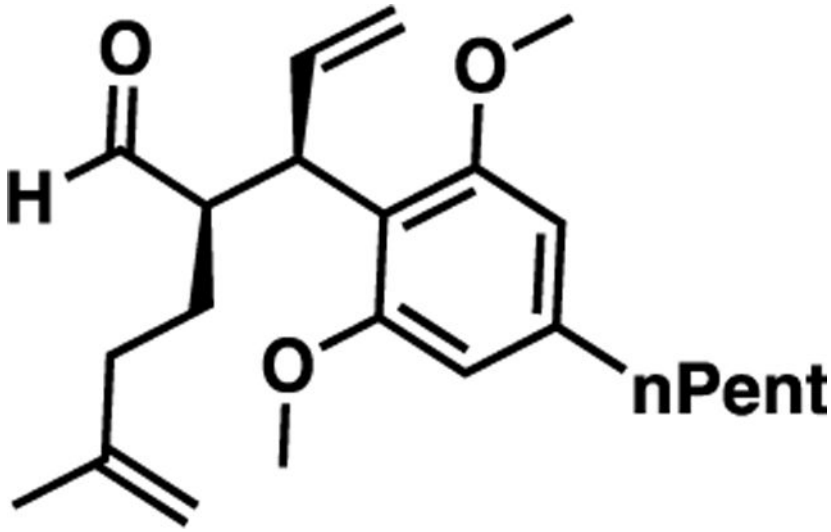

The general procedure was followed using 5-((11b*S*)-dinaphtho[2,1-*d*:1′,2′-*f*][1,3,2]dioxaphosphepin-4-yl)-5*H*-dibenzo[*b*,*f*]azepine (411 mg, 0.81 mmol, 12 mol %) and (*S*)-α,α-Bis[3,5-bis(trifluoromethyl)phenyl]-2-pyrrolidinemethanol trimethylsilyl ether (605 mg, 1.01 mmol, 15 mol %) to produce a clear, colorless oil (1.17 g, 3.27 mmol, 49%).

Matched literature data.[35] R_f = 0.538 [toluene:DCM (4:1)]; $[a]_D^{20}$+49.2 (*c* 1.1, $CHCl_3$) (literature: $[a]^{25}_D$ +50.4 (*c* 1.0, $CHCl_3$)); ^{1}H NMR (500 MHz, chloroform-*d*) δ 9.40 (d, *J* = 3.8 Hz, 1H), 6.40 (s, 2H), 6.32 (ddd, *J* = 17.1, 9.9, 8.8 Hz, 1H), 5.17 (dt, *J* = 17.0, 1.4 Hz, 1H), 5.09 (dd, *J* = 10.0, 2.0 Hz, 1H), 4.83–4.72 (m, 3H), 4.25 (t, *J* = 9.5 Hz, 1H), 3.85 (s, 6H), 3.00 (ddt, *J* = 10.4, 6.7, 3.3 Hz, 1H), 2.66–2.51 (m, 2H), 2.13–1.97 (m, 2H), 1.78 (d, *J* = 7.9 Hz, 5H), 1.72–1.57 (m, 3H), 1.47–1.29 (m, 5H), 0.97 (t, *J* = 6.9 Hz, 3H). ^{13}C NMR (126 MHz, chloroform-*d*) δ 204.9, 157.7, 145.5, 143.5, 138.4, 115.9, 114.2, 110.2, 104.5, 55.6, 53.1, 40.6, 36.5, 35.1, 31.6, 31.0, 26.2, 22.6, 22.4, 14.1; TOF-MS (ESI+) *m*/*z* $[M+Na]^+$ calculated for $C_{23}H_{34}O_3Na$ $(M+Na)^+$ 381.2400, found 381.2399.

(S)-2-((R)-1-(2,6-Dimethoxy-4-pentylphenyl)allyl)-5-methylhex-5-enal.

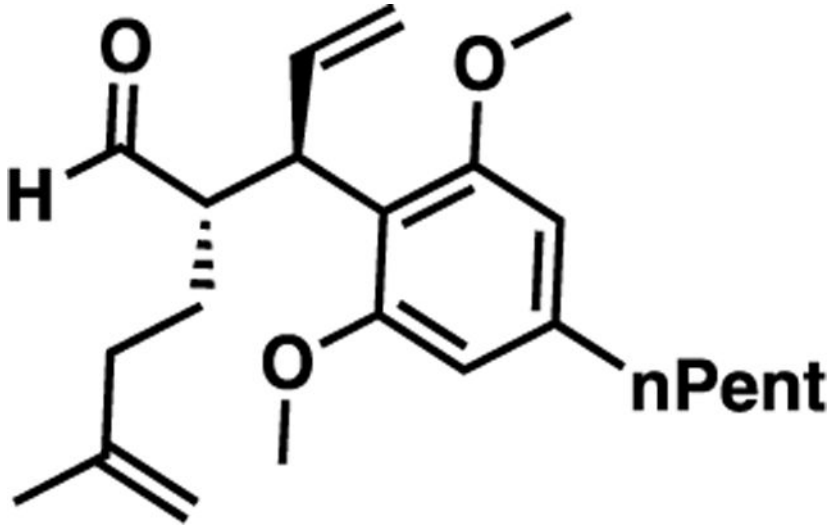

The general procedure was followed using 5-((11b*S*)-dinaphtho[2,1-*d*:1′,2′-*f*][1,3,2]dioxaphosphepin-4-yl)-5*H*-dibenzo[*b*,*f*]azepine (230 mg, 0.454 mmol) and (*R*)-bis(3,5-bis(trifluoromethyl)phenyl)-(pyrrolidin-2-yl)methanol trimethylsilyl ether (339 mg, 0.568 mmol) to produce a clear, yellow oil (590 mg, 1.65 mmol, 43%).

Matched literature data.[35] R_f = 0.466 [toluene:DCM (4:1)]; $[a]_D^{20}$ +21.1 (*c* 1.035, $CHCl_3$) (literature: $[a]^{25}_D$ +22.3 (*c* 1.0, $CHCl_3$)); ^{1}H NMR (500 MHz, chloroform-*d*) *δ* 9.61 (dd, *J* = 4.4, 0.8 Hz, 1H), 6.36 (s, 2H), 6.24 (ddd, *J* = 17.0, 10.0, 8.9 Hz, 1H), 5.05 (ddd, *J* = 17.1, 1.9, 0.9 Hz, 1H), 4.95 (dd, *J* = 10.0, 1.8 Hz, 1H), 4.63 (t, *J* = 1.8 Hz, 1H), 4.54 (dt, *J* = 2.5, 1.2 Hz, 1H), 4.29 (t, *J* = 9.5 Hz, 1H), 3.79 (s, 6H), 3.05 (tt, *J* = 9.8, 3.9 Hz, 1H), 2.61–2.48 (m, 2H), 1.98–1.77 (m, 2H), 1.66–1.54 (m, 2H), 1.53 (t, *J* = 1.1 Hz, 3H), 1.44–1.27 (m, 5H), 0.90 (t, *J* = 6.8 Hz, 3H). ^{13}C NMR (126 MHz, chloroform-*d*) *δ* 206.2, 158.1, 145.1, 143.3, 138.6, 115.6, 114.3, 110.4, 104.5, 55.5, 52.8, 40.2, 36.5, 34.7, 31.6, 31.1, 25.8, 22.6, 22.1, 14.1; TOF-MS (ESI+) *m*/*z* $[M+Na]^+$ calculated for $C_{23}H_{34}O_3Na$ $(M+Na)^+$ 381.2400, found 381.2399.

(R)-2-((S)-1-(2,6-Dimethoxy-4-pentylphenyl)allyl)-5-methylhex-5-enal.

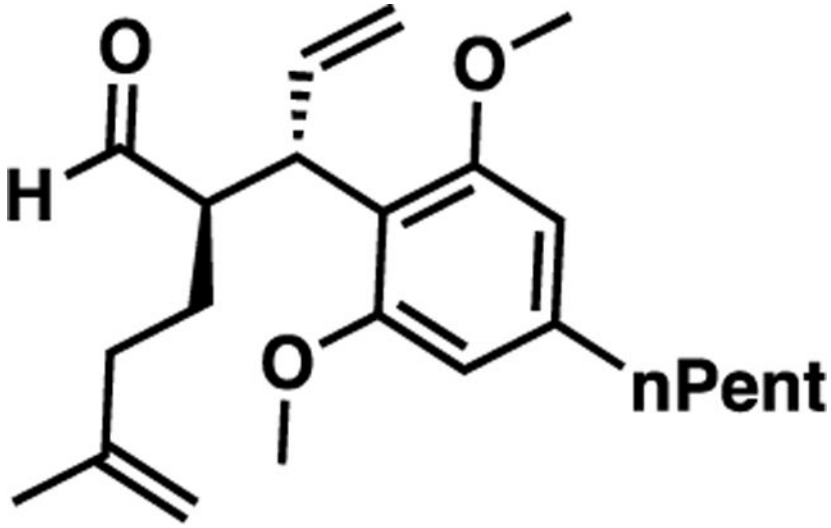

The general procedure was followed using 5-((11b*R*)-dinaphtho[2,1-*d*:1′,2′-*f*][1,3,2]dioxaphosphepin-4-yl)-5*H*-dibenzo[*b*,*f*]azepine (230 mg, 0.454 mmol) and (*S*)-bis(3,5-bis(trifluoromethyl)phenyl)-(pyrrolidin-2-yl)methanol trimethylsilyl ether (339 mg, 0.568 mmol) to produce yellow, clear oil (555 mg, 1.55 mmol, 41%).

Matched literature data.[35] R_f = 0.486 [toluene:DCM (4:1)]; $[a]_D^{20}$ −22.4 (*c* 1.03, $CHCl_3$) (literature: $[a]^{25}_D$ −21.5 (*c* 1.0, $CHCl_3$)); ^{1}H NMR (500 MHz, chloroform-*d*) *δ* 9.62 (d, *J* = 4.3 Hz, 1H), 6.37 (s, 2H), 6.24 (ddd, *J* = 17.1, 10.0, 8.8 Hz, 1H), 5.05 (ddd, *J* = 17.1, 1.8, 0.9 Hz, 1H), 4.95 (dd, *J* = 10.0, 1.8 Hz, 1H), 4.66–4.61 (m, 1H), 4.54 (dd, *J* = 2.3, 1.2 Hz, 1H), 4.29 (t, *J* = 9.6 Hz, 1H), 3.79 (s, 6H), 3.06 (tt, *J* = 9.8, 3.9 Hz, 1H), 2.67–2.48 (m, 2H), 2.00–1.76 (m, 2H), 1.60 (tdd, *J* = 18.2, 8.4, 5.3 Hz, 3H), 1.53 (t, *J* = 1.0 Hz, 3H), 1.44–1.27 (m, 5H), 0.94–0.87 (m, 3H). ^{13}C NMR (126 MHz, chloroform-*d*) *δ* 206.3, 158.1, 145.2, 143.3, 138.5, 129.0, 128.2, 125.3, 115.6, 114.3, 110.3, 104.5, 55.6, 52.9, 40.2, 36.5, 34.7, 31.6, 31.1, 25.8, 22.6, 22.1, 14.1; TOF-MS (ESI+) *m*/*z* $[M+Na]^+$ calculated for $C_{23}H_{34}O_3$ $(M+Na)^+$ 381.2400, found 381.2399.

(S)-2-((S)-1-(2,6-Dimethoxy-4-pentylphenyl)allyl)-5-methylhex-5-enal.

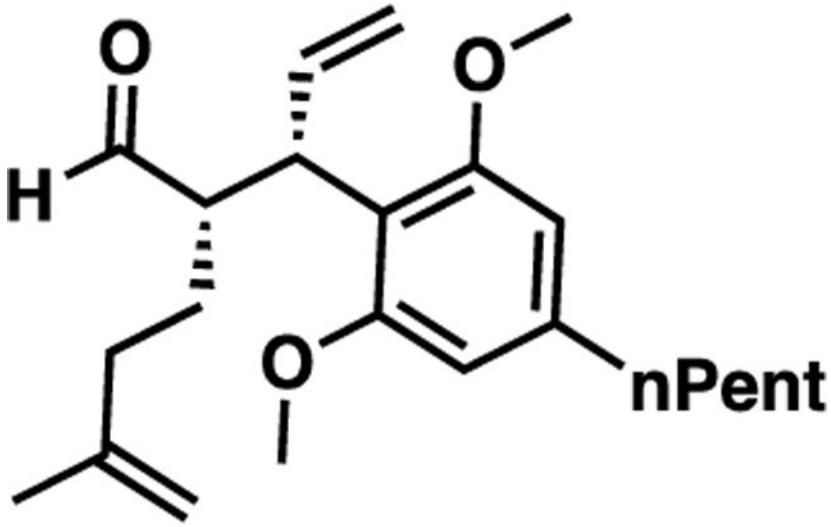

The general procedure was followed using 5-((11b*R*)-dinaphtho[2,1-*d*:1′,2′-*f*][1,3,2]dioxaphosphepin-4-yl)-5*H*-dibenzo[*b*,*f*]azepine (230 mg, 0.454 mmol) and (*R*)-bis(3,5-bis(trifluoromethyl)phenyl)-(pyrrolidin-2-yl)methanol trimethylsilyl ether (339 mg, 0.568 mmol) to produce clear, colorless oil (583 mg, 1.63 mmol, 43%).

Matched literature data.[35] R_f = 0.513 [toluene:DCM (4:1)]; $[a]_D^{20}$ −50.7 (*c* 0.95, $CHCl_3$) (literature: $[a]^{25}_D$ −52.4 (*c* 1.0, $CHCl_3$)); ^{1}H NMR (500 MHz, chloroform-*d*) *δ* 9.33 (d, *J* = 3.9 Hz, 1H), 6.33 (s, 2H), 6.25 (ddd, *J* = 17.1, 10.0, 8.8 Hz, 1H), 5.10 (dt, *J* = 17.1, 1.4 Hz, 1H), 5.02 (dd, *J* = 9.9, 1.9 Hz, 1H), 4.71 (t, *J* = 1.8 Hz, 1H), 4.70–4.66 (m, 1H), 4.18 (t, *J* = 9.5 Hz, 1H), 3.78 (s, 7H), 2.93 (dtd, *J* = 10.4, 6.6, 3.9 Hz, 1H), 2.52 (dd, *J* = 9.0, 6.8 Hz, 2H), 1.98 (p, *J* = 7.5 Hz, 2H), 1.71 (d, *J* = 7.9 Hz, 5H), 1.58 (ddd, *J* = 19.2, 10.5, 5.9 Hz, 2H), 1.33 (qd, *J* = 7.0, 3.2 Hz, 4H), 0.90 (t, *J* = 6.9 Hz, 3H). ^{13}C NMR (126 MHz, chloroform-*d*) *δ* 205.1, 157.8, 145.6, 143.6, 138.5, 116.1, 114.3, 110.3, 104.7, 55.7, 53.2, 40.8, 36.7, 35.2, 31.8, 31.2, 26.4, 22.7, 22.6, 14.2; TOF-MS (ESI+) *m*/*z* $[M+Na]^+$ calculated for $C_{23}H_{34}O_3Na$ $(M+Na)^+$ 381.2400, found 381.2399.

General Procedure for Ring-Closing Metathesis.

Synthesis was done as previously published with modifications.[35]

To a flame-dried round-bottom flask equipped with a stir bar and argon inlet, (*S*/*R*)-2-((*S*/*R*)-1-(2,6-dimethoxy-4-pentylphenyl)allyl)-5-methylhex-5-enal (92 mg, 0.257 mmol) was dissolved in Et_2O (4.6 mL). To the reaction flask, Grubb's II catalyst (4.4 mg, 0.005 mmol, 2 mol %) and CuI (1.5 mg, 0.008 mmol, 3 mol %) were added, and the light red solution was purged with argon. The argon inlet was replaced with a reflux condenser, and the reaction was heated to 40 °C (oil bath temperature) for 3 h. The brown solution was directly added to a silica plug (4:1 hexanes:Et_2O) for purification.

(1R,2R)-2′,6′-Dimethoxy-5-methyl-4′-pentyl-1,2,3,4-tetrahydro-[1,1′-biphenyl]-2-Carbaldehyde.

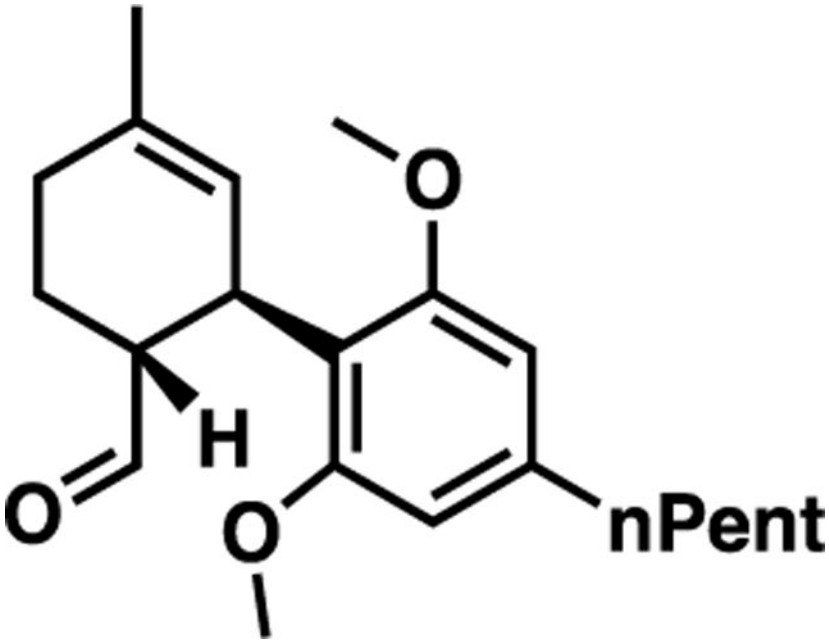

The general procedure was followed using *R*)-2-((*R*)-1-(2,6-dimethoxy-4-pentylphenyl)allyl)-5-methylhex-5-enal (92 mg, 0.257 mmol) to yield a brown oil (84.5 mg, 0.256 mmol, >99%).

Matched literature data.[35] R_f = 0.677 [hexanes:Et_2O (4:1)]; $[a]_D^{20}$ −111.0 (*c* 0.995, $CHCl_3$) (literature: $[a]^{25}_D$ −111.1 (*c* 1.0, $CHCl_3$)); ^{1}H NMR (500 MHz, chloroform-*d*) *δ* 9.51 (d, *J* = 2.4 Hz, 1H), 6.36 (s, 2H), 5.30–5.12 (m, 1H), 4.18 (ddt, *J* = 9.0, 4.4, 2.1 Hz, 1H), 3.75 (s, 6H), 2.96 (ddt, *J* = 12.5, 10.6, 2.8 Hz, 1H), 2.55 (dd, *J* = 8.9, 6.8 Hz, 2H), 2.22–2.09 (m, 1H), 2.09–1.95 (m, 2H), 1.69 (d, *J* = 2.2 Hz, 4H), 1.63 (q, *J* = 7.4 Hz, 2H), 1.35 (tt, *J* = 6.3, 3.7 Hz, 4H), 0.92 (t, *J* = 6.8 Hz, 3H). ^{13}C NMR (126 MHz, chloroform-*d*) *δ* 206.6, 158.6, 143.2, 131.5, 124.4, 116.4, 104.8, 55.9, 50.2, 36.6, 32.6, 31.8, 31.2, 29.0, 23.8, 23.5, 22.7, 14.2; TOF-MS (ESI+) *m*/*z* $[M+Na]^+$ calculated for $C_{21}H_{30}O_3Na$ $(M+Na)^+$ 353.2087, found 353.2089.

(1R,2S)-2′,6′-Dimethoxy-5-methyl-4′-pentyl-1,2,3,4-tetrahydro-[1,1′-biphenyl]-2-carbaldehyde.

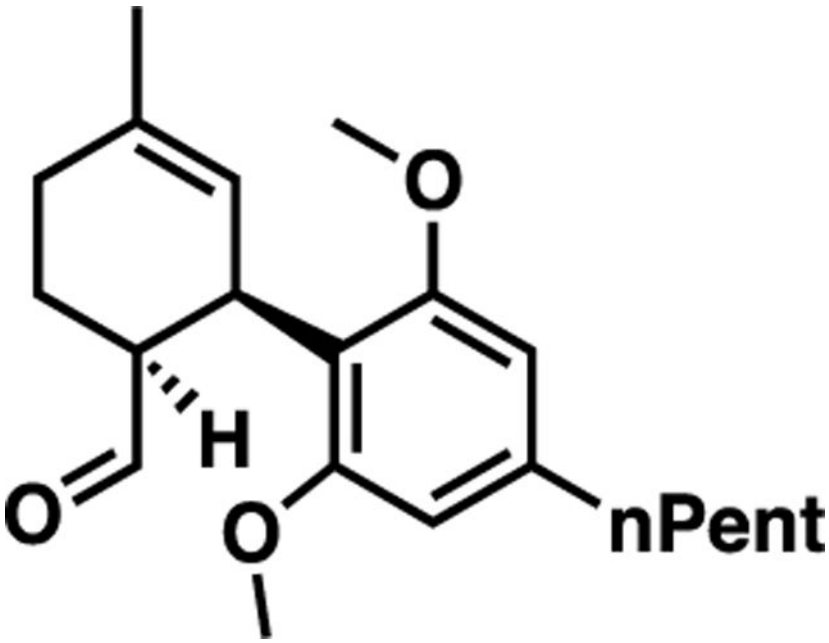

The general procedure was followed using (*S*)-2-((*R*)-1-(2,6-dimethoxy-4-pentylphenyl)allyl)-5-methylhex-5-enal (0.90 g, 2.5 mmol) to yield a brown oil (0.83 g, 2.51 mmol, 99%).

Matched literature data.[35] R_f = 0.357 [hexanes:Et_2O (9:1)]; $[a]_D^{20}$ −57.1 (*c* 1.04, $CHCl_3$) (literature: $[a]^{25}_D$ −46.4 (*c* 1.0, $CHCl_3$)); ^{1}H NMR (500 MHz, chloroform-*d*) *δ* 9.55 (d, *J* = 2.2 Hz, 1H), 6.36 (s, 2H), 5.42 (dq, *J* = 2.9, 1.6 Hz, 1H), 4.37 (dt, *J* = 5.6, 2.7 Hz, 1H), 3.74 (s, 6H), 2.69–2.44 (m, 3H), 2.32–2.10 (m, 2H), 2.03–1.79 (m, 2H), 1.77–1.66 (m, 3H), 1.66–1.55 (m, 2H), 1.35 (tt, *J* = 6.0, 3.5 Hz, 4H), 0.91 (t, *J* = 6.8 Hz, 3H). ^{13}C NMR (126 MHz, chloroform-*d*) *δ* 206.8, 158.5, 143.4, 130.6, 124.5, 115.4, 104.6, 55.7, 49.2, 36.6, 33.1, 31.8, 31.2, 27.1, 23.8, 23.4, 22.7, 14.2; TOF-MS (ESI+) *m*/*z* $[M+Na]^+$ calculated for $C_{21}H_{30}O_3Na$ $(M+Na)^+$ 353.2087, found 353.2087.

(1S,2R)-2′,6′-Dimethoxy-5-methyl-4′-pentyl-1,2,3,4-tetrahydro-[1,1′-biphenyl]-2-carbaldehyde.

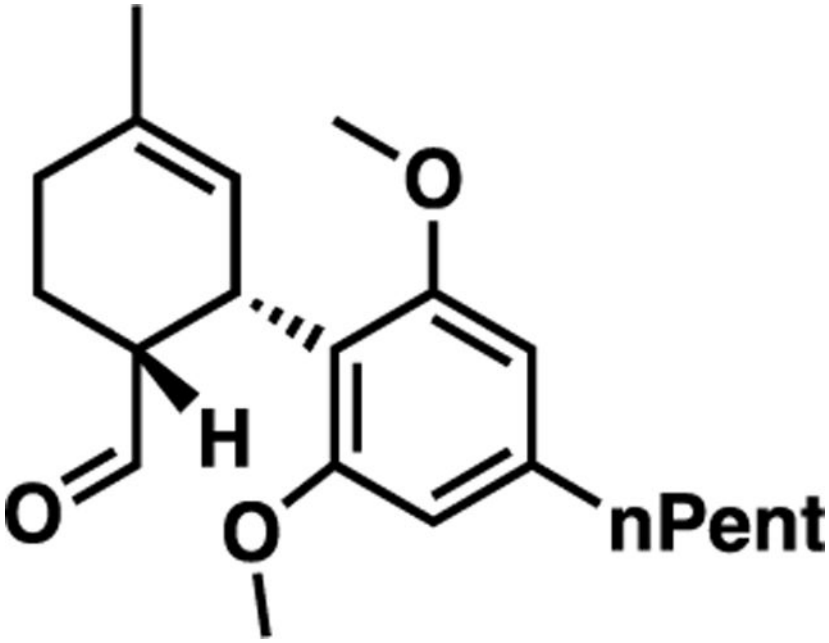

The general procedure metathesis was followed using (*R*)-2-((*S*)-1-(2,6-dimethoxy-4-pentylphenyl)allyl)-5-methylhex-5-enal (600 mg, 1.67 mmol) to yield a clear, light brown oil (550 mg, 1.67 mmol, >99%).

Matched literature data.[35] R_f = 0.528 [hexanes:Et_2O (4:1)]; $[a]_D^{20}$ +53.1 (*c* 1.04, $CHCl_3$) (literature: $[a]^{25}_D$ +50.9 (*c* 1.0, $CHCl_3$); ^{1}H NMR (500 MHz, chloroform-*d*) *δ* 9.54 (d, *J* = 2.3 Hz, 1H), 6.35 (d, *J* = 2.1 Hz, 2H), 5.42 (d, *J* = 3.0 Hz, 1H), 4.37 (dt, *J* = 5.3, 2.8 Hz, 1H), 3.73 (d, *J* = 2.1 Hz, 6H), 2.56 (qd, *J* = 7.9, 7.5, 2.5 Hz, 3H), 2.34–2.12 (m, 2H), 2.02–1.79 (m, 2H), 1.68 (t, *J* = 2.0 Hz, 3H), 1.61 (t, *J* = 7.3 Hz, 2H), 1.34 (pt, *J* = 8.2, 5.9, 4.0 Hz, 4H), 0.91 (td, *J* = 7.0, 2.2 Hz, 3H). ^{13}C NMR (126 MHz, chloroform-*d*) *δ* 206.8, 158.5, 143.4, 130.6, 124.5, 115.4, 104.6, 77.2, 55.7, 49.2, 36.6, 33.1, 31.8, 31.2, 27.1, 23.8, 23.4, 22.7, 14.2; TOF-MS (ESI+) *m*/*z* $[M+Na]^+$ calculated for $C_{21}H_{30}O_3Na$ $(M+Na)^+$ 353.2087, found 353.2089.

(1S,2S)-2′,6′-Dimethoxy-5-methyl-4′-pentyl-1,2,3,4-tetrahydro-[1,1′-biphenyl]-2-carbaldehyde.

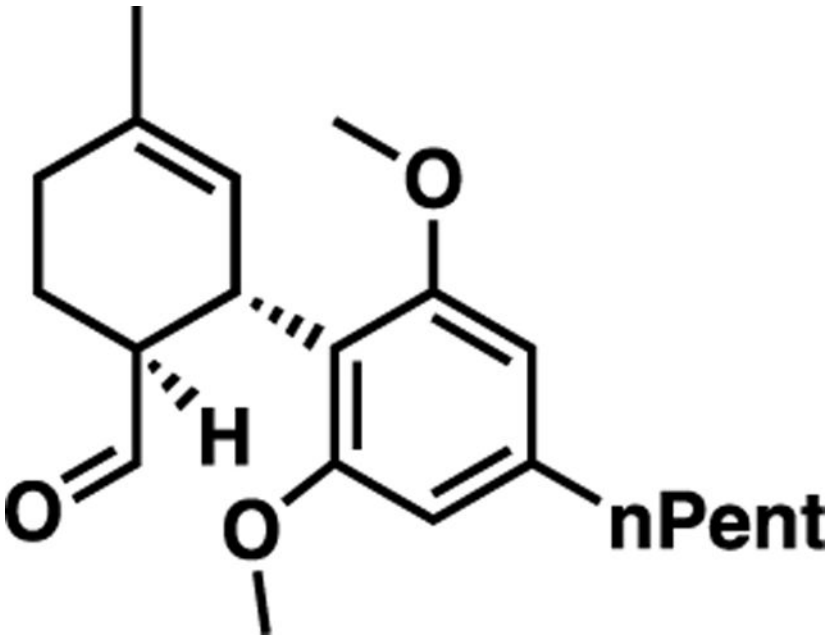

The general procedure was followed using (*S*)-2-((*S*)-1-(2,6-dimethoxy-4-pentylphenyl)allyl)-5-methylhex-5-enal (780 mg, 2.18 mmol) to yield a clear brown oil (710 mg, 2.15 mmol, 99%).

Matched literature data.[35] R_f = 0.475 [hexanes:Et_2O (6:1)]; $[a]_D^{20}$ +124.7 (*c* 0.95, $CHCl_3$) (literature: $[a]^{25}_D$ +114.8 (*c* 1.0, $CHCl_3$); ^{1}H NMR (500 MHz, chloroform-*d*) *δ* 9.50 (d, *J* = 2.4 Hz, 1H), 6.36 (s, 2H), 5.19 (dt, *J* = 2.3, 1.2 Hz, 1H), 4.24–4.10 (m, 1H), 3.75 (s, 6H), 2.96 (ddt, *J* = 12.3, 10.6, 2.8 Hz, 1H), 2.59–2.51 (m, 2H), 2.23–2.07 (m, 1H), 2.07–1.96 (m, 2H), 1.68 (dt, *J* = 2.7, 1.3 Hz, 4H), 1.64–1.56 (m, 2H), 1.41–1.29 (m, 4H), 0.91 (t, *J* = 6.9 Hz, 2H). ^{13}C NMR (126 MHz, chloroform-*d*) *δ* 206.7, 158.6, 143.3, 131.5, 124.4, 116.5, 104.8, 55.9, 50.2, 36.7, 32.7, 31.8, 31.2, 29.1, 23.8, 23.5, 22.7, 14.2; TOF-MS (ESI+) *m*/*z* $[M+Na]^+$ calculated for $C_{21}H_{30}O_3Na$ $(M+Na)^+$ 353.2087, found 353.2088.

General Procedure for Homologation.

To a flame-dried round-bottom flask under an inert atmosphere, triphenylphosphine (2.19 g, 8.36 mmol) was dissovled in DCM (16.7 mL), and the reaction flask was cooled to 0 °C. Upon addition of CBr_4 (1.39 g, 4.18 mmol), the orange solution was warmed to room temperature for 30 min and then cooled back down to 0 °C. A solution of 2′,6′-dimethoxy-5-methyl-4′-pentyl-1,2,3,4-tetrahydro-[1,1′-biphenyl]-2-carbaldehyde (690 mg, 2.09 mmol) in DCM (0.3 mL) was added. The reaction aged at 0 °C until TLC [hexanes:Et_2O (6:1)] revealed complete conversion of starting material. To the vigorously stirring solution, cold hexanes were added, and a white precipitate (triphenylphosphine oxide) was produced. The mixture was filtered through a Celite plug and washed with cold hexanes (150 mL). The filtrate was concentrated, which precipitated more triphenylphosphine oxide.

The residue was redissolved in cold hexanes (100 mL), filtered through a Celite plug, and concentrated again. The crude oil was dissolved in THF (6 mL), and the reaction flask was cooled to −78 °C. Upon complete addition of ^{n}BuLi (1.69 mL, 4.18 mmol, 2.48 M in hexanes), the reaction aged at −78 °C until TLC [5% Et_2O in petroleum ether] revealed complete conversion of the crude intermediate. The solution was quenched with saturated aqueous NH_4Cl (100 mL), and the solution was diluted with Et_2O (80 mL). The layers were separated, and the aqueous layer was washed with Et_2O (3 × 50 mL). Combined organic layers were washed with brine (100 mL), dried over $MgSO_4$, and concentrated *in vacuo*. The crude oil was purified via flash column chromatography [petroleum ether ≥ 5% Et_2O in petroleum ether].

(1R,2R)-2-Ethynyl-2′,6′-dimethoxy-5-methyl-4′-pentyl-1,2,3,4-tetrahydro-1,1′-biphenyl.

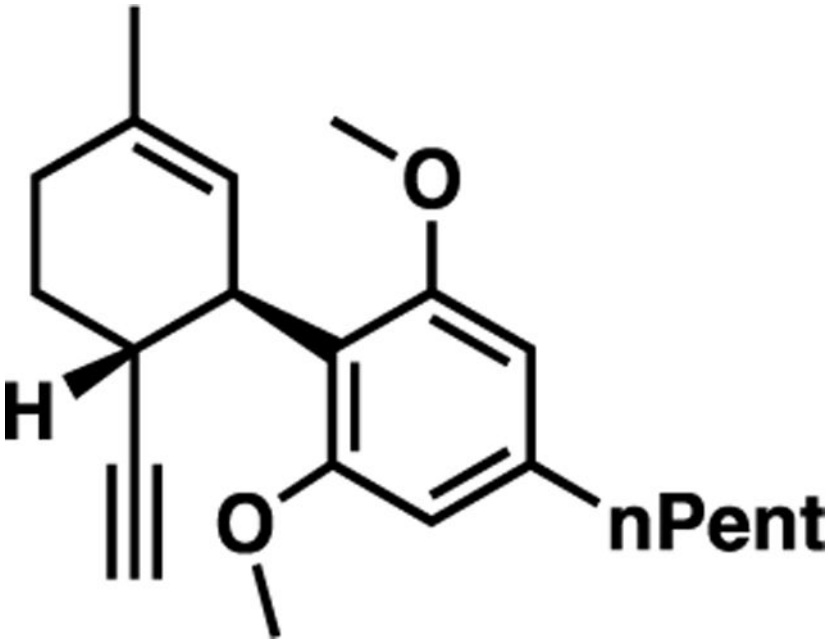

General procedure was followed using (1*R*,2*R*)-2′,6′-dimethoxy-5-methyl-4′-pentyl-1,2,3,4-tetrahydro-[1,1′-biphenyl]-2-carbaldehyde (300 mg, 0.91 mmol), and purification produced an off-white solid (296 mg, 0.907 mmol, 90%).

R_f = 0.714 [hexanes:Et_2O (9:1)]; $[a]_D^{20}$ −133.5 (*c* 1.105, $CHCl_3$); ^{1}H NMR (500 MHz, chloroform-*d*) *δ* 6.40 (d, *J* = 2.1 Hz, 2H), 5.18 (s, 1H), 4.23–4.00 (m, 1H), 3.79 (s, 6H), 3.15 (tt, *J* = 7.7, 4.0 Hz, 1H), 2.69–2.49 (m, 2H), 2.15 (t, *J* = 2.6 Hz, 1H), 2.07–1.78 (m, 3H), 1.68 (d, *J* = 8.5 Hz, 6H), 1.52–1.20 (m, 4H), 1.04–0.82 (m, 3H). ^{13}C NMR (101 MHz, chloroform-*d*) *δ* 158.9, 142.7, 131.1, 124.9, 117.9, 105.3, 88.9, 67.5, 56.2, 37.9, 36.6, 31.9, 31.2, 30.7, 29.9, 29.6, 23.5, 22.7, 14.2; TOF-MS (ESI+) *m*/*z* $[M+Na]^+$ calculated for $C_{22}H_{30}O_2Na$ $(M+Na)^+$ 349.2138, found 349.2139.

(1R,2S)-2-Ethynyl-2′,6′-dimethoxy-5-methyl-4′-pentyl-1,2,3,4-tetrahydro-1,1′-biphenyl.

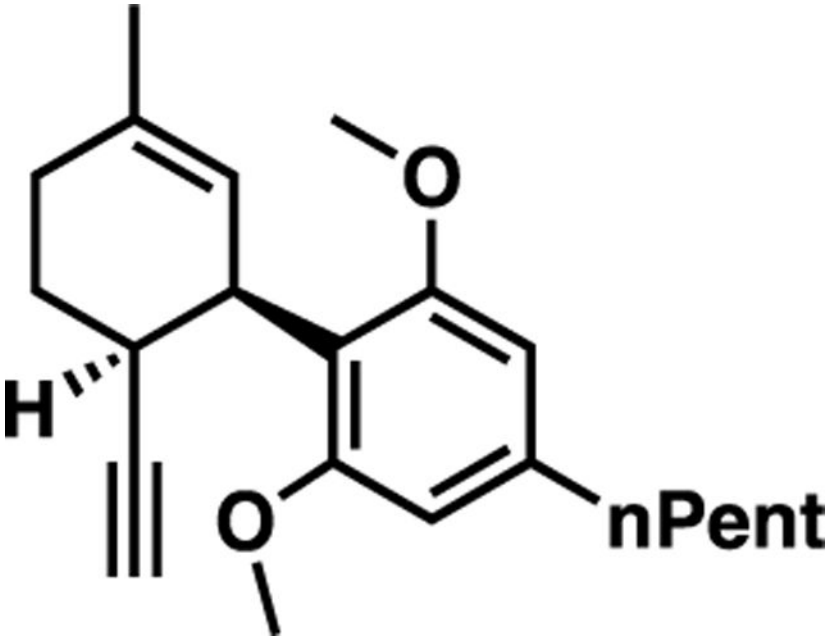

General procedure was followed using (1*R*,2*S*)-2′,6′-dimethoxy-5-methyl-4′-pentyl-1,2,3,4-tetrahydro-[1,1′-biphenyl]-2-carbaldehyde (0.50 g, 1.51 mmol), and purification produced a clear colorless oil (368 mg, 1.13 mmol, 75%).

R_f = 0.667 [hexanes:Et_2O (6:1)]; ^{1}H NMR (500 MHz, chloroform-*d*) δ 6.37 (s, 2H), 5.47 (s, 1H), 4.10 (dq, *J* = 5.5, 2.7 Hz, 1H), 3.73 (s, 6H), 3.00 (dq, *J* = 6.2, 3.0 Hz, 1H), 2.56 (t, *J* = 7.9 Hz, 3H), 2.42–2.24 (m, 1H), 2.11–1.97 (m, 1H), 1.97–1.81 (m, 3H), 1.74 (d, *J* = 11.0 Hz, 4H), 1.63 (t, *J* = 7.7 Hz, 3H), 1.35 (p, *J* = 4.0 Hz, 5H), 0.99–0.81 (m, 4H). ^{13}C NMR (151 MHz, chloroform-*d*) δ 159.3, 142.7, 129.3, 124.3, 116.6, 104.9, 87.3, 67.6, 55.9, 36.7, 35.7, 31.9, 31.2, 30.3, 28.3, 27.2, 23.9, 22.8, 14.2; TOF-MS (APCI+) *m*/*z* $[M+H]^+$ calculated for $C_{22}H_{31}O_2$ $(M+H)^+$ 327.2319, found 327.2320.

(1S,2R)-2-Ethynyl-2′,6′-dimethoxy-5-methyl-4′-pentyl-1,2,3,4-tetrahydro-1,1′-biphenyl.

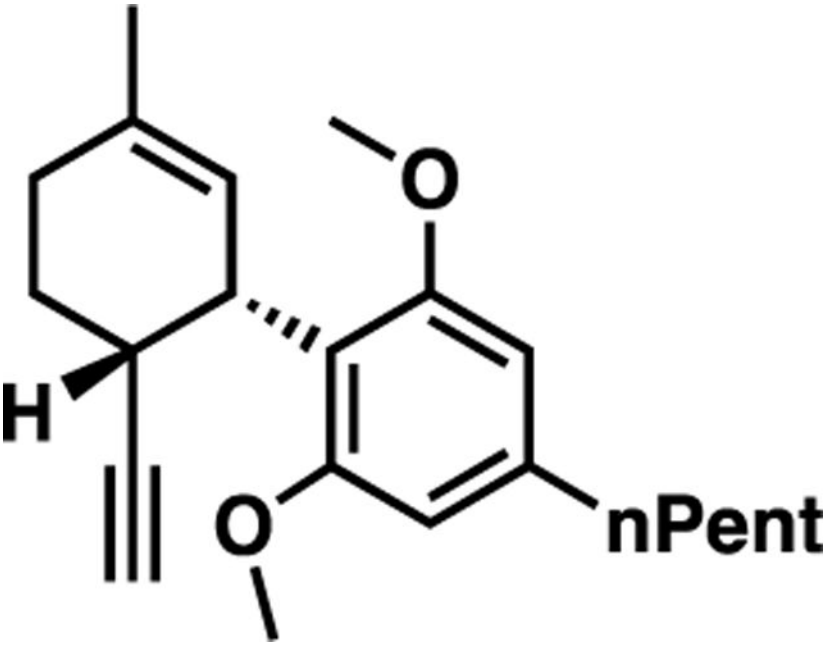

General procedure was followed using (1*S*,2*R*)-2′,6′-dimethoxy-5-methyl-4′-pentyl-1,2,3,4-tetrahydro-[1,1′-biphenyl]-2-carbaldehyde (0.69 g, 2.09 mmol), and purification produced a clear colorless oil (337 mg, 1.03 mmol, 50%).

R_f = 0.667 [hexanes:Et_2O (6:1)]; ^{1}H NMR (500 MHz, chloroform-*d*) δ 6.37 (d, J = 3.3 Hz, 2H), 5.47 (dq, J = 3.0, 1.5 Hz, 1H), 4.11 (dq, J = 5.8, 2.7 Hz, 1H), 3.74 (d, J = 7.4 Hz, 6H), 3.00 (dq, J = 6.1, 3.0 Hz, 1H), 2.66–2.49 (m, 2H), 2.40–2.26 (m, 1H), 2.04 (dtd, J = 12.7, 6.8, 6.3, 2.5 Hz, 1H), 1.96–1.82 (m, 2H), 1.80–1.68 (m, 4H), 1.68–1.56 (m, 2H), 1.35 (dt, J = 8.9, 3.1 Hz, 4H), 0.98–0.83 (m, 3H). ^{13}C NMR (126 MHz, chloroform-*d*) δ 159.3, 142.7, 129.3, 124.3, 116.6, 104.9, 87.3, 67.7, 56.0, 36.7, 35.7, 31.9, 31.2, 30.3, 28.3, 27.2, 23.9, 22.8, 14.2; TOF-MS (GC) m/z $[M+H]^+$ calculated for $C_{22}H_{31}O_2$ $(M+H)^+$ 327.2319, found 327.2315.

(1S,2S)-2-Ethynyl-2′,6′-dimethoxy-5-methyl-4′-pentyl-1,2,3,4-tetrahydro-1,1′-biphenyl.

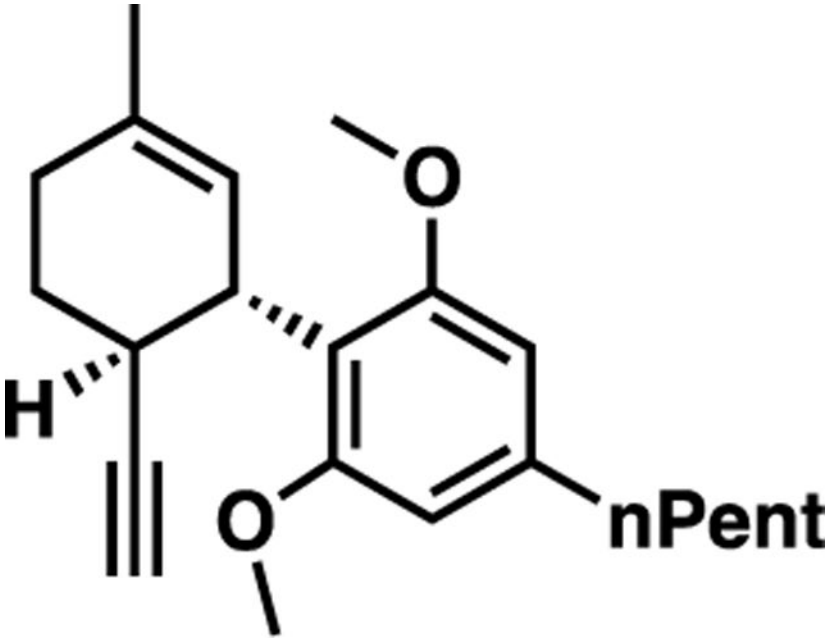

General procedure was followed using (1*S*,2*S*)-2′,6′-dimethoxy-5-methyl-4′-pentyl-1,2,3,4-tetrahydro-[1,1′-biphenyl]-2-carbaldehyde (355 mg, 1.075 mmol), and purification produced an off-white solid (308 mg, 0.944 mmol, 88%).

R_f = 0.418 [hexanes:Et_2O (9:1)]; $[a]_D^{20}$ +117.0 (*c* 0.950, $CHCl_3$); ^1H NMR (500 MHz, chloroform) δ 6.38 (s, 2H), 5.16 (s, 1H), 4.05 (d, *J* = 10.3 Hz, 1H), 3.76 (s, 6H), 3.19–3.04 (m, 1H), 2.61–2.49 (m, 2H), 2.16–2.07 (m, 2H), 2.01–1.91 (m, 1H), 1.89–1.74 (m, 2H), 1.70–1.57 (m, 5H), 1.41–1.28 (m, 4H), 0.97–0.83 (m, 3H). ^{13}C NMR (126 MHz, chloroform-*d*) δ 159.0, 142.7, 131.2, 124.9, 118.0, 105.3, 89.0, 67.6, 56.3, 37.9, 36.7, 31.9, 31.2, 30.7, 29.9, 29.6, 23.6, 22.7, 14.2; TOF-MS (ESI+) *m*/*z* $[M+Na]^+$ calculated for $C_{22}H_{30}O_2Na$ $(M+Na)^+$ 349.2138, found 349.2135.

General Procedure for Carboalumination.

To a flame-dried round-bottom flask under an inert atmosphere and equipped with a stir bar, Cp_2ZrCl_2 (552 mg, 1.89 mmol) was dissolved in DCE (4.7 mL). The reaction flask was cooled to 0 °C, and then Me_3Al (543 mL, 5.66 mmol, neat) was added dropwise. Upon complete addition, (1*S*/*R*,2*S*/*R*)-2-ethynyl-2′,6′-dimethoxy-5-methyl-4′-pentyl-1,2,3,4-tetrahydro-1,1′-biphenyl (308 mg, 0.944 mmol) was added to the pale-yellow solution. The ice bath was removed, and the reaction was stirred at room temperature for 20 h. The reaction was cooled to 0 °C and quenched with water (10 mL) that was added very slowly. The layers were separated, and the aqueous layer was washed with Et_2O (3 × 20 mL). Combined organic layers were washed with brine (50 mL), dried over $MgSO_4$, and concentrated *in vacuo*. Crude oil was purified via flash column chromatography [petroleum ether ≥ petroleum ether:Et_2O (98:2)].

(1R,2R)-2′,6′-Dimethoxy-5-methyl-4′-pentyl-2-(prop-1-en-2-yl)-1,2,3,4-tetrahydro-1,1′-biphenyl.

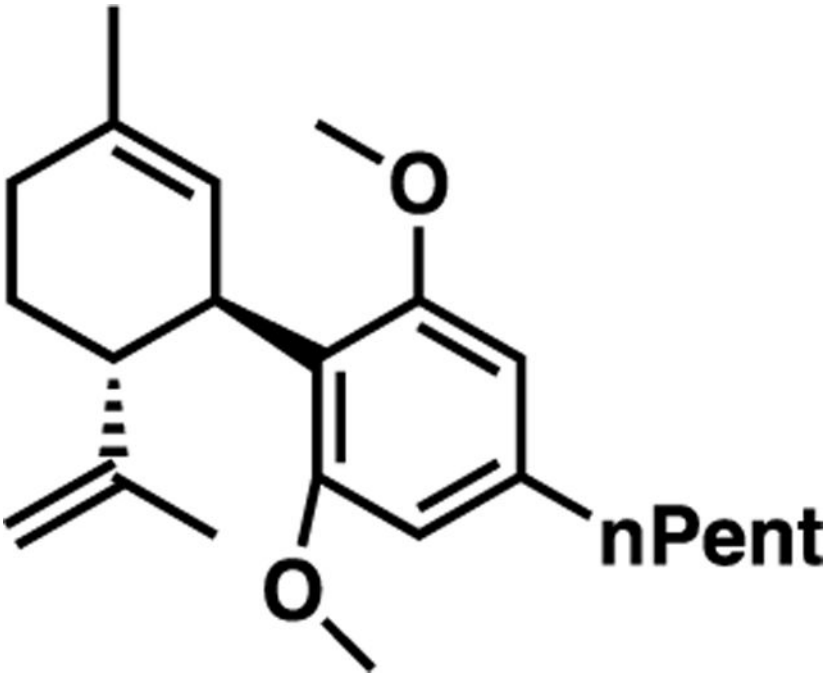

The general procedure was followed using (1*R*,2*R*)-2-ethynyl-2′,6′-dimethoxy-5-methyl-4′-pentyl-1,2,3,4-tetrahydro-1,1′-biphenyl (308 mg, 0.944 mmol) to produce a clear, yellow oil (233 mg, 0.681 mmol, 55%).

R_f = 0.794 [hexanes:Et_2O (9:1)]; $[a]_D^{20}$ −175.5 (*c* 1.14, $CHCl_3$); ^{1}H NMR (500 MHz, chloroform-*d*) *δ* 6.38 (s, 2H), 5.16 (s, 1H), 4.05 (d, *J* = 10.3 Hz, 1H), 3.76 (s, 6H), 3.22–3.02 (m, 1H), 2.61–2.49 (m, 2H), 2.20–2.05 (m, 2H), 1.95 (dd, *J* = 15.7, 5.9 Hz, 1H), 1.88–1.75 (m, 2H), 1.64 (d, *J* = 12.3 Hz, 6H), 1.41–1.29 (m, 3H), 0.97–0.83 (m, 3H). ^{13}C NMR (126 MHz, chloroform-*d*) *δ* 149.5, 141.9, 131.2, 125.9, 118.9, 109.6, 55.9, 45.2, 36.4, 36.1, 31.7, 31.0, 30.8, 29.7, 23.5, 22.6, 19.1, 14.1; TOF-MS (ESI+) *m*/*z* $[M+Na]^+$ calculated for $C_{23}H_{34}O_2Na$ $(M+Na)^+$ 365.2451, found 365.2452.

(1S,2S)-2′,6′-Dimethoxy-5-methyl-4′-pentyl-2-(prop-1-en-2-yl)-1,2,3,4-tetrahydro-1,1′-biphenyl.

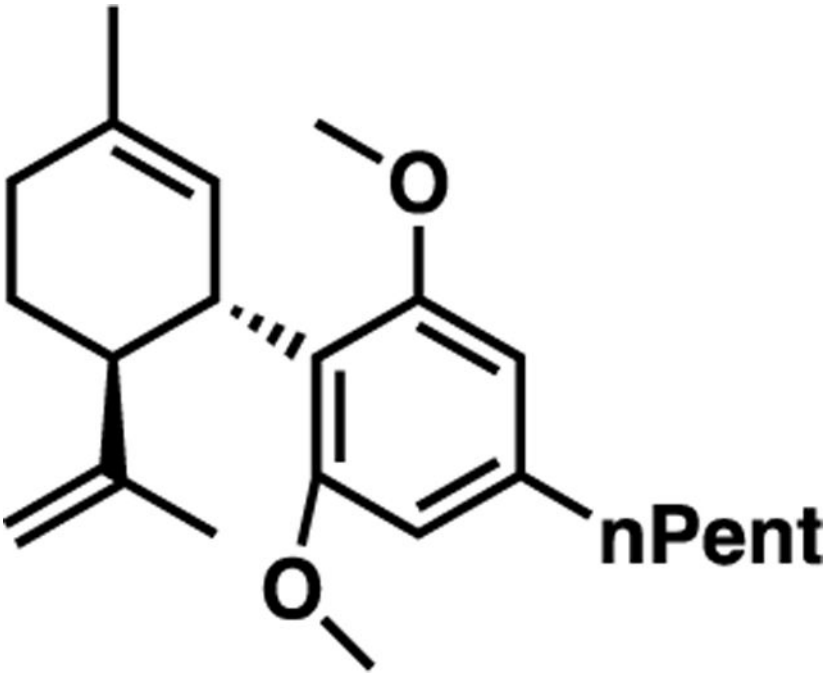

The general procedure was followed using (1*S*,2*S*)-2-ethynyl-2′,6′-dimethoxy-5-methyl-4′-pentyl-1,2,3,4-tetrahydro-1,1′-biphenyl (108 mg, 0.33 mmol) to produce a clear, light yellow oil (59 mg, 0.172 mmol, 55%).

R_f = 0.794 [hexanes:Et_2O (9:1)]; $[a]_D^{20}$ +121.8 (*c* 1.00, $CHCl_3$); ^{1}H NMR (500 MHz, chloroform-*d*) *δ* 6.34 (d, *J* = 1.9 Hz, 2H), 5.22 (s, 1H), 4.44 (dt, *J* = 9.9, 2.1 Hz, 2H), 4.00 (ddt, *J* = 8.9, 4.6, 2.3 Hz, 1H), 3.74 (d, *J* = 1.9 Hz, 6H), 3.02–2.81 (m, 1H), 2.54 (td, *J* = 7.8, 1.9 Hz, 2H), 2.26–2.12 (m, 1H), 2.04–1.93 (m, 1H), 1.82–1.70 (m, 2H), 1.68 (s, 3H), 1.61 (s, 5H), 1.35 (qt, *J* = 7.3, 3.2 Hz, 4H), 0.91 (td, *J* = 7.0, 2.1 Hz, 3H). ^{13}C NMR (126 MHz, chloroform-*d*) *δ* 149.7, 142.0, 131.3, 126.1, 119.1, 109.7, 56.1, 45.4, 36.6, 36.3, 36.3, 31.9, 31.2, 30.9, 29.9, 23.6, 22.7, 19.2, 14.2; TOF-MS (+EI-EIC) *m*/*z* $[M]^+$ calculated for $C_{23}H_{34}O_2$ $(M)^+$ 342.256, found 365.2554.

General Procedure for Demethylation of Antidiastereomers.

To a flame-dried round-bottom flask under an inert atmosphere, (1*S*/*R*,2*S*/*R*)-2′,6′-dimethoxy-5-methyl-4′-pentyl-2-(prop-1-en-2-yl)-1,2,3,4-tetrahydro-1,1′-biphenyl (100 mg, 0.292 mmol) was dissolved in hexanes (6 mL). To the reaction flask at room temperature, 9-I-9-BBN (0.614 mL, 0.614 mmol, 1 M in hexanes) was added dropwise, and the red-orange solution aged for 1 h. TLC revealed full conversion of starting material. Volatile compounds were removed under reduced pressure, and the orange/red residue was redissolved in Et_2O (10 mL). Ethanolamine (0.039 mL, 0.642 mmol) was added dropwise, and a white solid (ethanolamine-9-BBN complex) precipitated out. The reaction stirred for an additional hour. The mixture was filtered, and the filtrate was concentrated *in vacuo*.

Characterization via GCMS revealed a complete didemethylated product. The crude oil was purified via flash column chromatography (4:1 hexanes:Et_2O).

(1′R,2′R)-5′-Methyl-4-pentyl-2′-(prop-1-en-2-yl)-1′,2′,3′,4′-tetrahydro-[1,1′-biphenyl]-2,6-diol (Synthetic (–)-CBD or JGC17).

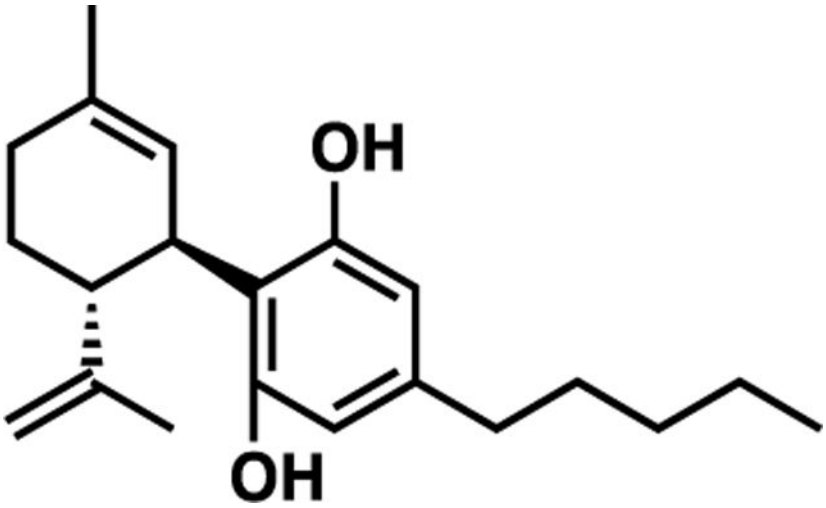

General procedure was followed using (1*R*,2*R*)-2′,6′-dimethoxy-5-methyl-4′-pentyl-2-(prop-1-en-2-yl)-1,2,3,4-tetrahydro-1,1′-biphenyl (100 mg, 0.292 mmol) to produce a clear, colorless oil (50 mg, 0.159 mmol, 54%).

Matched literature data.[47] R_f = 0.468 [hexanes:Et_2O (4:1)]; $[a]_D^{20}$ −75.6 (*c* 0.766, $CHCl_3$); ^1H NMR (500 MHz, chloroform-*d*) *δ* 6.13–6.08 (m, 2H), 5.91 (s, 1H), 5.49 (d, *J* = 2.8 Hz, 1H), 4.72 (s, 1H), 4.57 (t, *J* = 1.8 Hz, 1H), 4.48 (d, *J* = 2.0 Hz, 1H), 3.78 (ddq, *J* = 9.2, 4.6, 2.3 Hz, 1H), 2.45–2.26 (m, 3H), 2.24–2.08 (m, 1H), 2.01 (ddt, *J* = 17.9, 5.0, 2.3 Hz, 1H), 1.83–1.64 (m, 5H), 1.58 (s, 3H), 1.47 (p, *J* = 7.5 Hz, 2H), 1.31–1.11 (m, 5H), 0.80 (t, *J* = 6.9 Hz, 3H). ^{13}C NMR (126 MHz, chloroform-*d*) *δ* 154.1, 148.2, 141.9, 138.9, 123.1, 112.8, 112.8, 109.8, 107.9, 76.3, 45.2, 36.2, 34.5, 30.5, 29.6, 29.4, 27.4, 22.6, 21.5, 19.4, 13.0; TOF-MS (ESI+) *m*/*z* $[M+H]^+$ calculated for $C_{21}H_{31}O_2$ $(M+H)^+$ 315.2319, found 315.2318.

(1′S,2′)-5′-Methyl-4-pentyl-2′-(prop-1-en-2-yl)-1′,2′,3′,4′-tetrahydro-[1,1′-biphenyl]-2,6-diol (Synthetic (+)-CBD or JGC18).

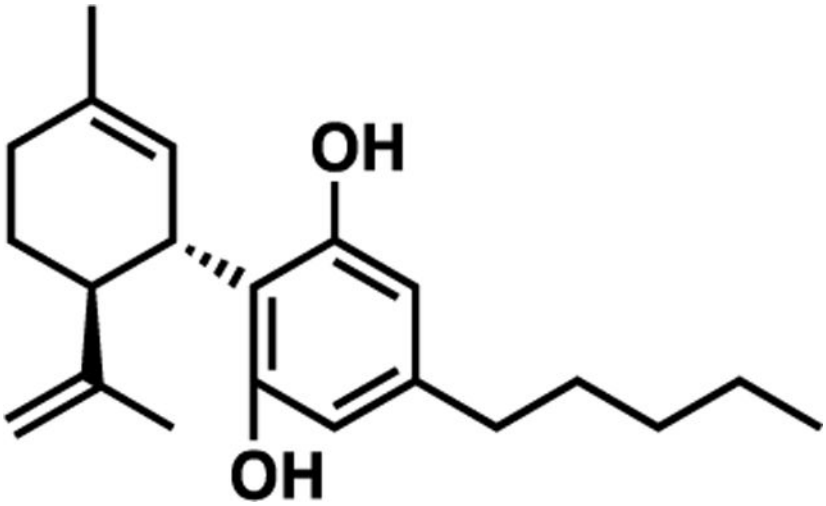

General procedure was followed using (1*S*,2*S*)-2′,6′-dimethoxy-5-methyl-4′-pentyl-2-(prop-1-en-2-yl)-1,2,3,4-tetrahydro-1,1′-biphenyl (50 mg, 0.146 mmol) to produce a clear, colorless oil (18 mg, 0.057 mmol, 39%).

Matched literature data.[50,57] R_f = 0.468 [hexanes:Et_2O (4:1)]; $[a]_D^{20}$ +74.9 (*c* 0.810, $CHCl_3$); ^{1}H NMR (500 MHz, chloroform-*d*) *δ* 6.41–6.08 (m, 2H), 5.97 (s, 1H), 5.57 (dt, *J* = 2.9, 1.6 Hz, 1H), 4.66 (p, *J* = 1.6 Hz, 1H), 4.56 (d, *J* = 2.0 Hz, 1H), 3.90–3.80 (m, 1H), 2.49–2.33 (m, 3H), 2.32–2.17 (m, 1H), 2.10 (ddt, *J* = 17.8, 5.0, 2.4 Hz, 1H), 1.90–1.70 (m, 6H), 1.66 (t, *J* = 1.1 Hz, 3H), 1.56 (p, *J* = 7.6 Hz, 2H), 1.41–1.18 (m, 4H), 0.88 (t, *J* = 7.0 Hz, 3H). ^{13}C NMR (126 MHz, chloroform-*d*) *δ* 154.1, 149.5, 143.2, 140.2, 124.3, 113.9, 110.9, 108.2, 46.3, 37.4, 35.6, 31.7, 30.8, 30.6, 28.6, 23.8, 22.7, 20.7, 14.2; TOF-MS (EI+) *m*/*z* $[M]^+$ calculated for $C_{21}H_{30}O_2$ $(M)^+$ 314.2240, found 314.2242.

General Procedure for Demethylation and Iodoborylation of Syn-Diastereomers.

To a flame-dried round-bottom flask under an inert atmosphere, 2-ethynyl-2′,6′-dimethoxy-5-methyl-4′-pentyl-1,2,3,4-tetrahydro-1,1′-biphenyl (590 mg, 1.81 mmol) was dissolved in DCM (36.2 mL) and the reaction solution was cooled to 0 °C. 9-I-9-BBN (1 M in hexanes, 5.79 mL, 5.79 mmol) was added dropwise to the stirring solution. Upon complete addition, the deep red solution aged at 0 °C for 6 h. TLC [hexanes:Et_2O (7:1)] revealed complete conversion of starting material. Glacial acetic acid (2 mL) was added to the cooled solution and aged for 1 h. Aqeous NaOH (15%, 20 mL) and H_2O_2 (30%, 4 mL) were added slowly, and the blue reaction solution was warmed to room temperature and aged for 30 min. The aqeous solution was extracted with hexanes (3 × 80 mL), and the combined organic layers were washed with water (50 mL), saturated aquous $NaHCO_3$ (50 mL), and brine (50 mL), dried over $MgSO_4$, and concentrated *in vacuo*. The orange residue was purified via flash column chromatography [hexanes à hexanes:Et_2O (94:6)]. Upon characterization by NMR, unexpected ring closure occurred to yield the following

products, not the desired 2′-(1-iodovinyl)-5′-methyl-4-pentyl-1′,2′,3′,4′-tetrahydro-[1,1′-biphenyl]-2,6-diol enantiomers.

(2R,5S,6R)-5-(1-Iodovinyl)-2-methyl-9-pentyl-3,4,5,6-tetrahydro-2H-2,6-methanobenzo[b]oxocin-7-ol (JGC21).

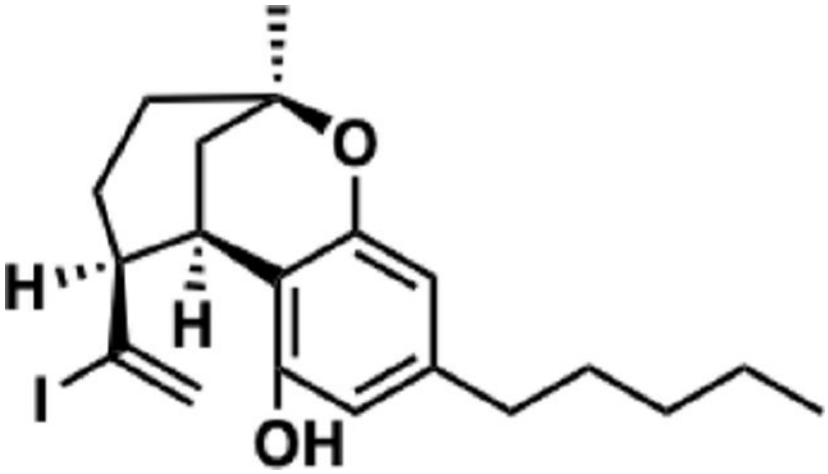

The general procedure was followed using (1*R*,2*S*)-2-ethynyl-2′,6′-dimethoxy-5-methyl-4′-pentyl-1,2,3,4-tetrahydro-1,1′-biphenyl (590 mg, 1.81 mmol) to produce a white solid (371 mg, 0.871 mmol, 48%).

R_f = 0.451 [hexanes:Et_2O (7:1)]; ^{1}H NMR (500 MHz, chloroform-*d*) δ 6.31–6.22 (m, 1H), 6.19 (d, J = 1.6 Hz, 1H), 5.76 (d, J = 2.4 Hz, 1H), 5.71–5.64 (m, 1H), 4.70 (s, 1H), 3.56 (d, J = 3.1 Hz, 1H), 2.71 (d, J = 10.4 Hz, 1H), 2.51–2.39 (m, 2H), 1.98 (d, J = 10.4 Hz, 1H), 1.89 (dd, J = 3.3, 1.4 Hz, 2H), 1.66–1.54 (m, 5H), 1.53 (s, 1H), 1.37 (s, 3H), 1.30 (dp, J = 6.8, 4.3, 2.8 Hz, 4H), 0.88 (t, J = 6.8 Hz, 3H). ^{13}C NMR (126 MHz, chloroform-*d*) δ 157.4, 154.3, 143.7, 126.0, 114.8, 107.9, 107.2, 105.7, 73.9, 57.1, 39.5, 37.1, 35.8, 31.8, 31.2, 30.7, 28.6, 24.3, 22.7, 14.2; TOF-MS (+EI) m/z $[M]^+$ calculated for $C_{20}H_{27}O_2I$ $(M)^+$ 426.1050, found 426.1057.

(2S,5R,6S)-5-(1-Iodovinyl)-2-methyl-9-pentyl-3,4,5,6-tetrahydro-2H-2,6-methanobenzo[b]oxocin-7-ol (JGC22).

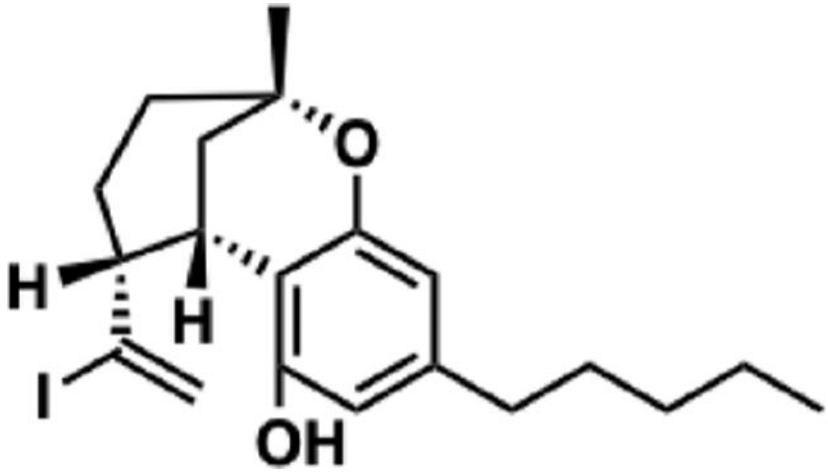

The general procedure was followed using (1*S*,2*R*)-2-ethynyl-2′,6′-dimethoxy-5-methyl-4′-pentyl-1,2,3,4-tetrahydro-1,1′-biphenyl (484 mg, 1.48 mmol) to produce a white solid (260 mg, 0.610 mmol, 42%).

R_f = 0.451 [hexanes:Et_2O (7:1)]; ^{1}H NMR (500 MHz, chloroform-*d*) δ 6.26 (d, J = 1.5 Hz, 1H), 6.19 (d, J = 1.6 Hz, 1H), 5.76 (d, J = 2.5 Hz, 1H), 5.68 (t, J = 1.9 Hz, 1H), 4.70 (s, 1H), 3.55 (s, 1H), 2.71 (d, J = 10.4 Hz, 1H), 2.51–2.37 (m, 2H), 1.98 (d, J = 10.5 Hz, 1H), 1.89 (d, J = 2.5 Hz, 2H), 1.55 (d, J = 22.9 Hz, 5H), 1.37 (s, 3H), 1.31 (q, J = 3.7, 3.3 Hz, 3H), 0.88 (t, J = 6.8 Hz, 3H). ^{13}C NMR (126 MHz, chloroform-*d*) δ 157.4, 154.3, 143.7, 126.0, 114.8, 107.9, 107.2, 105.7, 73.9, 57.1, 39.5, 37.1, 35.8, 31.8, 31.2, 30.7, 28.6, 24.3, 22.7, 14.2; TOF-MS (+ESI) *m*/*z* $[M+H]^+$ calculated for $C_{20}H_{28}O_2I$ $(M+H)^+$ 427.1128, found 427.1130.

General Procedure for Kumada Cross-Coupling.

To a flame-dried round-bottom flask under an inert atmosphere, tetrakis-(triphenylphosphine) palladium(0) (0.141 mmol, 163 mg) was added to a solution of 5-(1-iodovinyl)-2-methyl-9-pentyl-3,4,5,6-tetrahydro-2*H*-2,6-methanobenzo[*b*]oxocin-7-ol (300 mg, 0.704 mmol) in THF (7.04 mL). The reaction vessel was purged and aged at room temperature for 15 min before being cooled to −20 °C. MeMgBr (1.0 M in hexanes, 2.46 mL, 2.46 mmol) was added dropwise to the stirring yellow solution. Upon complete addition, the solution was warmed to room temperature and then further to 50 °C. The reaction was monitored by TLC [hexanes:Et_2O (7:1)], and after 2 h, the starting material was completely consumed. The orange solution was cooled to room temperature and then to 0 °C before quenching with aqueous saturated NH_4Cl (5 mL). The aqueous layer was extracted with ether (3 × 10 mL). The combined organic layers were washed with water (15 mL) and brine (15 mL), dried over $MgSO_4$, and concentrated *in vacuo*. The crude oil was purified via flash column chromatography [hexanes:Et_2O (100:0) → (95:5)].

(2R,5S,6R)-2-Methyl-9-pentyl-5-(prop-1-en-2-yl)-3,4,5,6-tetrahydro-2H-2,6-methanobenzo[b]oxocin-7-ol (JGC19).

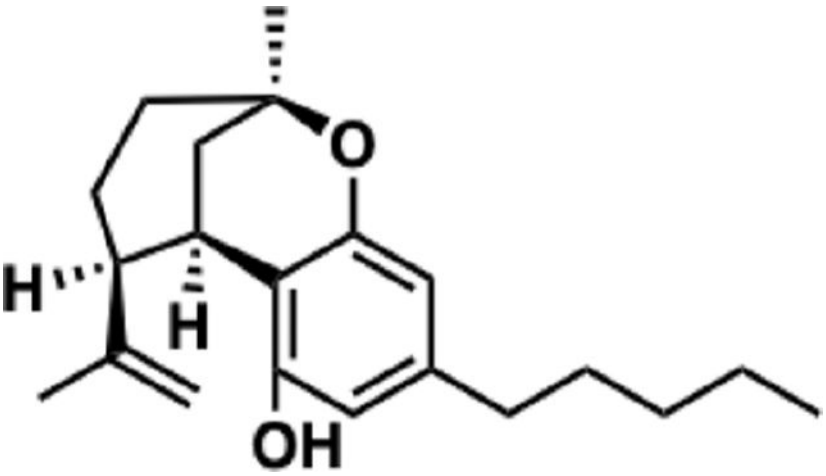

The general procedure was followed using (5a*R*,9*S*,9a*R*)-9-(1-iodovinyl)-6-methyl-3-pentyl-5a,6,7,8,9,9a-hexahydrodibenzo[*b*,*d*]-furan-1-ol (300 mg, 0.704 mmol) to produce a clear oil (128 mg, 0.408 mmol, 58%).

R_f = 0.440 [hexanes:Et_2O (7:1)]; ^{1}H NMR (500 MHz, chloroform-*d*) δ 6.29 (s, 1H), 6.19 (d, *J* = 1.6 Hz, 1H), 4.96–4.79 (m, 2H), 4.65 (s, 1H), 3.31 (q, *J* = 3.2 Hz, 1H), 2.46 (t, *J* = 7.8 Hz, 2H), 2.36 (dt, *J* = 11.8, 3.2 Hz, 1H), 2.02 (dq, *J* = 8.1, 2.9 Hz, 1H), 1.92 (dd, *J* = 12.9, 2.8 Hz, 1H), 1.82 (t, *J* = 3.1 Hz, 1H), 1.79 (s, 3H), 1.66–1.49 (m, 4H), 1.45 (d, *J* = 7.1 Hz, 1H), 1.37 (s, 3H), 1.32 (qd, *J* = 6.2, 4.1, 2.6 Hz, 4H), 0.89 (t, *J* = 6.7 Hz, 3H). ^{13}C NMR (126 MHz, chloroform-*d*) δ 157.2, 153.7, 150.0, 143.2, 111.7, 108.2, 108.1, 107.4, 73.9, 48.5, 39.7, 37.7, 35.8, 33.1, 33.1, 31.8, 30.8, 28.9, 23.0, 22.7, 22.6, 14.2; TOF-MS (EI+) *m*/*z* $[M]^+$ calculated for $C_{21}H_{30}O_2$ $(M)^+$ 314.2252, found 314.2246.

(2S,5R,6S)-2-Methyl-9-pentyl-5-(prop-1-en-2-yl)-3,4,5,6-tetrahydro-2H-2,6-methanobenzo[b]oxocin-7-ol (JGC20).

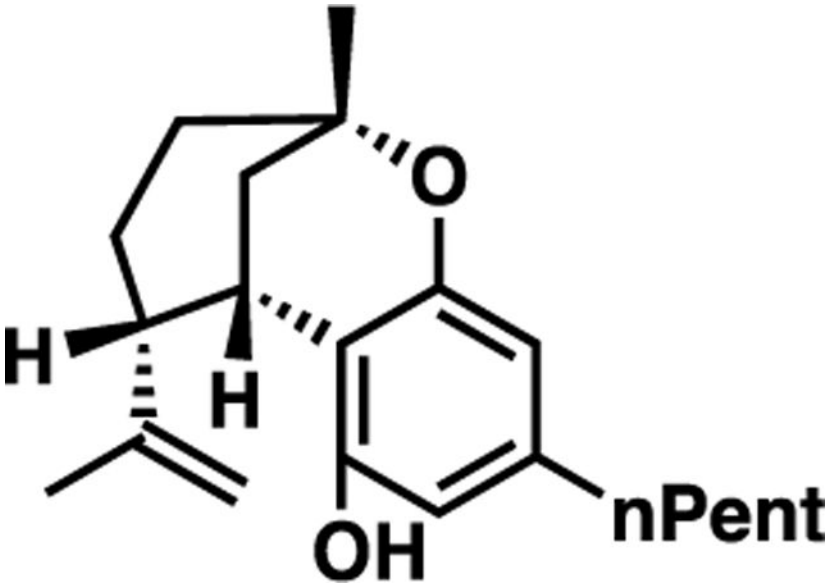

The general procedure was followed using (5a*S*,9*R*,9a*S*)-9-(1-iodovinyl)-6-methyl-3-pentyl-5a,6,7,8,9,9a-hexahydrodibenzo[*b*,*d*]-furan-1-ol (243 mg, 0.570 mmol) to produce a clear oil (107 mg, 0.341 mmol, 60%).

R_f = 0.440 [hexanes:Et_2O (7:1)]; ^{1}H NMR (500 MHz, chloroform-*d*) δ 6.29 (d, *J* = 1.5 Hz, 1H), 6.19 (d, *J* = 1.5 Hz, 1H), 4.94–4.80 (m, 2H), 4.65 (dt, *J* = 2.0, 1.0 Hz, 1H), 3.31 (q, *J* = 3.1 Hz, 1H), 2.51–2.41 (m, 2H), 2.36 (dt, *J* = 11.8, 3.3 Hz, 1H), 2.03 (dt, *J* = 9.0, 2.6 Hz, 1H), 1.92 (dd, *J* = 13.0, 2.8 Hz, 1H), 1.82 (t, *J* = 3.2 Hz, 1H), 1.79 (d, *J* = 1.3 Hz, 3H), 1.62–1.53 (m, 4H), 1.49–1.42 (m, 1H), 1.37 (s, 3H), 1.35–1.26 (m, *J* = 4.3 Hz, 4H), 0.89 (t, *J* = 6.8 Hz, 3H). ^{13}C NMR (126 MHz, chloroform-*d*) δ 157.2, 153.7, 150.0, 143.2, 111.7, 108.2, 108.1, 107.4, 73.9, 48.5, 39.7, 37.7, 35.8, 33.1, 31.8, 30.8, 28.9, 23.1, 22.7, 22.6, 14.2; TOF-MS (EI+) *m*/*z* $[M]^+$ calculated for $C_{21}H_{30}O_2$ $(M)^+$ 314.2252, found 314.2244.

Lipid Tail Derivatives of (–)-Cannabidiol.

Starting materials were synthesized as previously published with modifications.[30,31,55–57]

General Procedure of Negishi Cross-Coupling.

Synthesis was done as previously published.[30]

To a flame-dried round-bottom flask under an inert atmosphere, anhydrous $ZnCl_2$ (146 mg, 1.07 mmol) and LiCl (45 mg, 1.07 mmol) were dissolved in THF (5 mL). The reaction flask was cooled to −10 °C, and RMgBr or RLi (1.07 mmol) was added dropwise. The solution aged for 15 min at −10 °C, was warmed to room temperature, and then stirred for an additional 1.5 h. A solution of (1′*R*,2′*R*)-5′-methyl-2′-(prop-1-en-2-yl)-4-(((trifluoromethyl)sulfonyl)oxy)-1′,2′,3′,4′-tetrahydro-[1,1′-biphenyl]-2,6-diyl bis(2,2-dimethylpropanoate) (400 mg, 0.714 mmol) in

THF (3.6 mL) was added to the reaction flask; then, $Pd(dppf)Cl_2$ (58 mg, 0.0714 mmol) was added. The reaction flask was purged and then heated to 55–65 °C. The reaction was monitored via TLC [hexanes:Et_2O (9:1)]. NOTE: the change in color from yellow-orange to deep wine red normally indicated that the reaction was complete. Upon cooling to room temperature, the reaction was quenched with saturated aqueous NH_4Cl (5 mL). The aqueous solution was extracted with Et_2O (3 × 10 mL), and combined organic layers were washed with water (15 mL) and brine (15 mL), dried over $MgSO_4$, and concentrated *in vacuo*. Crude oil was purified via flash column chromatography.

(1′R,2′R)-4,5′-Dimethyl-2′-(prop-1-en-2-yl)-1′,2′,3′,4′-tetrahydro-[1,1′-biphenyl]-2,6-diyl Bis(2,2-dimethylpropanoate).

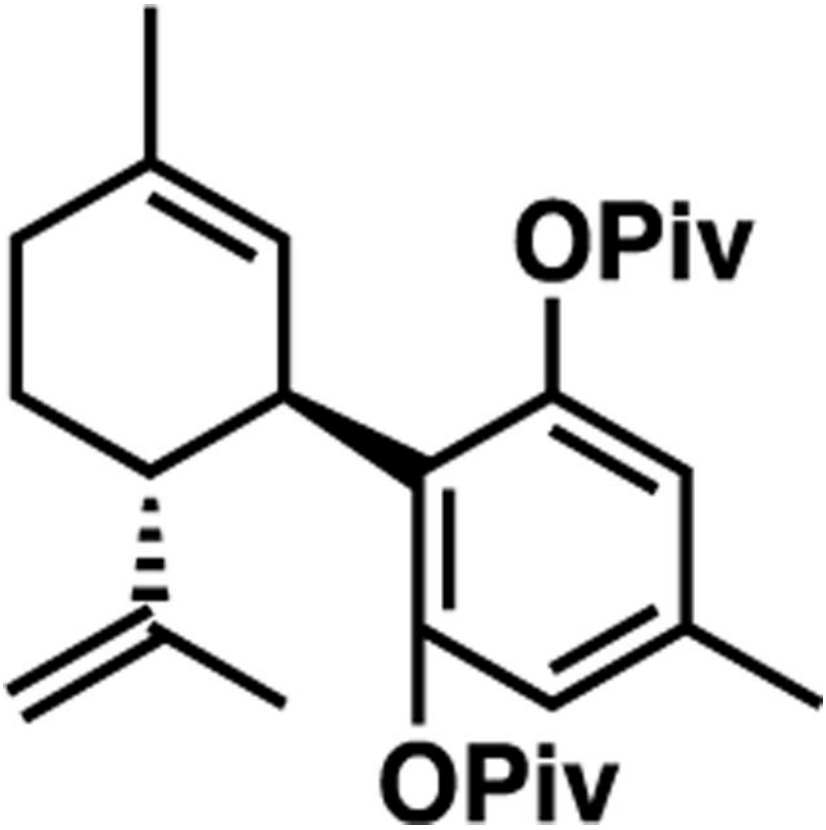

Synthesis was done as previously published with modification.[58]

To a flame-dried round-bottom flask under an inert atmosphere, $Pd(dppf)Cl_2$ (58 mg, 0.0714 mmol) was dissolved in THF (5 mL). The reaction flask was cooled to 0 °C, and DIBAL (1 M in hexanes, 14.5 mL, 0.0714 mmol) was added dropwise. The solution aged at 0 °C for 10 min; then, a solution of (1′*R*,2′*R*)-5′-methyl-2′-(prop-1-en-2-yl)-4-(((trifluoromethyl)sulfonyl)oxy)-1′,2′,3′,4′-tetrahydro-[1,1′-biphenyl]-2,6-diyl bis(2,2-dimethylpropanoate) (400 mg, 0.714 mmol) in THF (3.6 mL) was added and stirred for 15 min. $ZnMe_2$ (2 M in toluene, 0.54 mL, 1.07 mL) was added dropwise at 0 °C. Upon complete addition, the reaction flask was warmed to room temperature and then further heated to 65 °C, and the reaction was monitored

via TLC [hexanes:Et_2O (9:1)]. The wine-red solution was cooled to room temperature and quenched with saturated aqueous NH_4Cl. The aqueous layer was washed with Et_2O (3 × 10 mL). Combined organic layers were washed with water (15 mL) and brine (15 mL), dried over $MgSO_4$, and concentrated *in vacuo*. The crude oil was purified via flash column chromatography [hexanes:Et_2O (22:3)] to produce a clear, colorless oil (230 mg, 0.540 mmol, 76%).

Matched literature data.[30] R_f = 0.189 [hexanes:Et_2O (9:1)]; ^{1}H NMR (400 MHz, chloroform-*d*) δ 6.58 (s, 2H), 5.24 (t, J = 1.8 Hz, 1H), 4.55 (d, J = 1.4 Hz, 2H), 3.51 (ddq, J = 11.2, 4.6, 2.4 Hz, 1H), 2.67 (ddd, J = 12.9, 10.8, 2.7 Hz, 1H), 2.27 (s, 3H), 2.19–1.95 (m, 2H), 1.81 (ddt, J = 10.5, 6.1, 2.2 Hz, 1H), 1.77–1.65 (m, 1H), 1.60 (t, J = 1.8 Hz, 3H), 1.54 (d, J = 1.8 Hz, 3H), 1.33 (s, 18H). ^{13}C NMR (101 MHz, chloroform-*d*) δ 176.8, 148.2, 137.0, 132.3, 126.3, 125.2, 110.9, 45.4, 39.3, 38.6, 30.9, 29.7, 27.4, 27.3, 23.4, 21.0, 20.1; TOF-MS (ESI+) m/z $[M+Na]^+$ calculated for $C_{27}H_{38}O_4Na$ $(M+Na)^+$ 449.2662; found 449.2664.

(1′R,2′R)-4-Ethyl-5′-methyl-2′-(prop-1-en-2-yl)-1′,2′,3′,4′-tetrahydro-[1,1′-biphenyl]-2,6-diyl Bis(2,2-dimethylpropanoate).

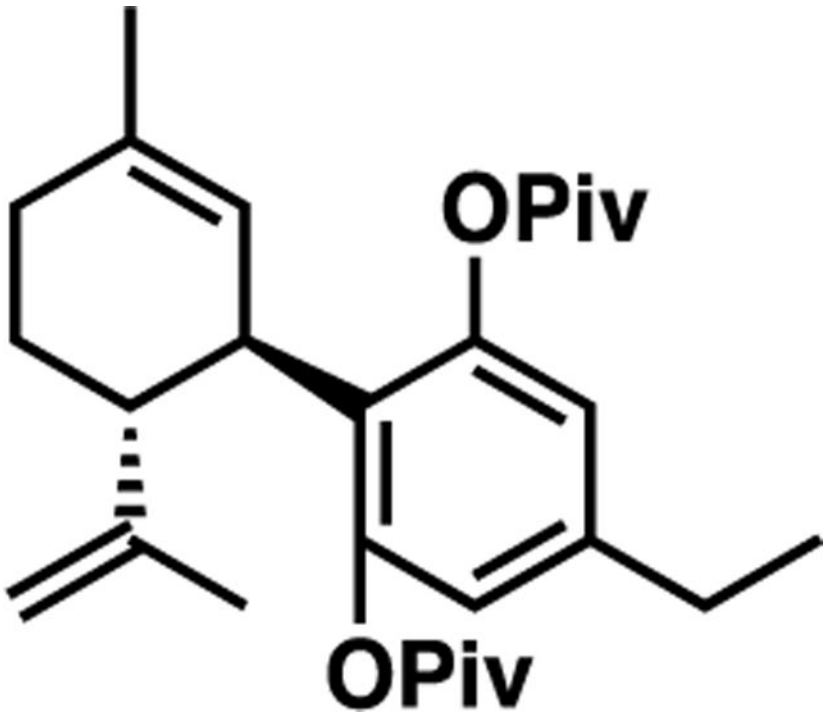

The general procedure above was followed using (1′*R*,2′*R*)-5′-methyl-2′-(prop-1-en-2-yl)-4-(((trifluoromethyl)sulfonyl)oxy)-1′,2′,3′,4′-tetrahydro-[1,1′-biphenyl]-2,6-diyl bis(2,2-dimethylpropanoate) (400 mg, 0.714 mmol), which upon purification [hexanes:Et_2O (93:7)] produced a clear, colorless oil (250 mg, 0.568 mmol, 80%).

R_f = 0.347 [hexanes:Et_2O (9:1)]; ^{1}H NMR (500 MHz, chloroform-*d*) δ 6.60 (s, 2H), 5.25 (t, J = 1.8 Hz, 1H), 4.55 (d, J = 2.0 Hz, 2H), 3.51 (ddt, J = 11.1, 4.6, 2.3 Hz, 1H), 2.68

(ddd, J = 13.0, 10.8, 2.6 Hz, 1H), 2.58 (q, J = 7.6 Hz, 2H), 2.19–2.05 (m, 1H), 2.02 (dd, J = 17.8, 5.8 Hz, 1H), 1.81 (ddt, J = 13.0, 6.2, 2.0 Hz, 1H), 1.69 (qd, J = 12.3, 5.9 Hz, 1H), 1.61 (t, J = 1.8 Hz, 3H), 1.54 (d, J = 1.4 Hz, 3H), 1.34 (s, 18H), 1.20 (t, J = 7.6 Hz, 3H). ^{13}C NMR (126 MHz, chloroform-d) δ 176.8, 148.3, 143.2, 132.2, 126.4, 125.2, 110.9, 45.3, 39.3, 38.7, 30.9, 29.7, 28.2, 27.4, 23.4, 20.2, 14.9; TOF-MS (APCI+) m/z $[M+H]^+$ calculated for $C_{28}H_{41}O_4$ $(M+H)^+$ 441.2999, found 441.3003.

(1′R,2′R)-5′-Methyl-2′-(prop-1-en-2-yl)-4-propyl-1′,2′,3′,4′-tetrahydro-[1,1′-biphenyl]-2,6-diyl Bis(2,2-dimethylpropanoate).

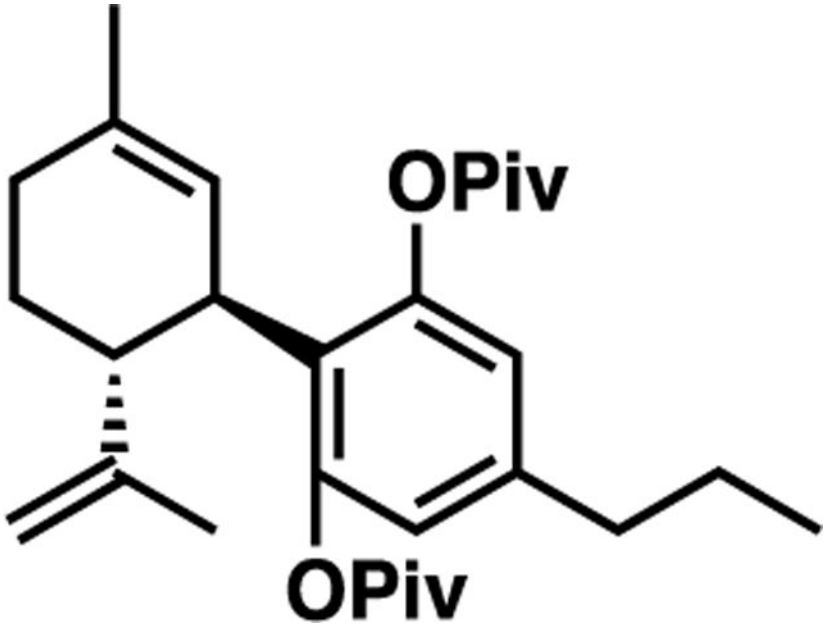

The general procedure above was followed using (1′R,2′R)-5′-methyl-2′-(prop-1-en-2-yl)-4-(((trifluoromethyl)sulfonyl)oxy)-1′,2′,3′,4′-tetrahydro-[1,1′-biphenyl]-2,6-diyl bis(2,2-dimethylpropanoate) (280 mg, 0.5 mmol), which upon purification [hexanes:Et_2O (93:7)] produced a clear, colorless oil (172 mg, 0.379 mmol, 75%).

Matched literature data.[30] R_f = 0.429 [hexanes:Et_2O (9:1)]; ^{1}H NMR (500 MHz, chloroform-d) δ 6.58 (s, 2H), 5.26 (t, J = 1.8 Hz, 1H), 4.55 (s, 2H), 3.52 (ddq, J = 11.1, 4.7, 2.4 Hz, 1H), 2.67 (ddd, J = 13.0, 10.7, 2.6 Hz, 1H), 2.51 (dd, J = 8.7, 6.8 Hz, 2H), 2.11 (ddt, J = 17.0, 10.8, 5.2 Hz, 1H), 2.02 (dd, J = 17.7, 5.7 Hz, 1H), 1.82 (ddt, J = 13.1, 6.2, 2.0 Hz, 1H), 1.76–1.65 (m, 1H), 1.62 (dt, J = 9.5, 6.6 Hz, 5H), 1.54 (s, 3H), 1.34 (s, 18H), 0.92 (t, J = 7.4 Hz, 3H). ^{13}C NMR (126 MHz, chloroform-d) δ 176.8, 148.2, 141.7, 132.2, 126.4, 125.2, 110.8, 45.3, 39.3, 38.7, 37.4, 30.9, 29.7, 27.4, 24.1, 23.4, 20.3, 13.9; TOF-MS (ESI+) m/z $[M+Na]^+$ calculated for $C_{29}H_{42}O_4Na$ $(M+Na)^+$ 477.2975, found 477.2976.

(1′R,2′R)-4-Butyl-5′-methyl-2′-(prop-1-en-2-yl)-1′,2′,3′,4′-tetrahydro-[1,1′-biphenyl]-2,6-diyl Bis(2,2-dimethylpropanoate).

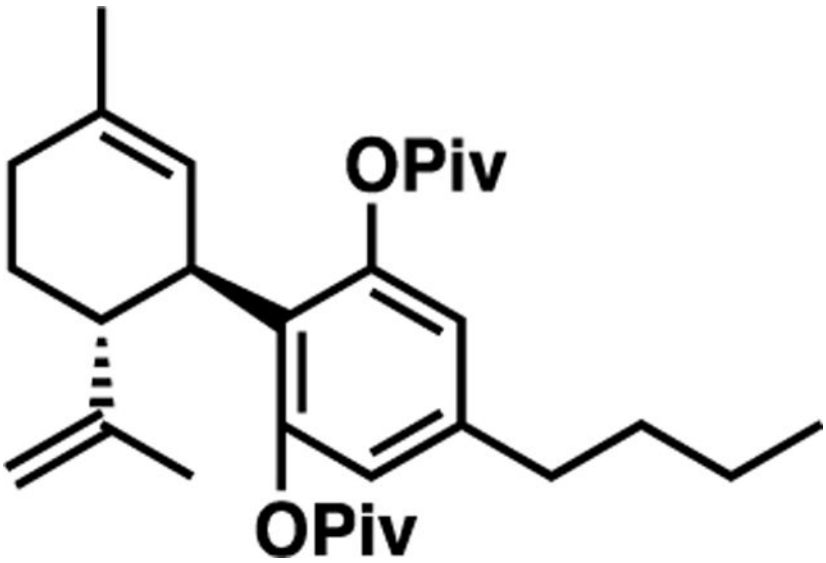

The general procedure above was followed using (1′*R*,2′*R*)-5′-methyl-2′-(prop-1-en-2-yl)-4-(((trifluoromethyl)sulfonyl)oxy)-1′,2′,3′,4′-tetrahydro-[1,1′-biphenyl]-2,6-diyl bis(2,2-dimethylpropanoate) (400 mg, 0.714 mmol), which upon purification [hexanes:Et_2O (93:7)] produced a clear, colorless oil (272 mg, 0.581 mmol, 81%).

Matched literature data.[30] R_f = 0.472 [hexanes:Et_2O (9:1)]; ^{1}H NMR (500 MHz, chloroform-*d*) *δ* 6.58 (s, 2H), 5.25 (p, *J* = 1.7 Hz, 1H), 4.55 (d, *J* = 1.4 Hz, 2H), 3.51 (ddt, *J* = 11.0, 4.5, 2.3 Hz, 1H), 2.67 (ddd, *J* = 13.0, 10.7, 2.6 Hz, 1H), 2.58–2.44 (m, 2H), 2.18–2.06 (m, 1H), 2.06–1.97 (m, 1H), 1.87–1.77 (m, 1H), 1.69 (ddt, *J* = 18.4, 12.4, 5.9 Hz, 1H), 1.63–1.50 (m, 9H), 1.33 (s, 20H), 0.91 (t, *J* = 7.4 Hz, 3H). ^{13}C NMR (126 MHz, chloroform-*d*) *δ* 176.6, 148.1, 141.9, 132.1, 126.2, 125.1, 110.7, 45.1, 39.2, 38.6, 35.0, 32.9, 30.8, 29.6, 27.2, 23.3, 22.5, 20.1, 13.9; TOF-MS (ESI+) *m*/*z* $[M+NH_4]^+$ calculated for $C_{30}H_{44}O_7NH_4$ $(M+NH_4)^+$ 486.3578, found 486.3583.

(1′R,2′R)-4-Hexyl-5′-methyl-2′-(prop-1-en-2-yl)-1′,2′,3′,4′-tetrahydro-[1,1′-biphenyl]-2,6-diyl Bis(2,2-dimethylpropanoate).

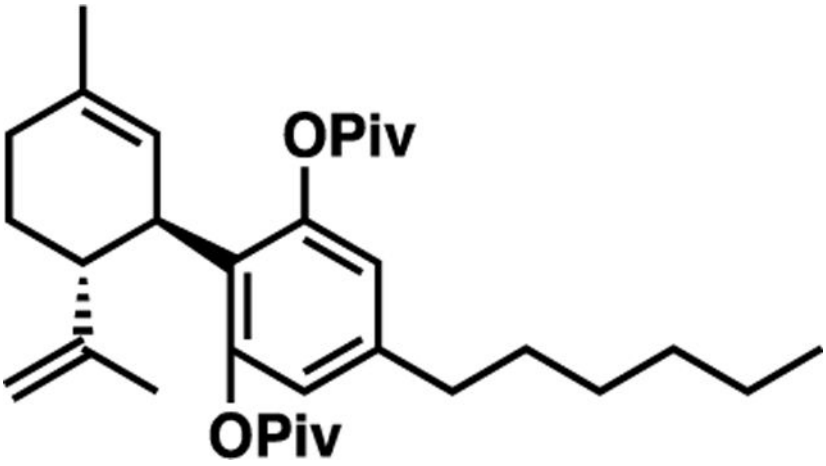

The general procedure above was followed using (1′*R*,2′*R*)-5′-methyl-2′-(prop-1-en-2-yl)-4-(((trifluoromethyl)sulfonyl)oxy)-1′,2′,3′,4′-tetrahydro-[1,1′-biphenyl]-2,6-diyl bis(2,2-dimethylpropanoate) (400 mg, 0.714 mmol), which upon purification [hexanes:Et_2O (95:5)] produced a clear, colorless oil (300 mg, 0.604 mmol, 85%).

R_f = 0.526 [hexanes:Et_2O (9:1)]; ^{1}H NMR (500 MHz, chloroform-*d*) δ 6.58 (s, 2H), 5.25 (p, *J* = 1.7 Hz, 1H), 4.55 (d, *J* = 1.4 Hz, 2H), 3.56–3.46 (m, 1H), 2.67 (ddd, *J* = 13.0, 10.7, 2.6 Hz, 1H), 2.58–2.45 (m, 2H), 2.10 (d, *J* = 12.6 Hz, 1H), 2.06–1.96 (m, 1H), 1.81 (ddt, *J* = 12.9, 6.1, 2.0 Hz, 1H), 1.69 (ddt, *J* = 18.4, 12.5, 5.9 Hz, 1H), 1.63–1.49 (m, 9H), 1.33 (s, 23H), 0.94–0.76 (m, 3H). ^{13}C NMR (126 MHz, chloroform-*d*) δ 176.8, 148.3, 142.1, 132.2, 126.4, 125.3, 110.9, 45.3, 39.3, 38.8, 35.5, 31.8, 30.9, 30.9, 29.7, 29.2, 27.4, 23.4, 22.7, 20.3, 14.2; TOF-MS (ESI+) *m*/*z* $[M+NH_4]^+$ calculated for $C_{32}H_{48}O_4NH_4$ $(M+NH_4)^+$ 514.3891, found 514.3893.

(1′R,2′R)-4-Heptyl-5′-methyl-2′-(prop-1-en-2-yl)-1′,2′,3′,4′-tetrahydro-[1,1′-biphenyl]-2,6-diyl Bis(2,2-dimethylpropanoate).

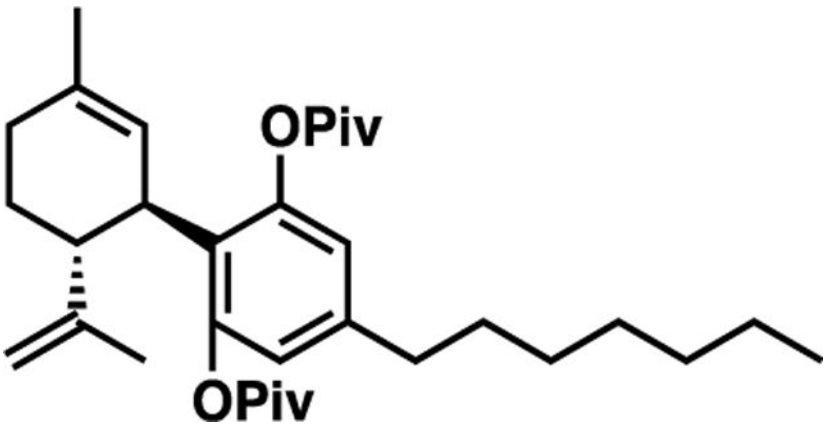

The general procedure above was followed using (1′*R*,2′*R*)-5′-methyl-2′-(prop-1-en-2-yl)-4-(((trifluoromethyl)sulfonyl)oxy)-1′,2′,3′,4′-tetrahydro-[1,1′-biphenyl]-2,6-diyl bis(2,2-dimethylpropanoate) (300 mg, 0.536 mmol), which upon purification [hexanes:Et_2O (95:5)] produced a clear, colorless oil (245 mg, 0.480 mmol, 90%).

R_f = 0.543 [hexanes:Et_2O (7:1)]; ^{1}H NMR (600 MHz, chloroform-*d*) δ 6.58 (s, 2H), 5.26 (s, 1H), 4.55 (d, *J* = 3.1 Hz, 2H), 3.52 (ddq, *J* = 11.1, 4.5, 2.3 Hz, 1H), 2.67 (td, *J* = 11.6, 10.7, 2.5 Hz, 1H), 2.52 (dd, *J* = 9.2, 6.8 Hz, 2H), 2.11 (tt, *J* = 10.4, 5.0 Hz, 1H), 2.07–1.95 (m, 1H), 1.81 (ddt, *J* = 13.0, 6.0, 1.9 Hz, 1H), 1.78–1.64 (m, 1H), 1.59 (d, *J* = 15.0 Hz, 5H), 1.54 (s, 3H), 1.49–1.19 (m, 26H), 0.87 (t, *J* = 6.9 Hz, 3H). ^{13}C NMR (151 MHz, chloroform-*d*) δ 176.6, 148.1, 141.9, 132.0, 126.2, 125.1, 110.7, 45.1, 39.2, 38.6, 35.3, 31.8, 30.9, 29.6, 29.3, 29.1, 27.2, 27.2, 23.3, 22.6, 20.1, 14.1; TOF-MS (ESI+) *m*/*z* $[M+Na]^+$ calculated for $C_{33}H_{50}O_4Na$ $(M+Na)^+$ 533.3601; found 533.3602.

(1′R,2′R)-5′-Methyl-4-octyl-2′-(prop-1-en-2-yl)-1′,2′,3′,4′-tetrahydro-[1,1′-biphenyl]-2,6-diyl Bis(2,2-dimethylpropanoate).

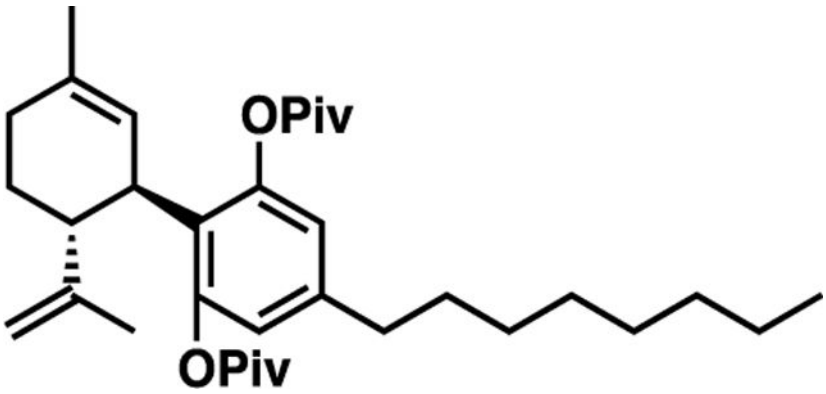

The general procedure above was followed using (1′*R*,2′*R*)-5′-methyl-2′-(prop-1-en-2-yl)-4-(((trifluoromethyl)sulfonyl)oxy)-1′,2′,3′,4′-tetrahydro-[1,1′-biphenyl]-2,6-diyl bis(2,2-dimethylpropanoate) (400 mg, 0.714 mmol), which upon purification [hexanes:Et_2O (95:5)] produced a clear, colorless oil (290 mg, 0.553 mmol, 78%).

R_f = 0.575 [hexanes:Et_2O (9:1)]; ^{1}H NMR (500 MHz, chloroform-*d*) δ 6.58 (s, 2H), 5.25 (p, *J* = 1.6 Hz, 1H), 4.55 (d, *J* = 1.4 Hz, 2H), 3.51 (ddq, *J* = 10.9, 4.4, 2.4 Hz, 1H), 2.67 (ddd, *J* = 13.0, 10.8, 2.6 Hz, 1H), 2.58–2.44 (m, 2H), 2.18–2.05 (m, 1H), 2.06–1.96 (m, 1H), 1.81 (ddt, *J* = 13.1, 6.3, 1.9 Hz, 1H), 1.69 (ddt, *J* = 18.4, 12.5, 5.9 Hz, 1H), 1.63–1.51 (m, 9H), 1.33 (s, 27H), 0.88 (t, *J* = 7.0 Hz, 3H). ^{13}C NMR (126 MHz, chloroform-*d*) δ 176.8, 148.3, 142.1, 132.2, 126.3, 125.2, 110.9, 45.3, 39.3, 38.8, 35.5, 32.0, 31.0, 30.9, 29.7, 29.6, 29.5, 29.4, 27.4, 23.4, 22.8, 20.3, 14.3; TOF-MS (ESI+) *m*/*z* $[M+NH_4]^+$ calculated for $C_{34}H_{52}O_4NH_4$ $(M+NH_4)^+$ 542.4204, found 542.4208.

(1′R,2′R)-5′-Methyl-2′-(prop-1-en-2-yl)-4-vinyl-1′,2′,3′,4′-tetrahydro-[1,1′-biphenyl]-2,6-diyl Bis(2,2-dimethylpropanoate).

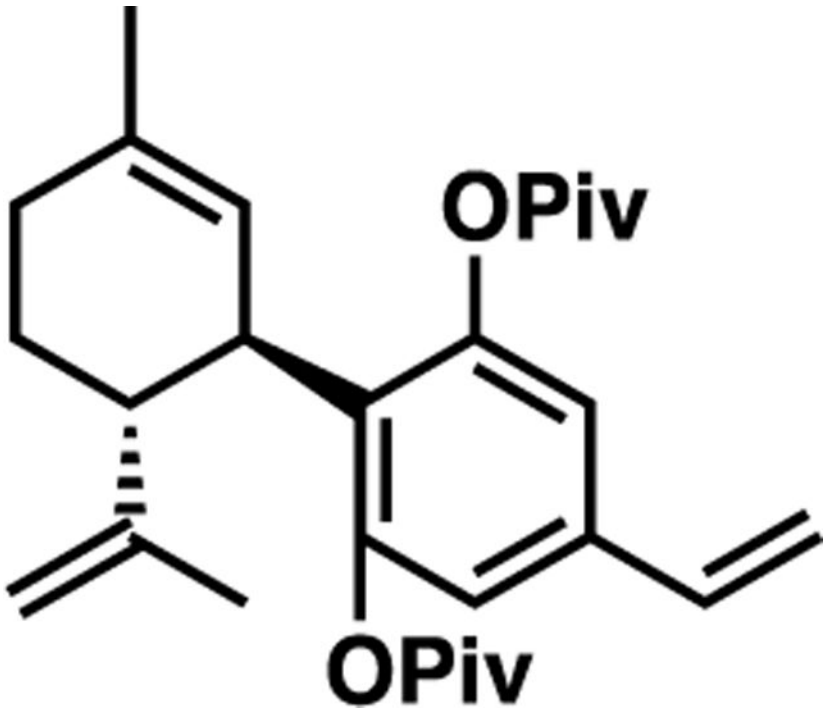

The general procedure above was followed using (1′*R*,2′*R*)-5′-methy-l2′-(prop-1-en-2-yl)-4-(((trifluoromethyl)sulfonyl)oxy)-1′,2′,3′,4′-tetrahydro-[1,1′-biphenyl]-2,6-diyl bis(2,2-dimethylpropanoate) (400 mg, 0.714 mmol), which upon purification [hexanes:Et_2O (95:5)] produced a clear, colorless oil (257 mg, 0.585 mmol, 82%).

Matched literature data.[30] R_f = 0.276 [hexanes:Et_2O (9:1)]; ^{1}H NMR (500 MHz, chloroform-*d*) δ 6.77 (d, *J* = 25.9 Hz, 2H), 6.57 (ddd, *J* = 17.6, 10.9, 3.7 Hz, 1H), 5.66 (d, *J* = 17.5 Hz, 1H), 5.24 (dd, *J* = 10.9, 3.0 Hz, 2H), 4.55 (dd, *J* = 3.5, 1.7 Hz, 2H), 3.53 (dtq, *J* = 10.9, 4.2, 2.1 Hz, 1H), 2.70 (ddd, *J* = 13.1, 10.7, 2.6 Hz, 1H), 2.12 (tt, *J* = 10.3, 4.9 Hz, 1H), 2.07–1.97 (m, 2H), 1.82 (ddt, *J* = 13.0, 6.2, 1.9 Hz, 1H), 1.71 (dd, *J* = 17.4, 11.5 Hz, 1H), 1.61 (t, *J* = 1.8 Hz, 3H), 1.55 (s, 3H), 1.34 (d, *J* = 5.6 Hz, 18H). ^{13}C NMR (126 MHz, chloroform-*d*) δ 176.6, 147.9, 136.7, 135.3, 132.3, 128.8, 124.7, 114.9, 110.9, 45.2, 39.2, 38.7, 30.8, 29.5, 27.2, 23.3, 19.9; TOF-MS (ESI+) *m*/*z* $[M+Na]^+$ calculated for $C_{28}H_{38}O_4Na$ $(M+Na)^+$ 461.2662; found 461.2662.

(1′R,2′R)-4-Allyl-5′-methyl-2′-(prop-1-en-2-yl)-1′,2′,3′,4′-tetrahydro-[1,1′-biphenyl]-2,6-diyl Bis(2,2-dimethylpropanoate).

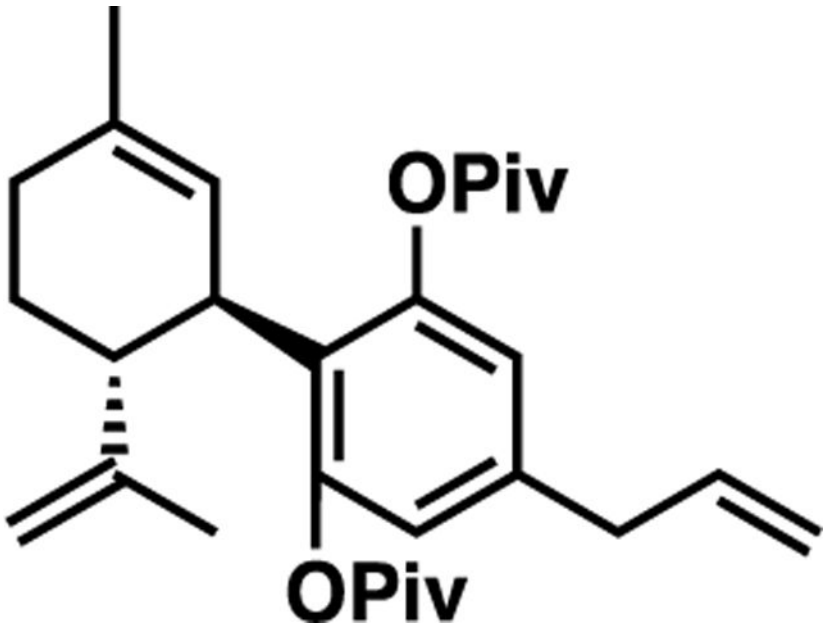

The general procedure above was followed using (1′*R*,2′*R*)-5′-methyl-2′-(prop-1-en-2-yl)-4-(((trifluoromethyl)sulfonyl)oxy)-1′,2′,3′,4′-tetrahydro-[1,1′-biphenyl]-2,6-diyl bis(2,2-dimethylpropanoate) (400 mg, 0.714 mmol), which upon purification [hexanes:Et_2O (95:5)] produced a clear, colorless oil (274 mg, 0.598 mmol, 85%). Characterization via GCMS revealed both *exo* and *endo* lipid tail formation (isomerization of allyl). Mixture was carried on to the next step.

R_f = 0.316 [hexanes:Et_2O (9:1)]; TOF-MS (ESI+) *m*/*z* $[M+Na]^+$ calculated for $C_{29}H_{40}O_4Na$ $(M+Na)^+$ 475.2819; found 475.2819.

(1′R,2′R)-4-Isobutyl-5′-methyl-2′-(prop-1-en-2-yl)-1′,2′,3′,4′-tetrahydro-[1,1′-biphenyl]-2,6-diyl Bis(2,2-dimethylpropanoate).

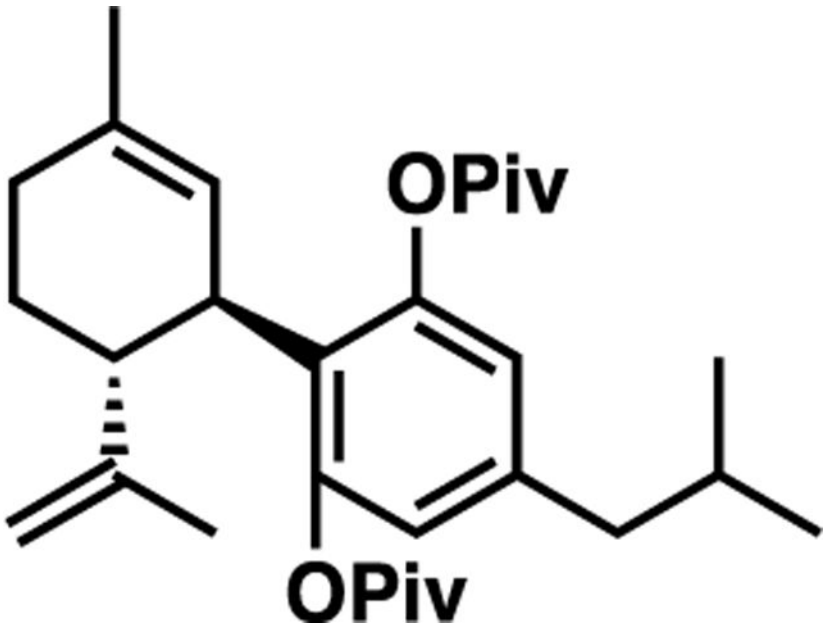

The general procedure above was followed using (1′*R*,2′*R*)-5′-methyl-2′-(prop-1-en-2-yl)-4-(((trifluoromethyl)sulfonyl)oxy)-1′,2′,3′,4′-tetrahydro-[1,1′-biphenyl]-2,6-diyl bis(2,2-dimethylpropanoate) (400 mg, 0.714 mmol), which upon purification [hexanes:Et_2O (9:1)] produced a clear, colorless oil (293 mg, 0.626 mmol, 88%).

R_f = 0.318 [hexanes:Et_2O (9:1)]; ^{1}H NMR (500 MHz, chloroform-*d*) δ 6.55 (s, 2H), 5.27 (t, *J* = 1.8 Hz, 1H), 4.54 (d, *J* = 1.4 Hz, 2H), 3.52 (ddq, *J* = 11.0, 4.5, 2.3 Hz, 1H), 2.66 (ddd, *J* = 13.0, 10.7, 2.6 Hz, 1H), 2.39 (d, *J* = 7.3 Hz, 2H), 2.11 (dq, *J* = 10.2, 5.5, 4.4 Hz, 1H), 2.04–1.95 (m, 1H), 1.89–1.77 (m, 2H), 1.76–1.64 (m, 1H), 1.61 (t, *J* = 1.7 Hz, 3H), 1.53 (d, *J* = 1.2 Hz, 3H), 1.33 (d, *J* = 6.4 Hz, 18H), 0.88 (dd, *J* = 6.6, 2.3 Hz, 6H). ^{13}C NMR (126 MHz, chloroform-*d*) δ 176.8, 148.3, 140.8, 132.2, 126.4, 125.2, 112.3, 110.8, 45.3, 44.8, 39.3, 38.9, 30.9, 30.1, 29.7, 27.4, 23.4, 22.5, 20.3; TOF-MS (ESI+) *m*/*z* $[M+Na]^+$ calculated for $C_{30}H_{44}O_4Na$ $(M+Na)^+$ 491.3132, found 491.3134.

(1′R,2′R)-4-(3,7-Dimethyloctyl)-5′-methyl-2′-(prop-1-en-2-yl)-1′,2′,3′,4′-tetrahydro-[1,1′-biphenyl]-2,6-diyl Bis(2,2-dimethylpropanoate).

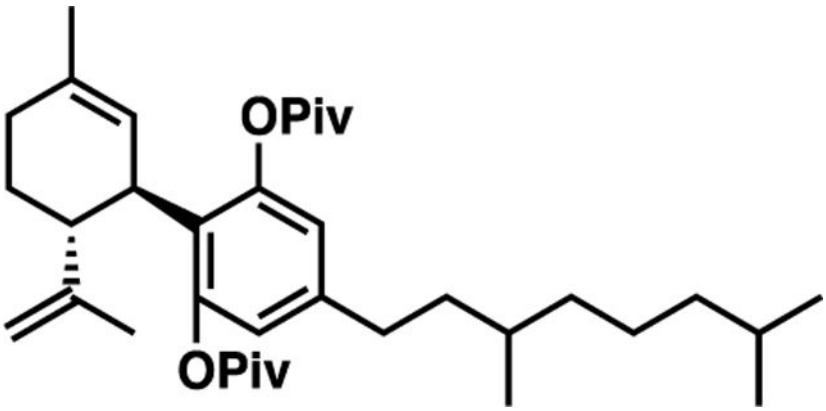

The general procedure above was followed using (1′*R*,2′*R*)-5′-methyl-2′-(prop-1-en-2-yl)-4-(((trifluoromethyl)sulfonyl)oxy)-1′,2′,3′,4′-tetrahydro-[1,1′-biphenyl]-2,6-diyl bis(2,2-dimethylpropanoate) (400 mg, 0.714 mmol), which upon purification [hexanes:Et_2O (95:5)] produced a clear, colorless oil (315 mg, 0.570 mmol, 80%).

R_f = 0.586 [hexanes:Et_2O (7:1)]; ^{1}H NMR (500 MHz, chloroform-*d*) δ 6.58 (s, 2H), 5.25 (s, 1H), 4.55 (s, 2H), 3.55–3.46 (m, 1H), 2.67 (ddd, *J* = 13.0, 10.7, 2.6 Hz, 1H), 2.53 (dddd, *J* = 44.4, 13.8, 10.8, 5.3 Hz, 2H), 2.10 (d, *J* = 12.0 Hz, 1H), 2.06–1.97 (m, 1H), 1.86–1.77 (m, 1H), 1.70 (dq, *J* = 18.9, 6.7, 6.3 Hz, 1H), 1.60 (d, *J* = 2.1 Hz, 3H), 1.56–1.49 (m, 4H), 1.45–1.38 (m, 1H), 1.33 (s, 18H), 1.32 (s, 6H), 1.18–1.06 (m, 3H), 0.88 (dd, *J* = 14.1, 6.4 Hz, 8H). ^{13}C NMR (126 MHz, chloroform-*d*) δ 176.6, 148.1, 142.2, 132.1, 126.2, 125.1, 110.7, 45.1, 39.3, 39.2, 38.6, 38.2, 37.1, 32.9, 32.7, 30.8, 29.6, 27.9, 27.2, 24.7, 23.3, 22.7, 22.6, 20.1, 19.6; TOF-MS (ESI+) *m*/*z* $[M+Na]^+$ calculated for $C_{36}H_{56}O_4Na$ $(M+Na)^+$ 575.4071; found 575.4071.

(1′R,2′R)-4-Isopropyl-5′-methyl-2′-(prop-1-en-2-yl)-1′,2′,3′,4′-tetrahydro-[1,1′-biphenyl]-2,6-diyl Bis(2,2-dimethylpropanoate).

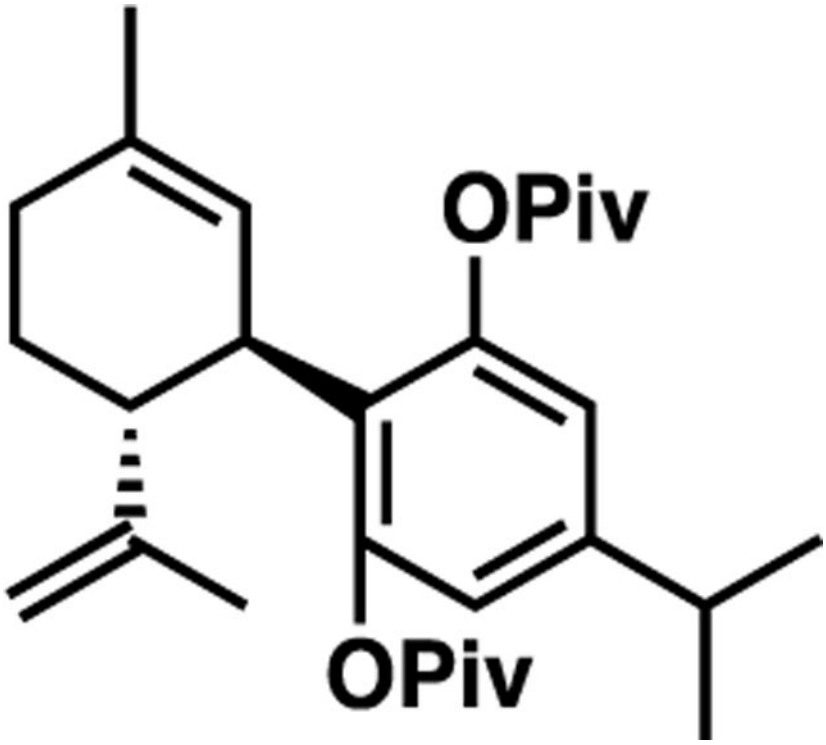

The general procedure above was followed using (1′*R*,2′*R*)-5′-methyl-2′-(prop-1-en-2-yl)-4-(((trifluoromethyl)sulfonyl)oxy)-1′,2′,3′,4′-tetrahydro-[1,1′-biphenyl]-2,6-diyl bis(2,2-dimethylpropanoate) (300 mg, 0.536 mmol), which upon purification [hexanes:Et_2O (93:7)] produced a clear, colorless oil (207 mg, 0.456 mmol, 85%).

Matched literature data.[30] R_f = 0.443 [hexanes:Et_2O (7:1)]; ^{1}H NMR (600 MHz, chloroform-*d*) δ 6.62 (s, 2H), 5.26 (t, *J* = 2.0 Hz, 1H), 4.56 (dd, *J* = 6.7, 1.9 Hz, 2H), 3.51 (ddq, *J* = 11.2, 4.7, 2.4 Hz, 1H), 2.83 (p, *J* = 6.9 Hz, 1H), 2.68 (ddd, *J* = 13.0, 10.8, 2.6 Hz, 1H), 2.19–2.07 (m, 1H), 2.07–1.95 (m, 1H), 1.82 (ddt, *J* = 13.1, 6.2, 1.9 Hz, 1H), 1.70 (dq, *J* = 20.8, 8.0, 7.0 Hz, 1H), 1.61 (d, *J* = 2.4 Hz, 3H), 1.54 (s, 3H), 1.34 (s, 18H), 1.21 (d, *J* = 7.0 Hz, 6H). ^{13}C NMR (151 MHz, chloroform-*d*) δ 176.6, 148.1, 147.7, 132.0, 126.3, 125.1, 110.7, 77.1, 45.1, 39.2, 38.7, 33.5, 30.8, 29.6, 27.2, 23.6, 23.2, 20.2; TOF-MS (ESI+) *m*/*z* $[M+Na]^+$ calculated for $C_{29}H_{42}O_4Na$ $(M+Na)^+$ 477.2975; found 477.2976.

(1′R,2′R)-5′-Methyl-4-(octan-2-yl)-2′-(prop-1-en-2-yl)-1′,2′,3′,4′-tetrahydro-[1,1′-biphenyl]-2,6-diyl Bis(2,2-dimethylpropanoate).

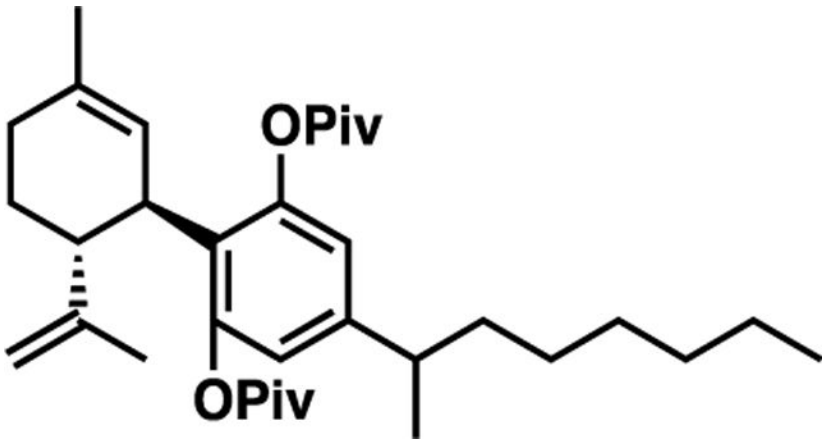

The general procedure for formation of alkylzinc and Negishi cross-coupling above was followed using (1′*R*,2′*R*)-5′-methyl-2′-(prop-1-en-2-yl)-4-(((trifluoromethyl)sulfonyl)oxy)-1′,2′,3′,4′-tetrahydro-[1,1′-biphenyl]-2,6-diyl bis(2,2-dimethylpropanoate) (300 mg, 0.536 mmol). Full conversion of starting material did not occur; however, purification [hexanes:DCM (6:4)] produced a clear, colorless oil (170 mg, 0.333 mmol, 62%). Characterization via GCMS showed a 1:1 ratio of branched linear products that were inseparable; crude mixture carried onto the next reaction without further purification.

R_f = 0.429 [hexanes:DCM (6:4)]; TOF-MS (ESI+) *m*/*z* $[M+Na]^+$ calculated for $C_{33}H_{50}O_4Na$ $(M+Na)^+$ 533.3601; found 533.3601.

General Procedure for Deprotection.

Synthesis was done as previously published.[30]

To a round-bottom flask under an inert atmosphere, piv-protected phenol (0.20 mmol) was dissolved in toluene (5 mL), and MeMgBr (3 M in hexanes, 1.0 mmol) was added dropwise at room temperature. The solution was then heated to 110 °C overnight. Upon cooling to room temperature, the reaction was quenched with saturated aqueous NH_4Cl (5 mL). The layers were separated, and the aqueous layer was washed with Et_2O (10 mL). Combined organic layers were washed with water (20 mL) and brine (20 mL), dried over $MgSO_4$, and concentrated *in vacuo*. The crude oil was purified via flash column chromatography.

(1′R,2′R)-4,5′-Dimethyl-2′-(prop-1-en-2-yl)-1′,2′,3′,4′-tetrahydro-[1,1′-biphenyl]-2,6-diol (JGC23).

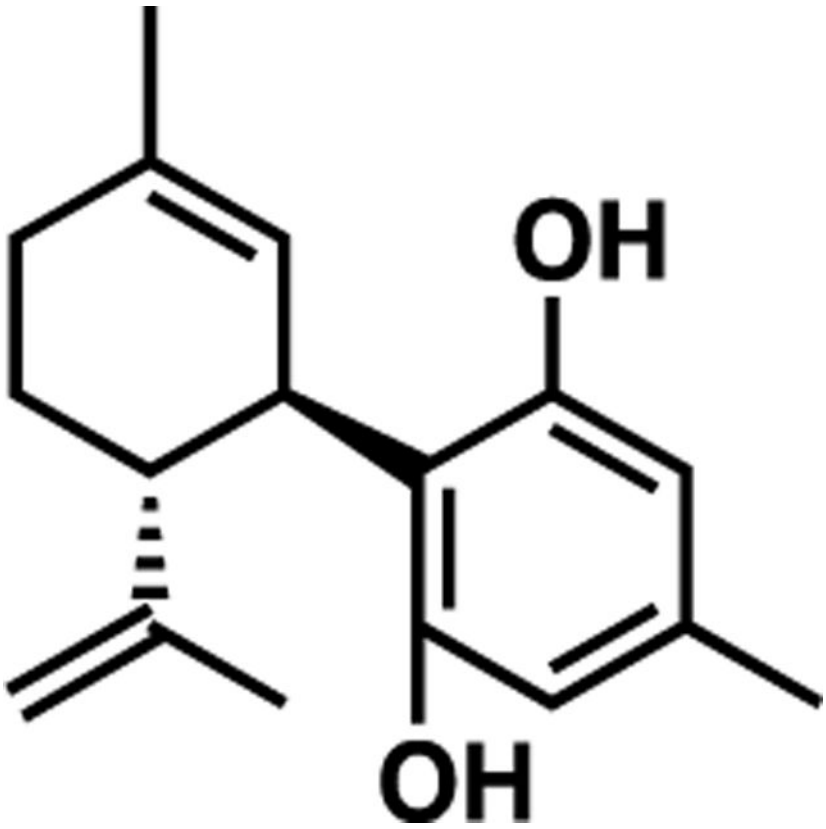

The general procedure above was followed using (1′*R*,2′*R*)-4,5′-dimethyl-2′-(prop-1-en-2-yl)-1′,2′,3′,4′-tetrahydro-[1,1′-biphenyl]-2,6-diyl bis(2,2-dimethylpropanoate) (236 mg, 0.554 mmol), which upon purification via flash column chromatography [hexanes:Et_2O (7:1)] produced a clear, colorless oil (100 mg, 0.387 mmol, 70%).

Matched literature data.[30] R_f = 0.219 [hexanes:Et_2O (7:1)]; ^{1}H NMR (500 MHz, chloroform-*d*) δ 6.21 (s, 1H), 6.20 (s, 1H), 5.95 (s, 1H), 5.55 (d, J = 2.8 Hz, 1H), 4.66 (p, J = 1.6 Hz, 1H), 4.56 (d, J = 2.1 Hz, 1H), 3.85 (ddt, J = 11.4, 4.6, 2.3 Hz, 1H), 2.47–2.33 (m, 1H), 2.20 (s, 4H), 2.15–2.03 (m, 1H), 1.87–1.74 (m, 5H), 1.66 (t, J = 1.1 Hz, 3H). ^{13}C NMR (126 MHz, chloroform-*d*) δ 149.5, 140.2, 138.1, 124.3, 113.7, 111.0, 46.3, 37.3, 30.6, 28.6, 23.8, 21.2, 20.6; TOF-MS (ESI+) m/z $[M+H]^+$ calculated for $C_{17}H_{23}O_2$ $(M+H)^+$ 259.1693, found 259.1694.

(1′R,2′R)-4-Ethyl-5′-methyl-2′-(prop-1-en-2-yl)-1′,2′,3′,4′-tetrahydro-[1,1′-biphenyl]-2,6-diol (JGC24).

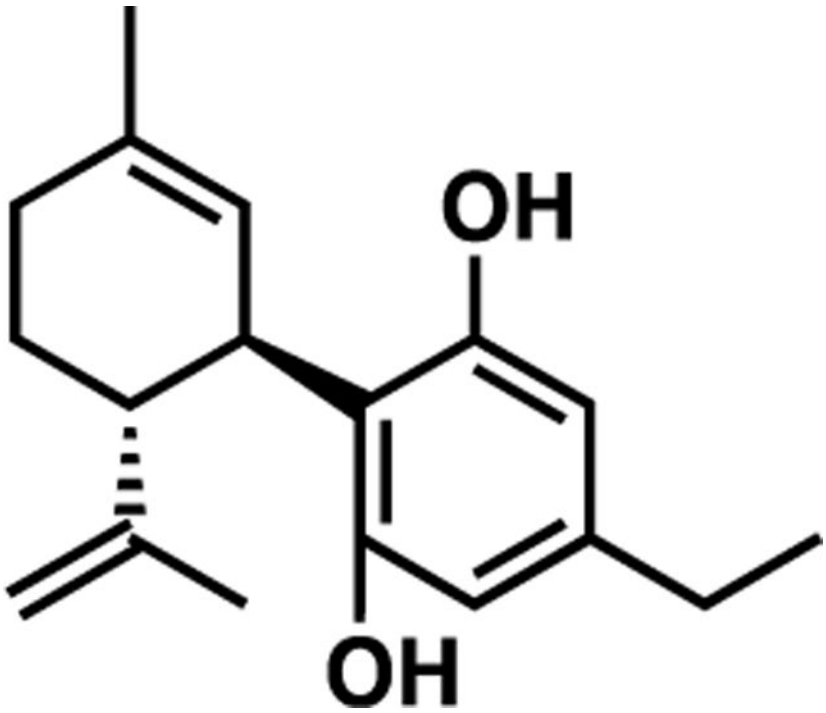

The general procedure above was followed using (1′*R*,2′*R*)-4-ethyl-5′-methyl-2′-(prop-1-en-2-yl)-1′,2′,3′,4′-tetrahydro-[1,1′-biphenyl]-2,6-diyl bis(2,2-dimethylpropanoate) (225 mg, 0.512 mmol), which upon purification via flash column chromatography [hexanes:Et_2O (7:1)] produced a clear, colorless oil (125 mg, 0.459 mmol, 90%).

R_f = 0.222 [hexanes:Et_2O (7:1)]; ^{1}H NMR (500 MHz, chloroform-*d*) δ 6.25 (s, 1H), 6.24 (s, 1H), 6.03 (s, 1H), 5.57 (d, J = 3.2 Hz, 1H), 4.66 (t, J = 1.8 Hz, 1H), 4.57 (d, J = 2.0 Hz, 1H), 3.90 (dtd, J = 8.7, 4.5, 2.3 Hz, 1H), 2.56–2.36 (m, 3H), 2.31–2.16 (m, 1H), 2.10 (ddt, J = 17.9, 5.0, 2.4 Hz, 1H), 1.81 (d, J = 15.2 Hz, 5H), 1.68 (s, 3H), 1.17 (t, J = 7.6 Hz, 3H). ^{13}C NMR (126 MHz, chloroform-*d*) δ 156.1, 149.2, 144.4, 140.1, 124.3, 113.9, 111.0, 109.2, 46.3, 37.1, 30.5, 28.5, 28.5, 23.8, 20.4, 15.1; TOF-MS (ESI+) m/z $[M+H]^+$ calculated for $C_{18}H_{23}O_2$ $(M+H)^+$ 273.1849, found 273.1849.

(1′R,2′R)-5′-Methyl-2′-(prop-1-en-2-yl)-4-propyl-1′,2′,3′,4′-tetrahydro-[1,1′-biphenyl]-2,6-diol (JGC25).

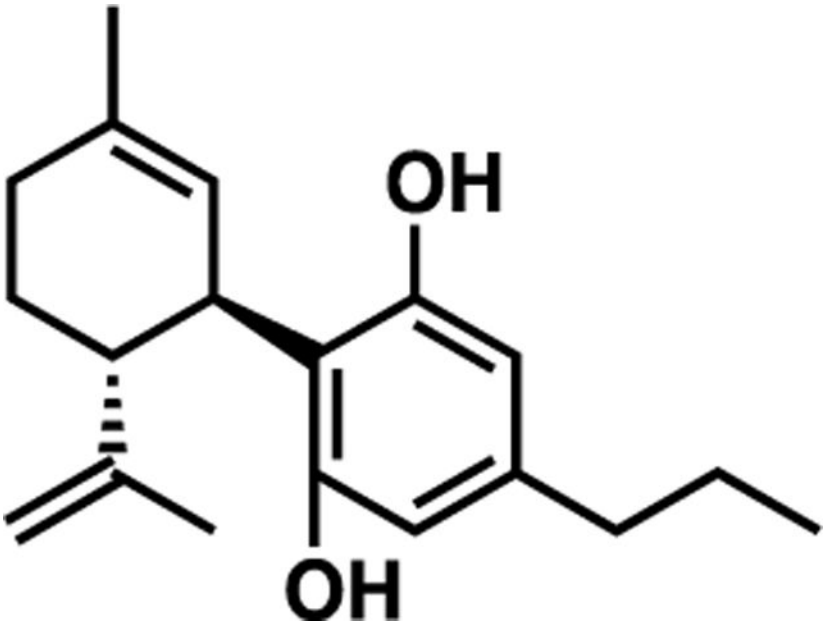

The general procedure above was followed using (1′*R*,2′*R*)-5′-methyl-2′-(prop-1-en-2-yl)-4-propyl-1′,2′,3′,4′-tetrahydro-[1,1′-biphenyl]-2,6-diyl bis(2,2-dimethylpropanoate) (144 mg, 0.317 mmol), which upon purification via flash column chromatography [hexanes:Et_2O (7:1)] produced a clear, colorless oil (74 mg, 0.259 mmol, 82%).

Matched literature data.[30] R_f = 0.429 [hexanes:Et_2O (7:1)]; ^{1}H NMR (500 MHz, chloroform-*d*) δ 6.21 (s, 1H), 6.20 (s, 1H), 5.98 (s, 1H), 5.66–5.47 (m, 1H), 4.71 (s, 1H), 4.66 (p, *J* = 1.6 Hz, 1H), 4.56 (d, *J* = 2.0 Hz, 1H), 3.86 (ddq, *J* = 10.9, 4.5, 2.1 Hz, 1H), 2.47–2.34 (m, 3H), 2.32–2.16 (m, 1H), 2.10 (ddt, *J* = 17.9, 5.1, 2.4 Hz, 1H), 1.90–1.72 (m, 4H), 1.66 (d, *J* = 1.3 Hz, 3H), 1.65–1.53 (m, 3H), 0.90 (t, *J* = 7.3 Hz, 3H). ^{13}C NMR (126 MHz, chloroform-*d*) δ 156.2, 149.5, 142.9, 140.2, 124.3, 113.9, 110.9, 109.0, 46.30, 37.7, 37.4, 30.56, 28.6, 27.4, 24.2, 23.8, 20.6, 13.9; TOF-MS (APCI+) *m*/*z* $[M+H]^+$ calculated for $C_{19}H_{27}O_2$ $(M+H)^+$ 287.2006, found 287.2009.

(1′R,2′R)-4-Butyl-5′-methyl-2′-(prop-1-en-2-yl)-1′,2′,3′,4′-tetrahydro-[1,1′-biphenyl]-2,6-diol (JGC26).

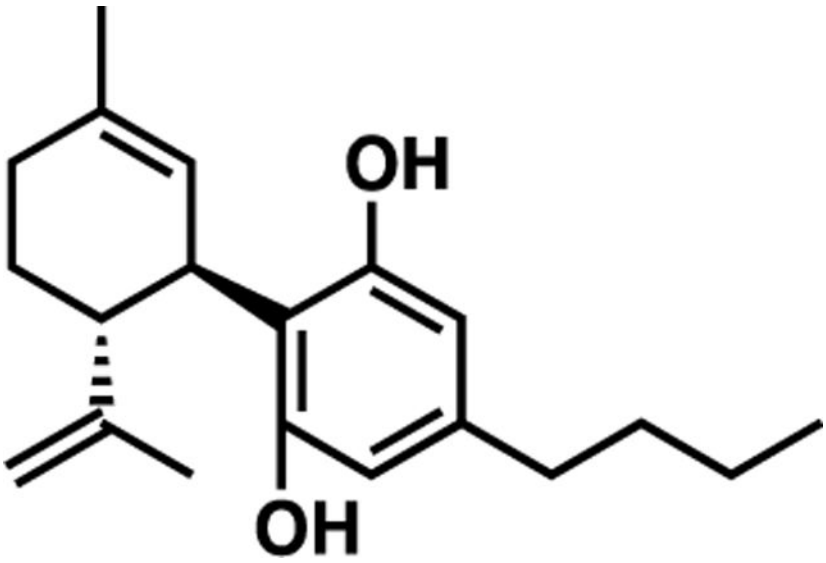

The general procedure above was followed using (1′*R*,2′*R*)-4-butyl-5′-methyl-2′-(prop-1-en-2-yl)-1′,2′,3′,4′-tetrahydro-[1,1′-biphenyl]-2,6-diyl bis(2,2-dimethylpropanoate) (204 mg, 0.436 mmol), which upon purification via flash column chromatography [hexanes:Et_2O (7:1)] produced a clear, colorless oil (103 mg, 0.343 mmol, 79%).

Matched literature data.[30] R_f = 0.273 [hexanes:Et_2O (7:1)]; ^{1}H NMR (500 MHz, chloroform-*d*) δ 6.22 (s, 1H), 6.21 (s, 1H), 5.96 (s, 1H), 5.62–5.49 (m, 1H), 4.66 (p, *J* = 1.6 Hz, 1H), 4.56 (d, *J* = 2.0 Hz, 1H), 3.85 (ddq, *J* = 8.9, 4.5, 2.4 Hz, 1H), 2.51–2.32 (m, 3H), 2.30–2.16 (m, 1H), 2.10 (ddt, *J* = 17.9, 5.1, 2.4 Hz, 1H), 1.89–1.70 (m, 4H), 1.65 (t, *J* = 1.0 Hz, 3H), 1.54 (tt, *J* = 9.1, 6.8 Hz, 2H), 1.39–1.18 (m, 3H), 0.90 (t, *J* = 7.4 Hz, 3H). ^{13}C NMR (126 MHz, chloroform-*d*) δ 149.5, 143.1, 140.2, 124.3, 113.9, 110.9, 46.3, 37.4, 35.3, 33.3, 30.6, 28.6, 23.8, 22.5, 20.7, 14.1; TOF-MS (ESI+) *m*/*z* $[M+H]^+$ calculated for $C_{20}H_{29}O_2$ $(M+H)^+$ 301.2162, found 301.2162.

(1′R,2′R)-4-Hexyl-5′-methyl-2′-(prop-1-en-2-yl)-1′,2′,3′,4′-tetrahydro-[1,1′-biphenyl]-2,6-diol (JGC27).

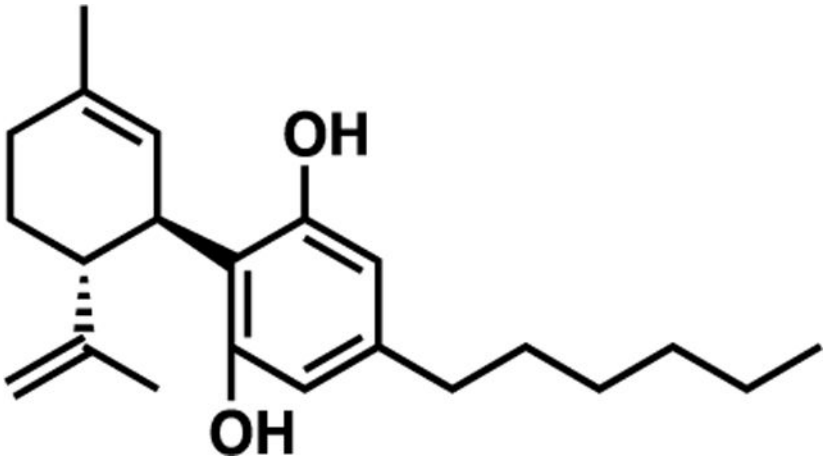

The general procedure above was followed using (1′*R*,2′*R*)-4-hexyl-5′-methyl-2′-(prop-1-en-2-yl)-1′,2′,3′,4′-tetrahydro-[1,1′-biphenyl]-2,6-diyl bis(2,2-dimethylpropanoate) (204 mg, 0.41 mmol), which upon purification via flash column chromatography [hexanes:Et_2O (7:1)] produced a clear, colorless oil (100 mg, 0.305 mmol, 74%).

R_f = 0.333 [hexanes:Et_2O (7:1)]; ^{1}H NMR (500 MHz, chloroform-*d*) *δ* 6.23 (s, 1H), 6.21 (s, 1H), 6.01 (s, 1H), 5.58 (d, *J* = 2.7 Hz, 1H), 4.88 (s, 1H), 4.66 (t, *J* = 1.8 Hz, 1H), 4.56 (d, *J* = 2.0 Hz, 1H), 3.87 (ddq, *J* = 10.9, 4.5, 2.4 Hz, 1H), 2.47–2.37 (m, 3H), 2.30–2.18 (m, 1H), 2.10 (ddt, *J* = 17.9, 5.0, 2.4 Hz, 1H), 1.89–1.72 (m, 5H), 1.67 (d, *J* = 1.2 Hz, 3H), 1.61–1.49 (m, 2H), 1.29 (dd, *J* = 6.7, 3.3 Hz, 6H), 0.97–0.74 (m, 3H). ^{13}C NMR (126 MHz, chloroform-*d*) *δ* 156.1, 149.3, 143.1, 140.1, 124.3, 113.9, 110.9, 109.8, 46.3, 37.3, 35.7, 31.8, 31.0, 30.5, 29.1, 28.5, 23.8, 22.7, 20.5, 14.2; TOF-MS (ESI+) *m*/*z* $[M+H]^+$ calculated for $C_{22}H_{33}O_2$ $(M+H)^+$ 329.2475, found329.2476.

(1′R,2′R)-4-Heptyl-5′-methyl-2′-(prop-1-en-2-yl)-1′,2′,3′,4′-tetrahydro-[1,1′-biphenyl]-2,6-diol (JGC32).

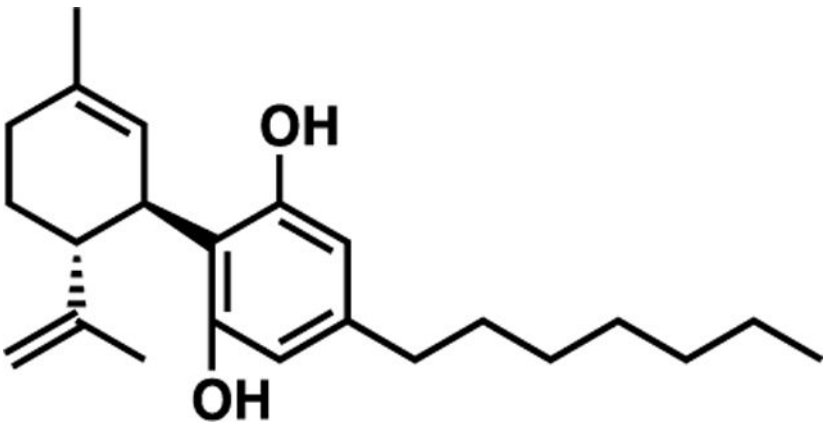

The general procedure above was followed using (1′*R*,2′*R*)-4-heptyl-5′-methyl-2′-(prop-1-en-2-yl)-1′,2′,3′,4′-tetrahydro-[1,1′-biphenyl]-2,6-diyl bis(2,2-dimethylpropanoate) (245

mg, 0.480 mmol), which upon purification via flash column chromatography [hexanes:Et_2O (7:1)] produced a clear, colorless oil (91 mg, 0.266 mmol, 55%).

R_f = 0.371 [hexanes:Et_2O (7:1)]; ^{1}H NMR (500 MHz, chloroform-*d*) δ 6.21 (s, 1H), 6.20 (s, 1H), 5.98 (s, 1H), 5.62–5.49 (m, 1H), 4.74 (s, 1H), 4.65 (t, J = 1.8 Hz, 1H), 4.55 (d, J = 2.0 Hz, 1H), 3.85 (ddq, J = 8.5, 4.4, 2.2 Hz, 1H), 2.47–2.35 (m, 3H), 2.31–2.16 (m, 1H), 2.14–2.03 (m, 1H), 1.87–1.71 (m, 5H), 1.65 (t, J = 1.1 Hz, 3H), 1.54 (t, J = 7.2 Hz, 2H), 1.35–1.18 (m, 8H), 0.87 (t, J = 6.9 Hz, 3H). ^{13}C NMR (126 MHz, chloroform-*d*) δ 156.0, 149.3, 143.0, 140.0, 124.2, 113.8, 110.9, 109.8, 46.2, 37.2, 35.5, 31.8, 30.9, 30.4, 29.3, 29.2, 28.4, 23.7, 22.7, 20.5, 14.1; TOF-MS (ESI+) m/z $[M+H]^+$ calculated for $C_{23}H_{35}O_2$ $(M+H)^+$ 343.2632; found 343.2632.

(1′R,2′R)-5′-Methyl-4-octyl-2′-(prop-1-en-2-yl)-1′,2′,3′,4′-tetrahydro-[1,1′-biphenyl]-2,6-diol (JGC28).

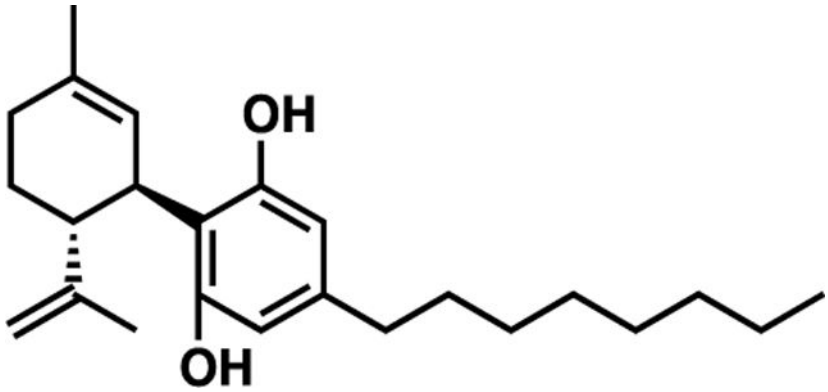

The general procedure above was followed using (1′*R*,2′*R*)-5′-methyl-4-octyl-2′-(prop-1-en-2-yl)-1′,2′,3′,4′-tetrahydro-[1,1′-biphenyl]-2,6-diyl bis(2,2-dimethylpropanoate) (263 mg, 0.502 mmol), which upon purification via flash column chromatography [hexanes:Et_2O (7:1)] produced a clear, colorless oil (128 mg, 0.359 mmol, 72%).

R_f = 0.536 [hexanes:Et_2O (7:1)]; ^{1}H NMR (500 MHz, chloroform-*d*) δ 6.35–6.09 (m, 2H), 5.97 (s, 1H), 5.57 (d, J = 2.7 Hz, 1H), 4.66 (t, J = 1.8 Hz, 1H), 4.56 (d, J = 2.0 Hz, 1H), 3.85 (ddq, J = 10.9, 4.6, 2.4 Hz, 1H), 2.50–2.32 (m, 3H), 2.23 (ddd, J = 16.0, 10.4, 4.6 Hz, 1H), 2.10 (ddt, J = 17.9, 5.0, 2.4 Hz, 1H), 1.81 (dt, J = 12.5, 2.4 Hz, 4H), 1.66 (s, 3H), 1.55 (p, J = 7.2 Hz, 3H), 1.33–1.20 (m, 10H), 0.88 (t, J = 6.9 Hz, 3H). ^{13}C NMR (126 MHz, chloroform-*d*) δ 149.5, 143.2, 140.2, 124.3, 113.9, 110.9, 46.3, 37.4, 35.7, 32.0, 31.1, 30.6, 29.6, 29.4, 29.4, 28.6, 23.8, 22.8, 20.7, 14.3; TOF-MS (APCI+) m/z $[M+H]^+$ calculated for $C_{24}H_{37}O_2$ $(M+H)^+$ 357.2788, found 357.2790.

(1′R,2′R)-5′-Methyl-2′-(prop-1-en-2-yl)-4-vinyl-1′,2′,3′,4′-tetrahydro-[1,1′-biphenyl]-2,6-diol (JGC29).

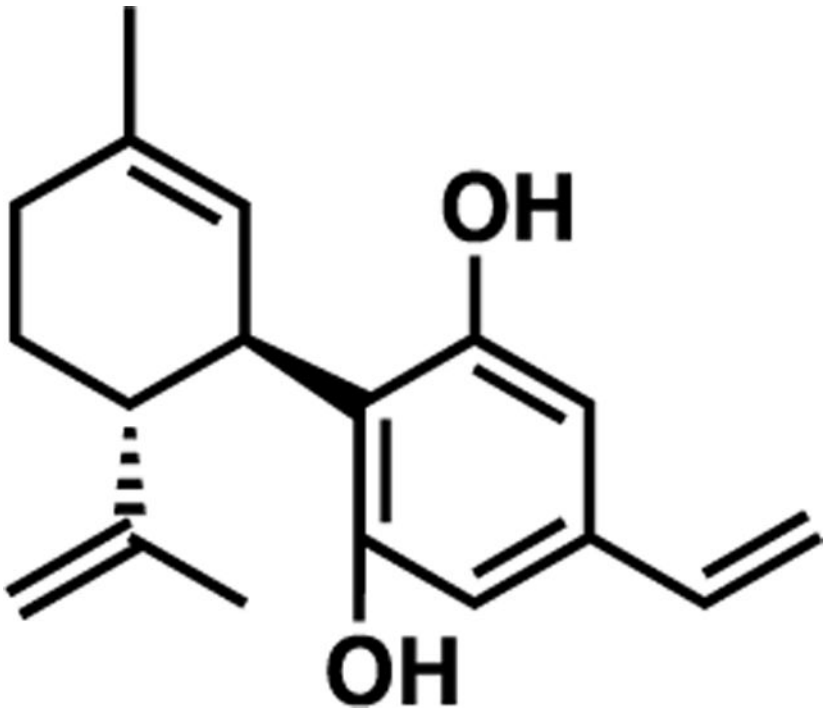

The general procedure above was followed using (1′*R*,2′*R*)-5′-methyl-2′-(prop-1-en-2-yl)-4-vinyl-1′,2′,3′,4′-tetrahydro-[1,1′-biphenyl]-2,6-diyl bis(2,2-dimethylpropanoate) (102 mg, 0.233 mmol), which upon purification via flash column chromatography [hexanes:Et_2O (7:1)] produced a clear, colorless oil (47 mg, 0.174 mmol, 75%).

Matched literature data.[30] R_f = 0.154 [hexanes:Et_2O (7:1)]; ^{1}H NMR (500 MHz, chloroform-*d*) δ 6.46 (s, 1H), 6.45 (s, 1H), 6.03 (s, 1H), 5.64 (d, J = 17.5 Hz, 1H), 5.58–5.50 (m, 1H), 5.18 (d, J = 10.7 Hz, 1H), 4.66 (p, J = 1.6 Hz, 1H), 4.56 (d, J = 2.0 Hz, 1H), 3.89 (ddq, J = 10.8, 4.5, 2.3 Hz, 1H), 2.42 (ddd, J = 13.7, 10.5, 3.4 Hz, 1H), 2.24 (ddt, J = 16.9, 12.7, 4.4 Hz, 1H), 2.10 (ddt, J = 20.6, 5.1, 2.5 Hz, 1H), 1.88–1.72 (m, 5H), 1.67 (s, 3H). ^{13}C NMR (126 MHz, chloroform-*d*) δ 149.2, 140.5, 137.5, 136.4, 123.9, 116.6, 113.9, 111.2, 46.3, 37.4, 30.6, 28.5, 23.8, 20.5; TOF-MS (ESI+) *m*/*z* $[M+H]^+$ calculated for $C_{18}H_{23}O_2$ $(M+H)^+$ 271.1693, found 271.1693.

(1′R,2′R)-4-Allyl-5′-methyl-2′-(prop-1-en-2-yl)-1′,2′,3′,4′-tetrahydro-[1,1′-biphenyl]-2,6-diol (JGC30).

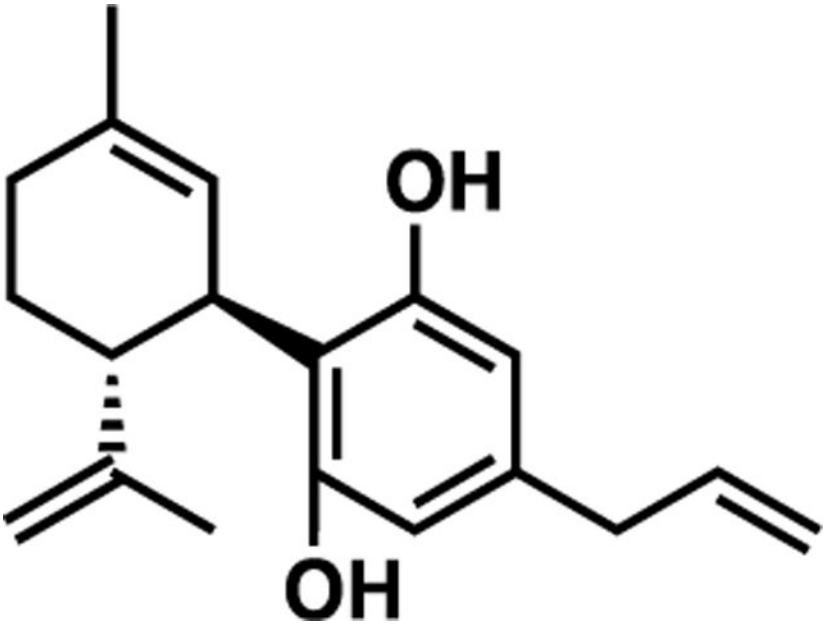

The general procedure above was followed using (1′*R*,2′*R*)-4-allyl-5′-methyl-2′-(prop-1-en-2-yl)-1′,2′,3′,4′-tetrahydro-[1,1′-biphenyl]-2,6-diyl bis(2,2-dimethylpropanoate) (104 mg, 0.230 mmol), which upon purification via flash column chromatography [hexanes:Et_2O (7:1)] produced a clear, colorless oil (30 mg, 0.106 mmol, 46%).

R_f = 0.194 [hexanes:Et_2O (7:1)]; ^{1}H NMR (500 MHz, chloroform-*d*) δ 6.23 (s, 1H), 6.22 (s, 1H), 5.92 (dtd, *J* = 18.2, 13.5, 13.1, 10.1 Hz, 2H), 5.56 (d, *J* = 2.9 Hz, 1H), 5.16–4.93 (m, 2H), 4.82–4.60 (m, 2H), 4.56 (d, *J* = 2.0 Hz, 1H), 3.86 (ddp, *J* = 11.1, 4.7, 2.4 Hz, 1H), 3.23 (d, *J* = 6.6 Hz, 2H), 2.41 (td, *J* = 11.0, 3.4 Hz, 1H), 2.33–2.16 (m, 1H), 2.10 (ddt, *J* = 17.8, 5.0, 2.4 Hz, 1H), 1.88–1.73 (m, 5H), 1.66 (s, 3H). ^{13}C NMR (126 MHz, chloroform-*d*) δ 149.3, 140.3, 140.2, 137.2, 124.1, 115.9, 114.4, 111.1, 110.1, 108.2, 46.3, 39.9, 37.3, 30.5, 28.5, 23.8, 20.5; TOF-MS (ESI+) *m*/*z* $[M+H]^+$ calculated for $C_{19}H_{25}O_2$ $(M+H)^+$ 285.1849, found 285.1850.

(1′R,2′R)-4-Isobutyl-5′-methyl-2′-(prop-1-en-2-yl)-1′,2′,3′,4′-tetrahydro-[1,1′-biphenyl]-2,6-diol (JGC31).

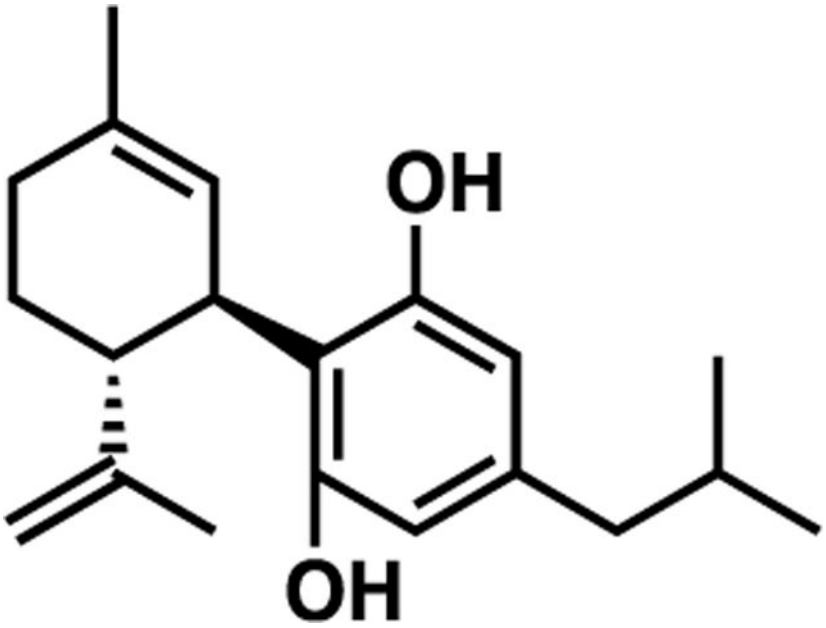

The general procedure above was followed using (1′*R*,2′*R*)-4-isobutyl-5′-methyl-2′-(prop-1-en-2-yl)-1′,2′,3′,4′-tetrahydro-[1,1′-biphenyl]-2,6-diyl bis(2,2-dimethylpropanoate) (282 mg, 0.602 mmol), which upon purification via flash column chromatography [hexanes:Et_2O (7:1)] produced a clear, colorless oil (122 mg, 0.373 mmol, 67%).

R_f = 0.306 [hexanes:Et_2O (7:1)]; ^{1}H NMR (500 MHz, chloroform-*d*) δ 6.19 (s, 1H), 6.18 (s, 1H), 5.97 (s, 1H), 5.58 (dt, *J* = 2.9, 1.6 Hz, 1H), 4.66 (p, *J* = 1.5 Hz, 1H), 4.55 (d, *J* = 2.0 Hz, 1H), 3.90–3.78 (m, 1H), 2.39 (ddd, *J* = 11.5, 10.2, 3.5 Hz, 1H), 2.35–2.18 (m, 3H), 2.10 (ddt, *J* = 17.9, 5.0, 2.4 Hz, 1H), 1.88–1.72 (m, 6H), 1.65 (t, *J* = 1.1 Hz, 3H), 0.87 (d, *J* = 6.6 Hz, 6H). ^{13}C NMR (126 MHz, chloroform-*d*) δ 149.6, 141.9, 140.2, 124.3, 113.9, 110.9, 46.3, 45.2, 37.5, 30.6, 30.0, 28.6, 23.8, 22.6, 22.5, 20.7; TOF-MS (ESI+) *m*/*z* $[M+H]^+$ calculated for $C_{20}H_{29}O_2$ $(M+H)^+$ 301.2162, found 301.2163.

(1′R,2′R)-4-(3,7-Dimethyloctyl)-5′-methyl-2′-(prop-1-en-2-yl)-1′,2′,3′,4′-tetrahydro-[1,1′-biphenyl]-2,6-diol (JGC33).

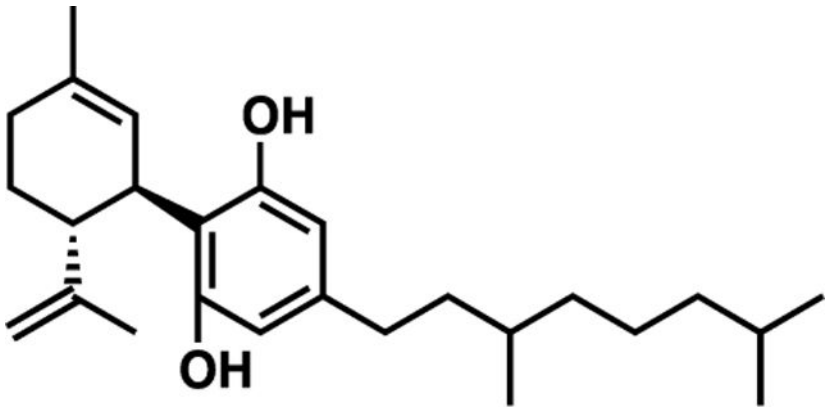

The general procedure above was followed using (1′*R*,2′*R*)-4-(3,7-dimethyloctyl)-5′-methyl-2′-(prop-1-en-2-yl)-1′,2′,3′,4′-tetrahydro-[1,1′-biphenyl]-2,6-diyl bis(2,2-dimethylpropanoate) (177 mg, 0.320 mmol), which upon purification via flash column chromatography [hexanes:Et_2O (7:1)] produced a clear, colorless oil (89 mg, 0.232 mmol, 72%).

R_f = 0.457 [hexanes:Et_2O (7:1)]; ^{1}H NMR (500 MHz, chloroform-*d*) δ 6.23 (s, 1H), 6.22 (s, 1H), 5.97 (s, 1H), 5.57 (dt, *J* = 2.8, 1.6 Hz, 1H), 4.67 (t, *J* = 1.8 Hz, 1H), 4.63 (s, 1H), 4.60–4.52 (m, 1H), 3.91–3.77 (m, 1H), 2.49 (ddd, *J* = 13.6, 10.3, 5.1 Hz, 1H), 2.45–2.36 (m, 2H), 2.29–2.18 (m, 1H), 2.10 (ddd, *J* = 15.3, 5.1, 2.6 Hz, 1H), 1.88–1.73 (m, 5H), 1.66 (t, *J* = 1.0 Hz, 3H), 1.63–1.47 (m, 2H), 1.47–1.19 (m, 4H), 1.12 (dddd, *J* = 13.3, 10.1, 7.2, 5.1 Hz, 3H), 0.93–0.82 (m, 8H). ^{13}C NMR (126 MHz, chloroform-*d*) δ 154.1, 149.5, 143.5, 140.2, 124.3, 113.9, 110.9, 109.9, 46.3, 39.5, 38.5, 37.4, 37.3, 33.2, 32.6, 30.6, 28.6, 28.1, 24.8, 23.8, 22.9, 22.8, 20.7, 19.8; TOF-MS (ESI−) *m*/*z* $[M-H]^-$ calculated for $C_{26}H_{39}O_2$ $[M-H]^-$ 383.2956, found 383.2949.

(1′R,2′R)-4-(3,7-Dimethyloctyl)-5′-methyl-2′-(prop-1-en-2-yl)-1′,2′,3′,4′-tetrahydro-[1,1′-biphenyl]-2,6-diol (JGC34).

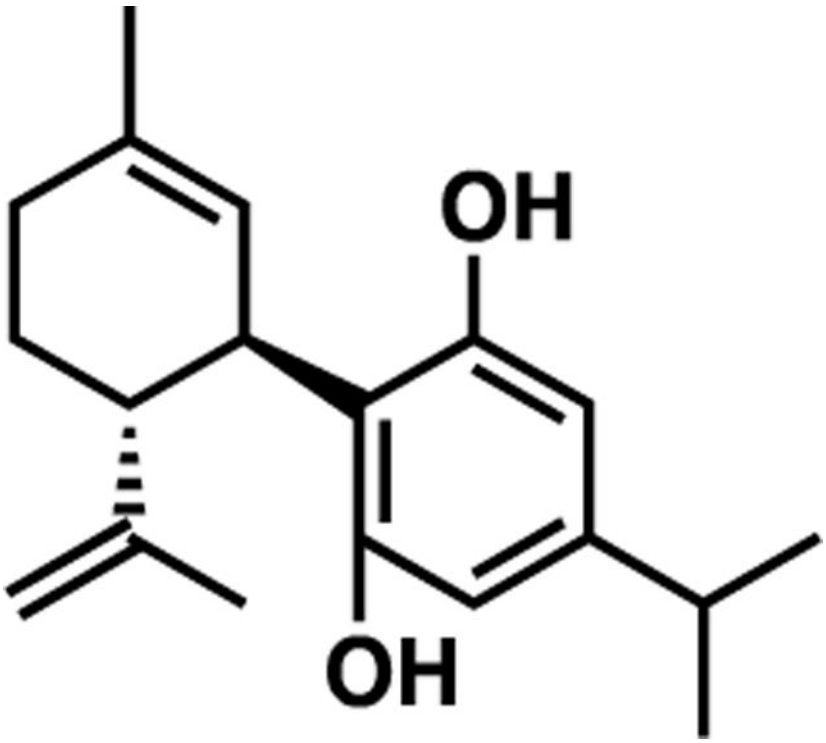

The general procedure above was followed using (1′*R*,2′*R*)-4-(3,7-dimethyloctyl)-5′-methyl-2′-(prop-1-en-2-yl)-1′,2′,3′,4′-tetrahydro-[1,1′-biphenyl]-2,6-diyl bis(2,2-dimethylpropanoate) (207 mg, 0.456 mmol), which upon purification via flash column chromatography [hexanes:Et_2O (7:1)] produced a clear, colorless oil (94 mg, 0.328 mmol, 72%).

Matched literature data.[30] R_f = 0.357 [hexanes:Et_2O (7:1)]; ^{1}H NMR (500 MHz, chloroform-*d*) δ 6.45–6.07 (m, 2H), 5.57 (dt, *J* = 2.8, 1.4 Hz, 1H), 4.66 (q, *J* = 1.7 Hz, 1H), 4.57 (d, *J* = 2.0 Hz, 1H), 3.85 (ddd, *J* = 9.2, 4.2, 2.1 Hz, 1H), 2.72 (p, *J* = 6.9 Hz, 1H), 2.40 (ddd, *J* = 13.3, 10.4, 3.5 Hz, 1H), 2.33–2.15 (m, 1H), 2.09 (ddt, *J* = 18.8, 5.9, 2.8 Hz, 1H), 1.89–1.72 (m, 5H), 1.65 (t, *J* = 1.1 Hz, 3H), 1.17 (d, *J* = 6.9 Hz, 6H). ^{13}C NMR (126 MHz, chloroform-*d*) δ 149.4, 149.1, 140.1, 124.1, 113.9, 110.9, 46.1, 37.3, 33.6, 30.4, 28.4, 23.7, 23.7, 20.6; TOF-MS (EI+) *m*/*z* $[M]^+$ calculated for $C_{19}H_{26}O_2$ $(M)^+$ 286.1927, found 286.1929.

(1′R,2′R)-4-(Heptan-2-yl)-5′-methyl-2′-(prop-1-en-2-yl)-1′,2′,3′,4′-tetrahydro-[1,1′-biphenyl]-2,6-diol (JGC35).

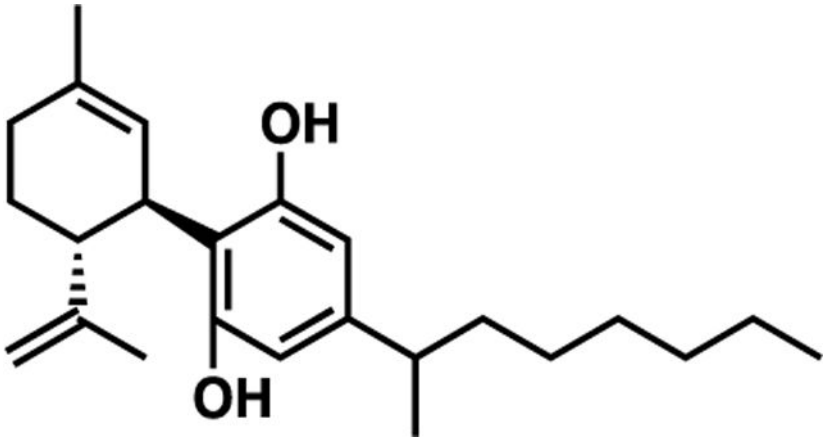

The general procedure above was followed using crude (50%) (1′*R*,2′*R*)-5′-methyl-4-(octan-2-yl)-2′-(prop-1-en-2-yl)-1′,2′,3′,4′-tetrahydro-[1,1′-biphenyl]-2,6-diyl bis(2,2-dimethylpropanoate) (170 mg, 0.333 mmol), which upon purification via flash column chromatography [hexanes:Et_2O (7:1)] produced a clear, colorless oil (37 mg, 0.108 mmol, 65%).

R_f = 0.469 [hexanes:Et_2O (6:1)]; ^{1}H NMR (500 MHz, chloroform-*d*) δ 6.21 (s, 1H), 6.20 (s, 1H), 5.99 (s, 1H), 5.65–5.50 (m, 1H), 4.66 (h, *J* = 1.7 Hz, 1H), 4.60–4.46 (m, 1H), 3.92–3.71 (m, 1H), 2.49 (ddt, *J* = 10.4, 7.0, 3.3 Hz, 1H), 2.39 (td, *J* = 10.9, 3.5 Hz, 1H), 2.28–2.17 (m, 1H), 2.15–2.03 (m, 1H), 1.89–1.72 (m, 5H), 1.63 (dt, *J* = 6.3, 1.1 Hz, 3H), 1.61–1.37 (m, 2H), 1.33–1.02 (m, 9H), 0.90–0.78 (m, 3H). ^{13}C NMR (126 MHz, chloroform-*d*) δ 149.5, 148.3, 140.1, 124.1, 113.9, 110.8, 46.1, 39.6, 38.2, 37.5, 31.9, 30.4, 28.4, 27.3, 23.7, 22.8, 22.6, 22.1, 20.7, 14.1; TOF-MS (ESI+) *m*/*z* $[M+H]^+$ calculated for $C_{23}H_{37}O_2$ $(M+H)^+$ 343.2632; found 343.2633.

Lipid Tail Derivatives of (+)-Cannabidiol.

Starting materials were synthesized as previously published with modifications.[30,31,58–60]

General Procedure of Negishi Cross-Coupling.

Synthesis was done as previously published with modifications.[30]

To a flame-dried round-bottom flask under an inert atmosphere, anhydrous $ZnCl_2$ (182 mg, 1.34 mmol) and LiCl (57 mg, 1.34 mmol) were dissolved in THF (5 mL). The reaction flask was cooled to −10 °C, and RMgBr or RLi (1.07 mmol) was added dropwise. The solution aged for 15 min at −10 °C, was warmed to room temperature, and then stirred for an additional 1.5 h. A solution of (1′*S*,2′*S*)-5′-methyl-2′-(prop-1-en-2-yl)-4-(((trifluoromethyl)-sulfonyl)oxy)-1′,2′,3′,4′-tetrahydro-[1,1′-biphenyl]-2,6-diyl bis(2,2-dimethylpropanoate) (500 mg, 0.893 mmol) in THF (4.5 mL) was added to the reaction flask; then, $Pd(dppf)Cl_2$ (73 mg, 0.089 mmol) was added. The reaction flask was purged and then heated to 55–65 °C. The reaction was monitored via TLC [hexanes:Et_2O

(9:1)]. NOTE: the change in color from yellow-orange to deep wine red normally indicated that the reaction was complete. Upon cooling to room temperature, the reaction was quenched with saturated aqueous NH_4Cl (5 mL). The aqueous solution was extracted with Et_2O (3 × 10 mL), and combined organic layers were washed with water (15 mL) and brine (15 mL), dried over $MgSO_4$, and concentrated *in vacuo*. Crude oil was purified via flash column chromatography.

(1′S,2′S)-4,5′-Dimethyl-2′-(prop-1-en-2-yl)-1′,2′,3′,4′-tetrahydro-[1,1′-biphenyl]-2,6-diyl Bis(2,2-dimethylpropanoate).

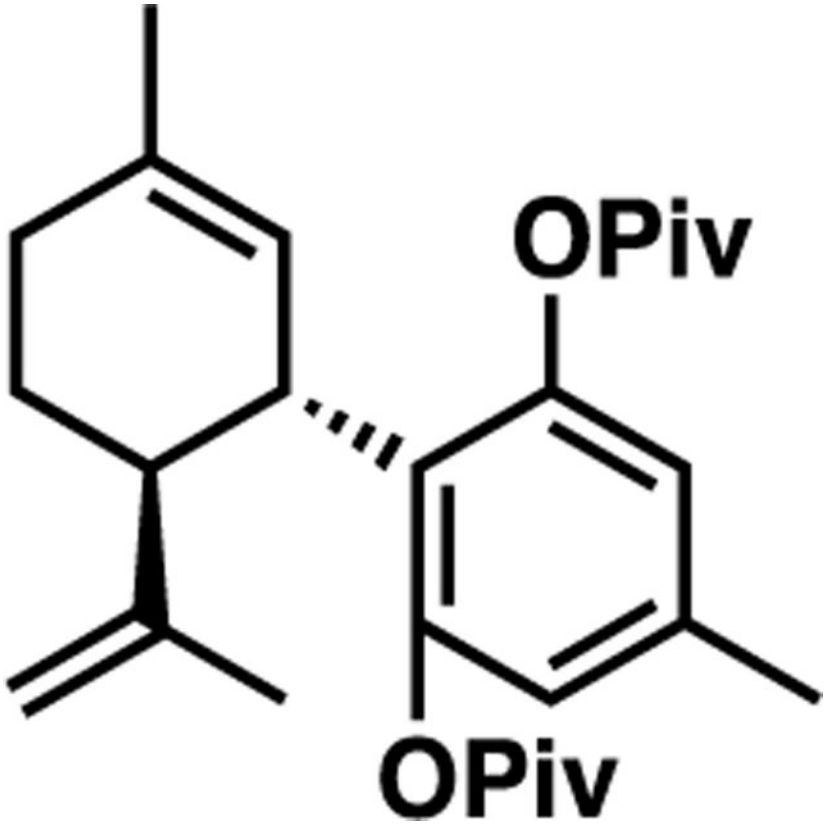

Synthesis was done as previously published with modification.[61]

To a flame-dried round-bottom flask under an inert atmosphere, $Pd(dppf)Cl_2$ (73 mg, 0.089 mmol) was dissolved in THF (5 mL). The reaction flask was cooled to 0 °C, and DIBAL (1 M in THF, 14.6 mL, 0.089 mmol) was added dropwise. The solution aged at 0 °C for 10 min; then, a solution of (1′*S*,2′*S*)-5′-methyl-2′-(prop-1-en-2-yl)-4-(((trifluoromethyl)sulfonyl)oxy)-1′,2′,3′,4′-tetrahydro-[1,1′-biphenyl]-2,6-diyl bis(2,2-dimethylpropanoate) (500 mg, 0.893 mmol) in THF (4.5 mL) was added and stirred for 15 min. $ZnMe_2$ (2 M in toluene, 0.67 mL, 1.34 mmol) was added dropwise at 0 °C. Upon complete addition, the reaction flask was warmed to room temperature and then further heated to 65 °C, and the reaction was monitored via TLC [hexanes:Et_2O (9:1)]. The wine-red solution was cooled to room temperature and quenched with saturated aqueous NH_4Cl. The aqueous layer was washed with Et_2O (3 × 10 mL). Combined organic layers

were washed with water (15 mL) and brine (15 mL), dried over $MgSO_4$, and concentrated *in vacuo*. The crude oil was purified via flash column chromatography [hexanes:Et_2O (22:3)] to produce a clear, colorless oil (306 mg, 0.717 mmol, 80%).

R_f = 0.189 [hexanes:Et_2O (9:1)]; ^{1}H NMR (500 MHz, chloroform-*d*) δ 6.59 (s, 2H), 5.25 (s, 1H), 4.56 (s, 2H), 3.52 (ddq, J = 11.1, 4.6, 2.4 Hz, 1H), 2.68 (ddd, J = 13.0, 10.9, 2.6 Hz, 1H), 2.28 (s, 3H), 2.11 (ddd, J = 17.1, 11.0, 4.8 Hz, 1H), 2.07–1.97 (m, 2H), 1.87–1.77 (m, 1H), 1.70 (dq, J = 18.7, 6.4 Hz, 2H), 1.61 (d, J = 2.4 Hz, 3H), 1.55 (s, 3H), 1.34 (s, 18H). ^{13}C NMR (126 MHz, chloroform-*d*) δ 176.8, 148.2, 137.0, 132.2, 126.3, 125.1, 110.9, 45.3, 39.3, 38.6, 30.9, 29.7, 27.3, 23.4, 20.9, 20.1; TOF-MS (ESI+) *m*/*z* $[M+Na]^+$ calculated for $C_{27}H_{38}O_4Na$ $(M+Na)^+$ 449.2662; found 449.2664.

(1′S,2′S)-4-Ethyl-5′-methyl-2′-(prop-1-en-2-yl)-1′,2′,3′,4′-tetrahydro-[1,1′-biphenyl]-2,6-diyl Bis(2,2-dimethylpropanoate).

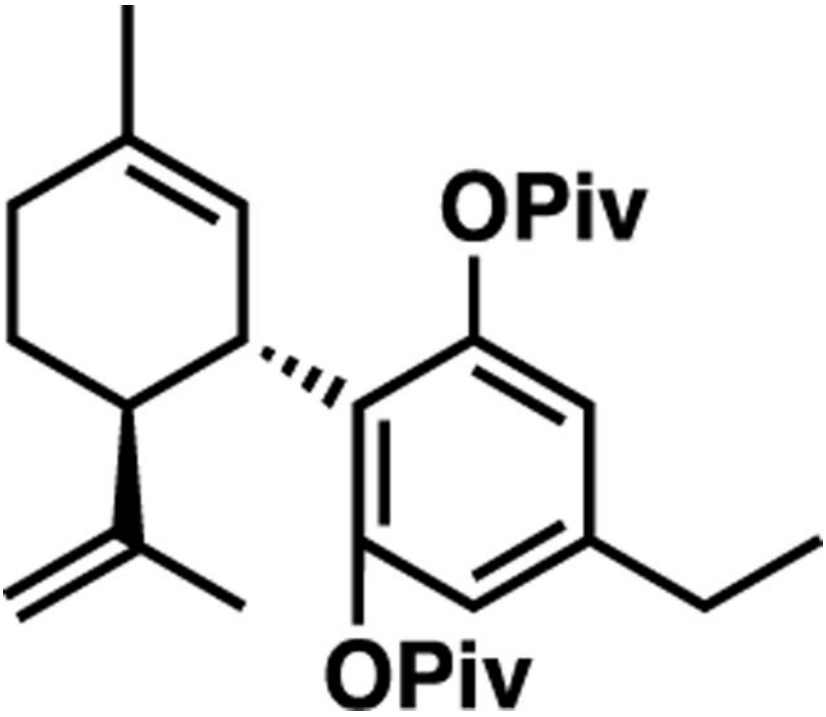

The general procedure above was followed using (1′*S*,2′*S*)-5′-methyl-2′-(prop-1-en-2-yl)-4-(((trifluoromethyl)sulfonyl)oxy)-1′,2′,3′,4′-tetrahydro-[1,1′-biphenyl]-2,6-diyl bis(2,2-dimethylpropanoate) (500 mg, 0.893 mmol), which upon purification [hexanes:Et_2O (93:7)] produced a clear, colorless oil (240 mg, 0.545 mmol, 61%).

R_f = 0.347 [hexanes:Et_2O (9:1)]; ^{1}H NMR (500 MHz, chloroform-*d*) δ 6.61 (s, 2H), 5.26 (s, 1H), 4.62–4.43 (m, 2H), 3.53 (ddq, J = 11.0, 4.6, 2.4 Hz, 1H), 2.69 (ddd, J = 13.0, 10.8, 2.6 Hz, 1H), 2.59 (q, J = 7.6 Hz, 2H), 2.20–1.91 (m, 2H), 1.82 (ddt, J = 13.0, 6.0, 2.0 Hz, 1H), 1.71 (dq, J = 18.2, 5.8 Hz, 2H), 1.64–1.59 (m, 3H), 1.56 (s, 3H), 1.35 (s, 18H), 1.21 (t, J = 7.6 Hz, 3H). ^{13}C NMR (126 MHz, chloroform-*d*) δ 176.7, 148.1, 143.1, 132.1, 126.4,

125.2, 110.9, 45.2, 39.2, 38.6, 30.8, 29.7, 28.2, 27.3, 23.3, 20.1, 14.8; TOF-MS (ESI+) *m*/*z* $[M+Na]^+$ calculated for $C_{28}H_{40}O_4Na$ $(M+Na)^+$ 463.2819, found 463.2822.

(1′S,2′S)-5′-Methyl-2′-(prop-1-en-2-yl)-4-propyl-1′,2′,3′,4′-tetrahydro-[1,1′-biphenyl]-2,6-diyl Bis(2,2-dimethylpropanoate).

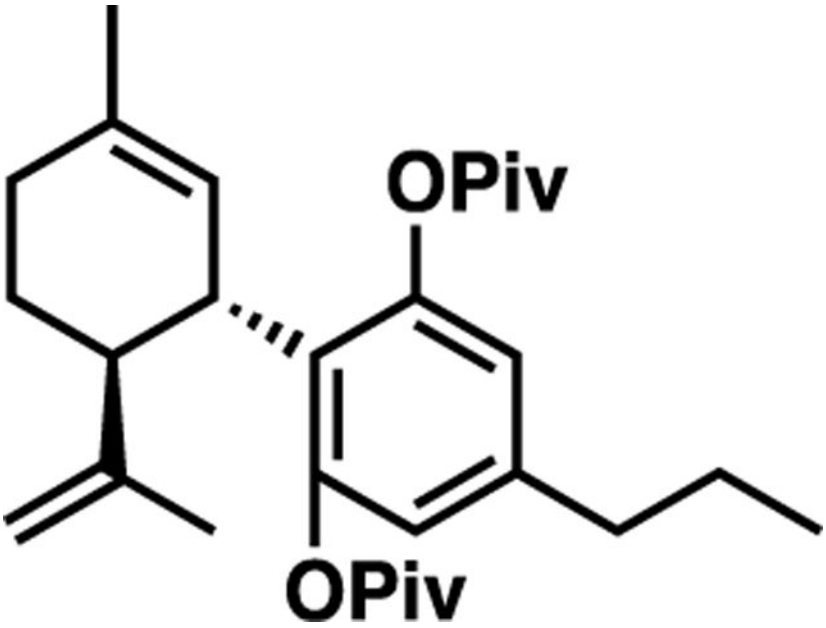

The general procedure above was followed using (1′*S*,2′*S*)-5′-methyl-2′-(prop-1-en-2-yl)-4-(((trifluoromethyl)sulfonyl)oxy)-1′,2′,3′,4′-tetrahydro-[1,1′-biphenyl]-2,6-diyl bis(2,2-dimethylpropanoate) (500 mg, 0.893 mmol), which upon purification [hexanes:Et_2O (93:7)] produced a clear, colorless oil (150 mg, 0.330 mmol, 37%).

R_f = 0.429 [hexanes:Et_2O (9:1)]; ^{1}H NMR (500 MHz, chloroform-*d*) *δ* 6.59 (s, 2H), 5.27 (s, 1H), 4.56 (d, *J* = 3.9 Hz, 2H), 3.53 (ddq, *J* = 11.0, 4.5, 2.4 Hz, 1H), 2.68 (ddd, *J* = 13.0, 10.8, 2.6 Hz, 1H), 2.58–2.46 (m, 2H), 2.21–1.96 (m, 2H), 1.82 (ddt, *J* = 13.1, 6.1, 2.0 Hz, 1H), 1.76–1.67 (m, 1H), 1.62 (q, *J* = 7.3 Hz, 5H), 1.55 (s, 3H), 1.33 (d, *J* = 7.0 Hz, 18H), 0.92 (t, *J* = 7.4 Hz, 3H). ^{13}C NMR (126 MHz, chloroform-*d*) *δ* 176.7, 148.1, 141.6, 132.1, 126.4, 125.1, 110.8, 45.2, 39.2, 38.7, 37.4, 30.8, 29.6, 27.3, 24.0, 23.3, 20.2, 13.8; TOF-MS (ESI+) *m*/*z* $[M+Na]^+$ calculated for $C_{29}H_{42}O_4Na$ $(M+Na)^+$ 477.2975, found 477.2975.

(1′S,2′S)-4-Butyl-5′-methyl-2′-(prop-1-en-2-yl)-1′,2′,3′,4′-tetrahydro-[1,1′-biphenyl]-2,6-diyl Bis(2,2-dimethylpropanoate).

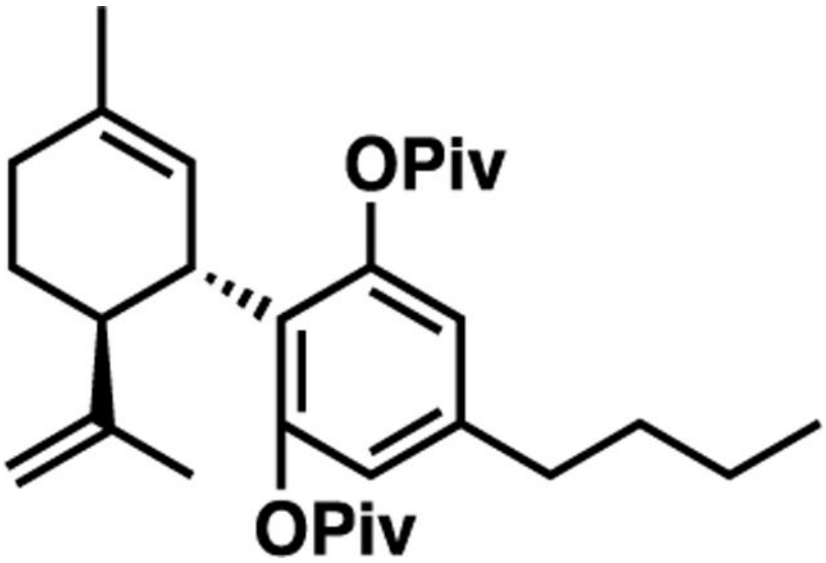

The general procedure above was followed using (1′*S*,2′*S*)-5′-methyl-2′-(prop-1-en-2-yl)-4-(((trifluoromethyl)sulfonyl)oxy)-1′,2′,3′,4′-tetrahydro-[1,1′-biphenyl]-2,6-diyl bis(2,2-dimethylpropanoate) (500 mg, 0.893 mmol), which upon purification [hexanes:Et_2O (93:7)] produced a clear, colorless oil (390 mg, 0.833 mmol, 93%).

R_f = 0.472 [hexanes:Et_2O (9:1)]; ^{1}H NMR (500 MHz, chloroform-*d*) δ 6.58 (s, 2H), 5.25 (t, *J* = 1.9 Hz, 1H), 4.55 (s, 2H), 3.51 (ddq, *J* = 11.0, 4.4, 2.3 Hz, 1H), 2.67 (ddd, *J* = 12.9, 10.6, 2.6 Hz, 1H), 2.58–2.44 (m, 2H), 2.10 (dq, *J* = 11.9, 6.4 Hz, 1H), 2.01 (dd, *J* = 17.7, 4.9 Hz, 1H), 1.82 (ddt, *J* = 15.1, 6.0, 2.0 Hz, 1H), 1.70 (dq, *J* = 18.4, 6.1 Hz, 1H), 1.61 (s, 3H), 1.61–1.51 (m, 5H), 1.34 (q, *J* = 6.8, 6.3 Hz, 20H), 0.91 (t, *J* = 7.4 Hz, 3H). ^{13}C NMR (126 MHz, chloroform-*d*) δ 176.8, 148.3, 142.0, 132.2, 126.3, 125.2, 123.7, 110.9, 45.3, 39.3, 38.7, 35.2, 33.2, 30.9, 29.7, 27.4, 23.4, 22.6, 20.3, 14.1; TOF-MS (ESI+) *m*/*z* $[M+Na]^+$ calculated for $C_{30}H_{44}O_7Na$ $(M+Na)^+$ 491.3132, found 491.3137.

(1′S,2′S)-4-Hexyl-5′-methyl-2′-(prop-1-en-2-yl)-1′,2′,3′,4′-tetrahydro-[1,1′-biphenyl]-2,6-diyl Bis(2,2-dimethylpropanoate).

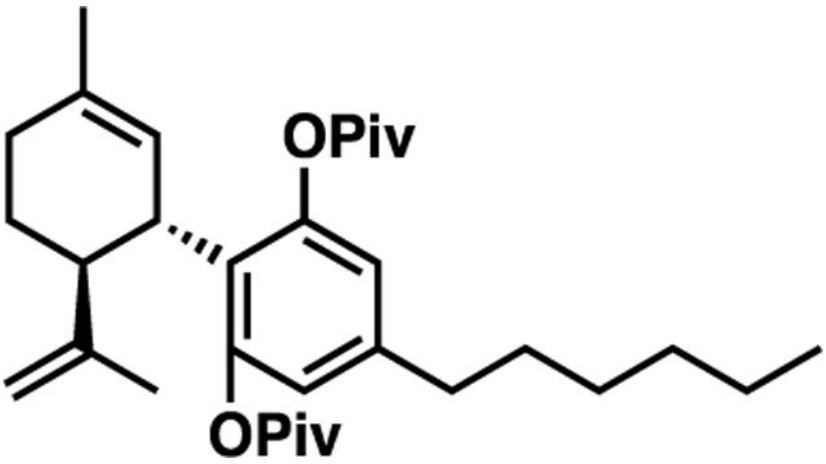

The general procedure above was followed using (1′*S*,2′*S*)-5′-methyl-2′-(prop-1-en-2-yl)-4-(((trifluoromethyl)sulfonyl)oxy)-1′,2′,3′,4′-tetrahydro-[1,1′-biphenyl]-2,6-diyl bis(2,2-dimethylpropanoate) (500 mg, 0.893 mmol), which upon purification [hexanes:Et_2O (95:5)] produced a clear, colorless oil (340 mg, 0.685 mmol, 77%).

R_f = 0.526 [hexanes:Et_2O (9:1)]; ^{1}H NMR (500 MHz, chloroform-*d*) δ 6.58 (s, 2H), 5.25 (s, 1H), 4.55 (s, 2H), 3.51 (ddq, *J* = 11.1, 4.6, 2.4 Hz, 1H), 2.67 (ddd, *J* = 13.0, 10.8, 2.6 Hz, 1H), 2.58–2.45 (m, 2H), 2.11 (ddd, *J* = 15.3, 10.3, 4.2 Hz, 1H), 2.01 (dd, *J* = 17.7, 5.0 Hz, 1H), 1.87–1.76 (m, 1H), 1.69 (dt, *J* = 18.6, 6.3 Hz, 1H), 1.57 (d, *J* = 33.9 Hz, 7H), 1.40–1.23 (m, 25H), 0.88 (d, *J* = 6.3 Hz, 3H). ^{13}C NMR (126 MHz, chloroform-*d*) δ 176.8, 148.3, 142.1, 132.2, 126.3, 125.2, 110.9, 45.3, 39.3, 38.7, 35.5, 31.8, 30.9, 30.9, 29.7, 29.2, 27.4, 23.4, 22.7, 20.3, 14.2; TOF-MS (ESI+) *m*/*z* $[M+Na]^+$ calculated for $C_{32}H_{48}O_4Na$ $(M+Na)^+$ 519.3445, found 519.3451.

(1′S,2′S)-4-Heptyl-5′-methyl-2′-(prop-1-en-2-yl)-1′,2′,3′,4′-tetrahydro-[1,1′-biphenyl]-2,6-diyl Bis(2,2-dimethylpropanoate).

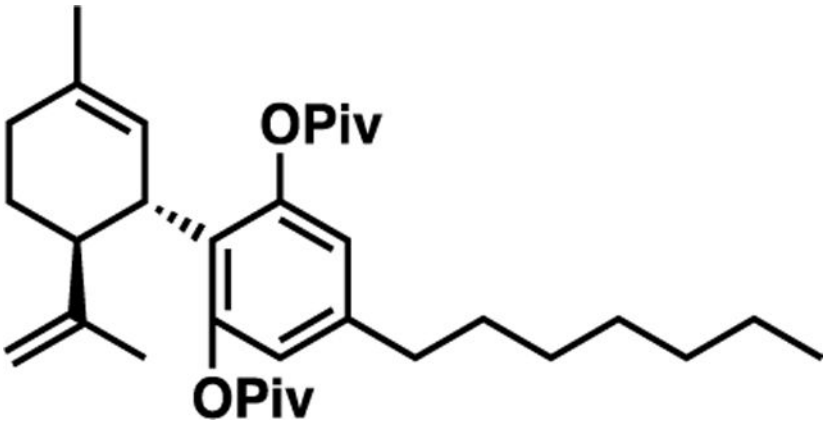

The general procedure above was followed using (1′*S*,2′*S*)-5′-methyl-2′-(prop-1-en-2-yl)-4-(((trifluoromethyl)sulfonyl)oxy)-1′,2′,3′,4′-tetrahydro-[1,1′-biphenyl]-2,6-diyl

bis(2,2-dimethylpropanoate) (500 mg, 0.893 mmol), which upon purification [hexanes:Et_2O (95:5)] produced a clear, colorless oil (300 mg, 0.588 mmol, 66%).

R_f = 0.543 [hexanes:Et_2O (7:1)]; ^{1}H NMR (500 MHz, chloroform-*d*) δ 6.58 (s, 2H), 5.25 (s, 1H), 4.55 (s, 2H), 3.51 (ddq, *J* = 11.0, 4.5, 2.4 Hz, 1H), 2.67 (ddd, *J* = 12.9, 10.6, 2.6 Hz, 1H), 2.51 (dd, *J* = 9.2, 6.8 Hz, 2H), 2.19–1.93 (m, 2H), 1.90–1.77 (m, 1H), 1.76–1.63 (m, 1H), 1.57 (d, *J* = 33.9 Hz, 8H), 1.42–1.21 (m, 26H), 0.87 (t, *J* = 6.7 Hz, 3H). ^{13}C NMR (126 MHz, chloroform-*d*) δ 176.8, 148.3, 142.1, 133.4, 132.2, 126.3, 125.2, 123.7, 110.9, 45.3, 39.3, 38.7, 35.5, 31.9, 31.0, 30.9, 29.7, 29.5, 29.2, 27.4, 23.4, 22.8, 20.3, 14.2; TOF-MS (ESI+) *m*/*z* $[M+Na]^+$ calculated for $C_{33}H_{50}O_4Na$ $(M+Na)^+$ 533.3601; found 533.3603.

(1′S,2′S)-5′-Methyl-4-octyl-2′-(prop-1-en-2-yl)-1′,2′,3′,4′-tetrahydro-[1,1′-biphenyl]-2,6-diyl Bis(2,2-dimethylpropanoate).

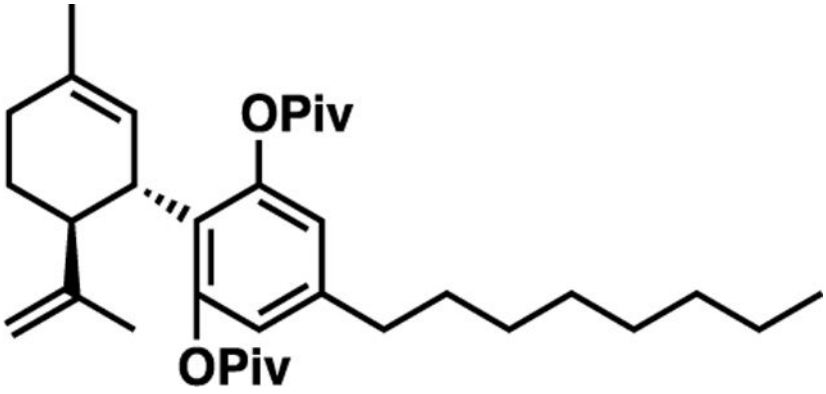

The general procedure above was followed using (1′*S*,2′*S*)-5′-methyl-2′-(prop-1-en-2-yl)-4-(((trifluoromethyl)sulfonyl)oxy)-1′,2′,3′,4′-tetrahydro-[1,1′-biphenyl]-2,6-diyl bis(2,2-dimethylpropanoate) (500 mg, 0.893 mmol), which upon purification [hexanes:Et_2O (95:5)] produced a clear, colorless oil (360 mg, 0.687 mmol, 77%).

R_f = 0.575 [hexanes:Et_2O (9:1)]; ^{1}H NMR (500 MHz, chloroform-*d*) δ 6.58 (s, 2H), 5.25 (s, 1H), 4.55 (s, 2H), 3.56–3.44 (m, 1H), 2.67 (ddd, *J* = 13.0, 10.8, 2.6 Hz, 1H), 2.51 (dd, *J* = 9.2, 6.9 Hz, 2H), 2.19–1.95 (m, 2H), 1.81 (ddd, *J* = 13.2, 6.1, 2.2 Hz, 1H), 1.76–1.63 (m, 1H), 1.63–1.51 (m, 7H), 1.42–1.17 (m, 29H), 0.88 (t, *J* = 6.9 Hz, 3H). ^{13}C NMR (126 MHz, chloroform-*d*) δ 176.8, 148.3, 142.1, 132.2, 126.3, 125.2, 110.9, 45.3, 39.3, 38.7, 35.5, 32.0, 31.0, 30.9, 29.7, 29.6, 29.5, 29.4, 27.4, 23.4, 22.8, 20.3, 14.3; TOF-MS (ESI+) *m*/*z* $[M+Na]^+$ calculated for $C_{34}H_{52}O_4Na$ $(M+Na)^+$ 547.3758, found 547.3759.

(1′S,2′S)-4-Isobutyl-5′-methyl-2′-(prop-1-en-2-yl)-1′,2′,3′,4′-tetrahydro-[1,1′-biphenyl]-2,6-diyl Bis(2,2-dimethylpropanoate).

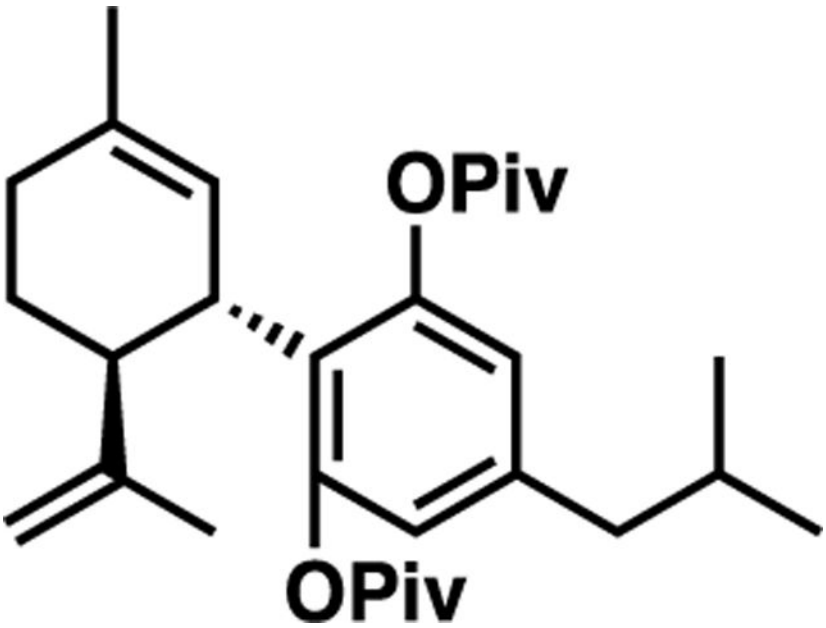

The general procedure above was followed using (1′*S*,2′*S*)-5′-methyl-2′-(prop-1-en-2-yl)-4-(((trifluoromethyl)sulfonyl)oxy)-1′,2′,3′,4′-tetrahydro-[1,1′-biphenyl]-2,6-diyl bis(2,2-dimethylpropanoate) (500 mg, 0.893 mmol). Complete conversion did not occur, and upon purification, [hexanes:Et_2O (9:1)] product and starting material were inseparable. Crude oil taken to next step without further purification.

R_f = 0.318 [hexanes:Et_2O (9:1)]; TOF-MS (ESI+) *m*/*z* $[M+Na]^+$ calculated for $C_{30}H_{44}O_4Na$ $(M+Na)^+$ 491.3132, found 491.3136.

(1′S,2′S)-4-(3,7-Dimethyloctyl)-5′-methyl-2′-(prop-1-en-2-yl)-1′,2′,3′,4′-tetrahydro-[1,1′-biphenyl]-2,6-diyl Bis(2,2-dimethylpropanoate).

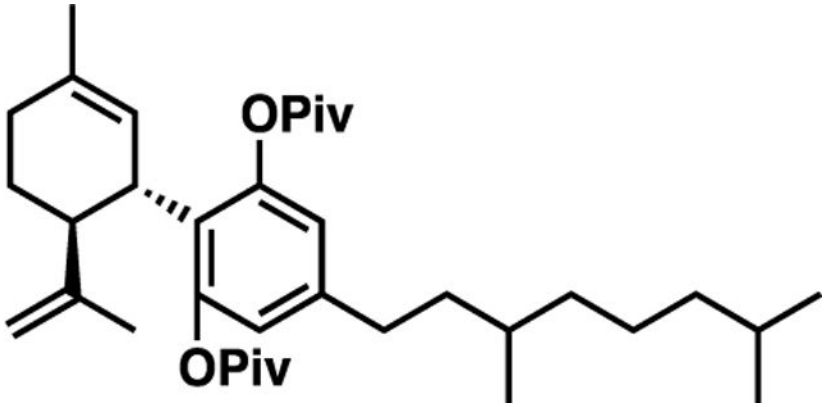

The general procedure above was followed using (1′*S*,2′*R*S-5′-methyl-2′-(prop-1-en-2-yl)-4-(((trifluoromethyl)sulfonyl)oxy)-1′,2′,3′,4′-tetrahydro-[1,1′-biphenyl]-2,6-diyl

bis(2,2-dimethylpropanoate) (500 mg, 0.893 mmol), which upon purification [hexanes:Et_2O (95:5)] produced a clear, colorless oil (412 mg, 0.745 mmol, 83%).

R_f = 0.586 [hexanes:Et_2O (7:1)]; ^{1}H NMR (500 MHz, chloroform-*d*) δ 6.59 (s, 2H), 5.26 (s, 1H), 4.56 (s, 2H), 3.52 (ddq, *J* = 11.0, 4.4, 2.3 Hz, 1H), 2.68 (ddd, *J* = 13.0, 10.5, 4.0 Hz, 1H), 2.63–2.43 (m, 2H), 2.12 (dt, *J* = 11.7, 5.7 Hz, 1H), 2.06–1.97 (m, 1H), 1.86–1.77 (m, 1H), 1.78–1.62 (m, 2H), 1.62 (d, *J* = 6.1 Hz, 3H), 1.54 (d, *J* = 4.0 Hz, 5H), 1.33 (d, *J* = 6.6 Hz, 24H), 1.19–1.07 (m, 3H), 0.87 (d, *J* = 6.6 Hz, 8H). ^{13}C NMR (126 MHz, chloroform-*d*) δ 176.7, 148.2, 142.3, 132.2, 126.3, 125.2, 123.7, 111.5, 110.9, 45.2, 39.4, 38.7, 38.3, 37.2, 33.0, 30.9, 29.7, 28.1, 27.3, 24.9, 23.4, 22.8, 22.8, 20.2, 19.7; TOF-MS (ESI+) *m*/*z* $[M+Na]^+$ calculated for $C_{36}H_{56}O_4Na$ $(M+Na)^+$ 575.4071; found 575.4073.

(1′*S*,2′*S*)-4-Isopropyl-5′-methyl-2′-(prop-1-en-2-yl)-1′,2′,3′,4′-tetrahydro-[1,1′-biphenyl]-2,6-diyl Bis(2,2-dimethylpropanoate).

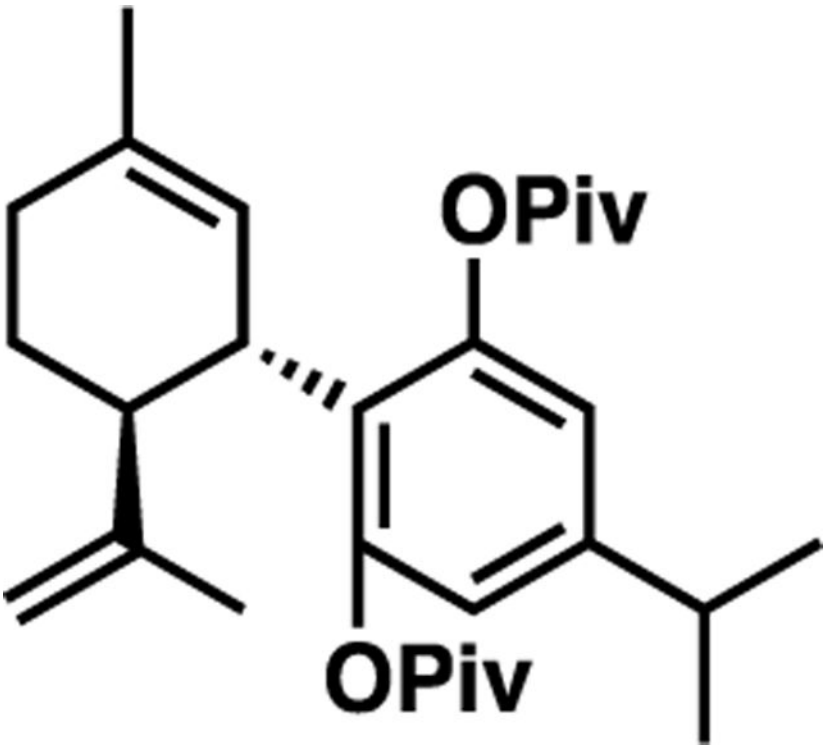

The general procedure above was followed using (1′*S*,2′*S*)-5′-methyl-2′-(prop-1-en-2-yl)-4-(((trifluoromethyl)sulfonyl)oxy)-1′,2′,3′,4′-tetrahydro-[1,1′-biphenyl]-2,6-diyl bis(2,2-dimethylpropanoate) (500 mg, 0.893 mmol), which upon purification [hexanes:Et_2O (93:7)] produced a clear, colorless oil (398 mg, 0.877 mmol, 98%).

R_f = 0.443 [hexanes:Et_2O (7:1)]; ^{1}H NMR (500 MHz, chloroform-*d*) δ 6.62 (s, 2H), 5.27 (s, 1H), 4.57 (dd, *J* = 7.0, 1.9 Hz, 2H), 3.52 (ddq, *J* = 11.0, 4.5, 2.3 Hz, 1H), 2.83 (p, *J* = 6.9 Hz, 1H), 2.69 (ddd, *J* = 13.2, 10.8, 2.6 Hz, 1H), 2.12 (ddd, *J* = 17.0, 11.0, 4.9 Hz, 1H), 2.02 (dd, *J* = 17.4, 6.0 Hz, 1H), 1.88–1.76 (m, 1H), 1.76–1.65 (m, 1H), 1.61 (d, *J* = 2.4 Hz, 3H), 1.55 (s, 3H), 1.35 (s, 18H), 1.22 (d, *J* = 6.9 Hz, 6H). ^{13}C NMR (126 MHz, chloroform-*d*) δ 176.6, 148.1, 147.8, 132.1, 126.4, 125.2, 110.8, 45.1, 39.2, 38.7, 33.5, 30.8, 29.7, 27.3, 23.6, 23.3,

20.2; TOF-MS (ESI+) *m*/*z* [M+Na]$^+$ calculated for $C_{29}H_{42}O_4Na$ (M+Na)$^+$ 477.2975; found 477.2976.

(1′S,2′S)-5′-Methyl-2′-(prop-1-en-2-yl)-4-vinyl-1′,2′,3′,4′-tetrahydro-[1,1′-biphenyl]-2,6-diyl Bis(2,2-dimethylpropanoate).

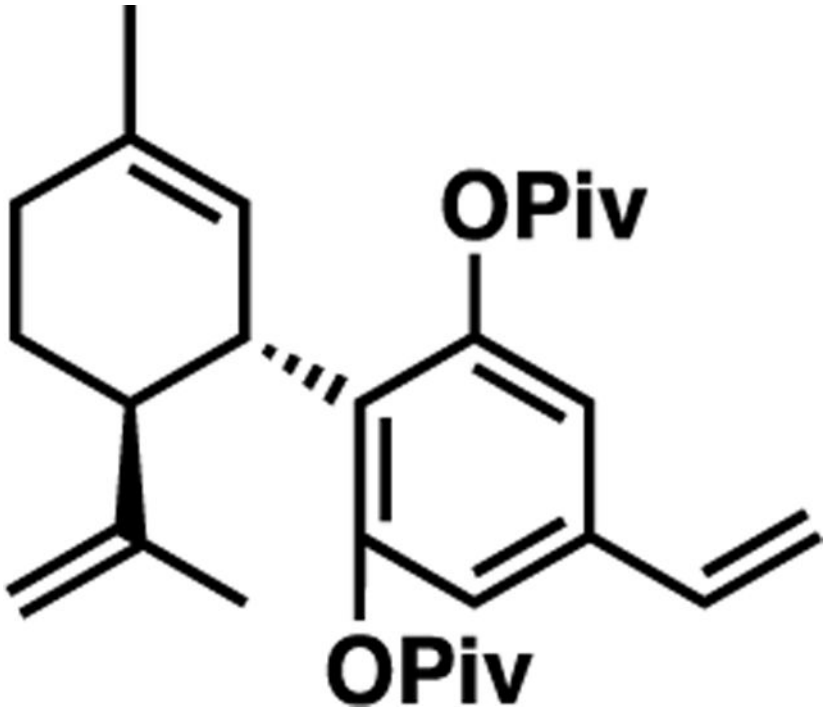

The general procedure above was followed using (1′*S*,2′*S*)-5′-methyl-2′-(prop-1-en-2-yl)-4-(((trifluoromethyl)sulfonyl)oxy)-1′,2′,3′,4′-tetrahydro-[1,1′-biphenyl]-2,6-diyl bis(2,2-dimethylpropanoate) (500 mg, 0.893 mmol), which upon purification [hexanes:Et_2O (95:5)] produced a clear, colorless oil (40 mg, 0.091 mmol, 10%).

R_f = 0.276 [hexanes:Et_2O (9:1)]; ^{1}H NMR (500 MHz, chloroform-*d*) *δ* 6.80 (s, 2H), 6.63–6.42 (m, 1H), 5.66 (d, *J* = 17.5 Hz, 1H), 5.24 (d, *J* = 10.9 Hz, 2H), 4.56 (d, *J* = 2.6 Hz, 2H), 3.54 (ddq, *J* = 11.1, 4.6, 2.4 Hz, 1H), 2.70 (ddd, *J* = 13.0, 10.7, 2.6 Hz, 1H), 2.20–1.95 (m, 2H), 1.91–1.76 (m, 1H), 1.77–1.64 (m, 1H), 1.61 (s, 3H), 1.55 (s, 3H), 1.35 (s, 18H). ^{13}C NMR (126 MHz, chloroform-*d*) *δ* 176.7, 148.0, 136.8, 135.4, 132.5, 128.9, 124.8, 115.0, 111.1, 45.3, 39.4, 38.8, 30.9, 29.7, 27.4, 23.4, 20.1; TOF-MS (ESI+) *m*/*z* [M+Na]$^+$ calculated for $C_{28}H_{38}O_4Na$ (M+Na)$^+$ 461.2667; found 461.2662.

(1′S,2′S)-4-Allyl-5′-methyl-2′-(prop-1-en-2-yl)-1′,2′,3′,4′-tetrahydro-[1,1′-biphenyl]-2,6-diyl Bis(2,2-dimethylpropanoate).

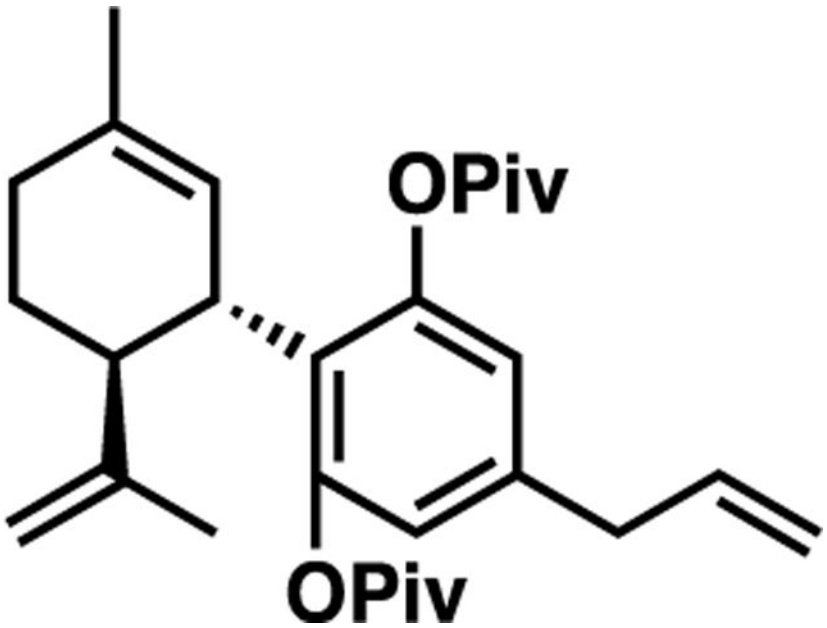

The general procedure above was followed using (1′*S*,2′*S*)-5′-methyl-2′-(prop-1-en-2-yl)-4-(((trifluoromethyl)sulfonyl)oxy)-1′,2′,3′,4′-tetrahydro-[1,1′-biphenyl]-2,6-diyl bis(2,2-dimethylpropanoate) (500 mg, 0.893 mmol), which upon purification [hexanes:Et_2O (95:5)] produced a clear, colorless oil (60 mg, 0.133 mmol, 15%). Characterization via GCMS revealed both *exo* and *endo* lipid tail formation (isomerization of allyl). Mixture was carried on to the next step.

R_f = 0.316 [hexanes:Et_2O (9:1)]; TOF-MS (ESI+) m/z $[M+Na]^+$ calculated for $C_{29}H_{40}O_4Na$ $(M+Na)^+$ 475.2819; found 475.2819.

General Procedure for Deprotection.

Synthesis was done as previously published with modifications.[30]

To a round-bottom flask under an inert atmosphere, piv-protected phenol (0.20 mmol) was dissolved in toluene (5 mL), and MeMgBr (3 M in hexanes, 1.0 mmol) was added dropwise at room temperature. The solution was then heated to 110 °C overnight. Upon cooling to room temperature, the reaction was quenched with saturated aqueous NH_4Cl (5 mL). The layers were separated, and the aqueous layer was washed with Et_2O (10 mL). Combined organic layers were washed with water (20 mL) and brine (20 mL), dried over $MgSO_4$, and concentrated *in vacuo*. The crude oil was purified via flash column chromatography.

(1′S,2′S)-4,5′-Dimethyl-2′-(prop-1-en-2-yl)-1′,2′,3′,4′-tetrahydro-[1,1′-biphenyl]-2,6-diol (JGC36).

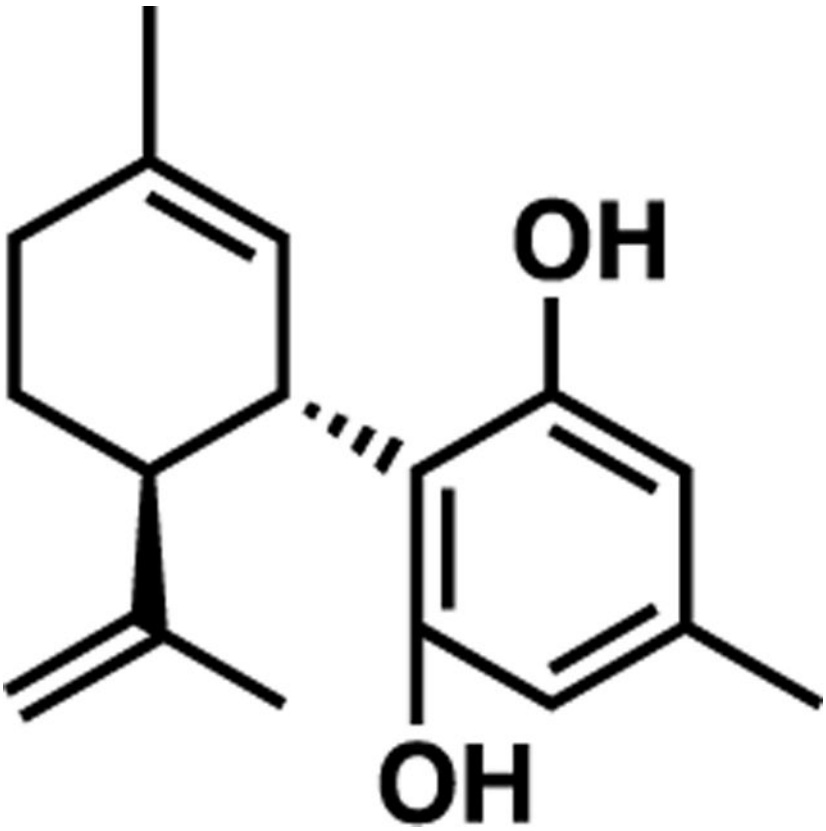

The general procedure above was followed using (1′*S*,2′*S*)-4,5′-dimethyl-2′-(prop-1-en-2-yl)-1′,2′,3′,4′-tetrahydro-[1,1′-biphenyl]-2,6-diyl bis(2,2-dimethylpropanoate) (306 mg, 0.717 mmol), which upon purification via flash column chromatography [hexanes:Et_2O (7:1)] produced a clear, colorless oil (71 mg, 0.275 mmol, 38%).

R_f = 0.219 [hexanes:Et_2O (7:1)]; ^{1}H NMR (500 MHz, chloroform-*d*) δ 6.21 (s, 1H), 6.20 (s, 1H), 5.96 (s, 1H), 5.59–5.49 (m, 1H), 4.80–4.49 (m, 2H), 3.85 (ddq, J = 9.1, 4.7, 2.4 Hz, 1H), 2.40 (td, J = 11.0, 3.4 Hz, 1H), 2.19 (s, 3H), 2.09 (ddt, J = 18.1, 5.2, 2.4 Hz, 1H), 1.91–1.73 (m, 6H), 1.66 (s, 3H). ^{13}C NMR (126 MHz, chloroform-*d*) δ 156.3, 149.5, 140.2, 138.0, 124.2, 113.7, 111.0, 108.8, 46.3, 37.2, 30.5, 28.6, 23.8, 21.2, 20.5; TOF-MS (APCI+) *m*/*z* $[M+H]^+$ calculated for $C_{17}H_{23}O_2$ $(M+H)^+$ 259.1693, found 259.1696.

(1′S,2′S)-4-Ethyl-5′-methyl-2′-(prop-1-en-2-yl)-1′,2′,3′,4′-tetrahydro-[1,1′-biphenyl]-2,6-diol (JGC37).

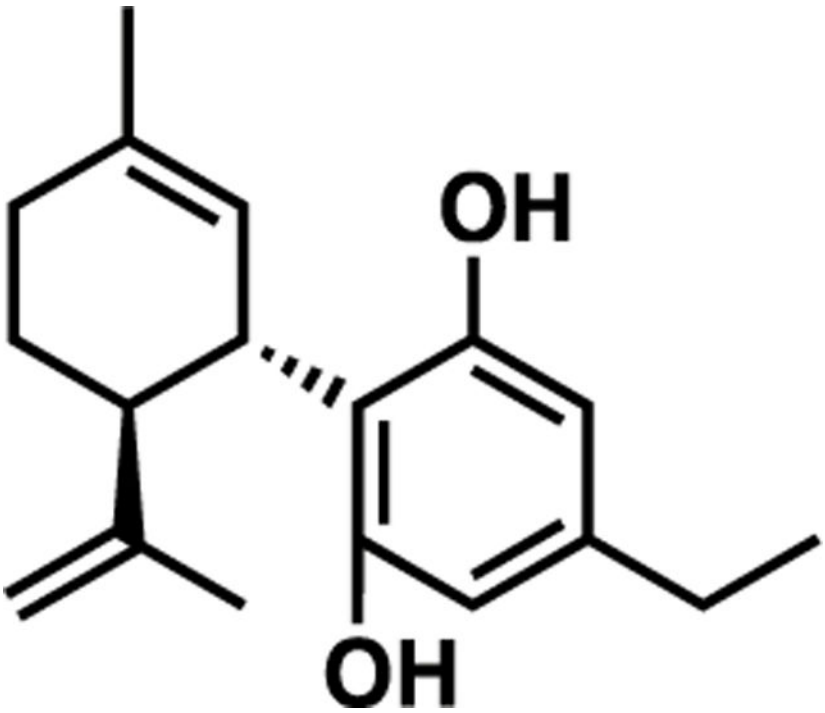

The general procedure above was followed using (1′*S*,2′*S*)-4-ethyl-5′-methyl-2′-(prop-1-en-2-yl)-1′,2′,3′,4′-tetrahydro-[1,1′-biphenyl]-2,6-diyl bis(2,2-dimethylpropanoate) (240 mg, 0.545 mmol), which upon purification via flash column chromatography [hexanes:Et_2O (7:1)] produced a clear, colorless oil (97.4 mg, 0.358 mmol, 66%).

R_f = 0.222 [hexanes:Et_2O (7:1)]; ^{1}H NMR (500 MHz, chloroform-*d*) δ 6.39–6.11 (m, 2H), 6.02 (s, 1H), 5.57 (d, *J* = 2.9 Hz, 1H), 4.66 (t, *J* = 1.7 Hz, 1H), 4.56 (d, *J* = 2.1 Hz, 1H), 3.95–3.82 (m, 1H), 2.49 (q, *J* = 7.6 Hz, 2H), 2.42 (td, *J* = 10.8, 3.4 Hz, 1H), 2.32–2.18 (m, 1H), 2.10 (ddt, *J* = 17.9, 5.0, 2.3 Hz, 1H), 1.81 (dd, *J* = 12.4, 3.1 Hz, 5H), 1.67 (s, 3H), 1.17 (t, *J* = 7.6 Hz, 3H). ^{13}C NMR (126 MHz, chloroform-*d*) δ 156.2, 149.3, 144.4, 140.1, 124.3, 113.9, 111.0, 109.3, 46.3, 37.2, 30.5, 28.5, 28.5, 23.8, 20.4, 15.1; TOF-MS (ESI+) *m*/*z* $[M+H]^+$ calculated for $C_{18}H_{23}O_2$ $(M+H)^+$ 273.1849, found 273.1848.

(1′S,2′S)-5′-Methyl-2′-(prop-1-en-2-yl)-4-propyl-1′,2′,3′,4′-tetrahydro-[1,1′-biphenyl]-2,6-diol (JGC38).

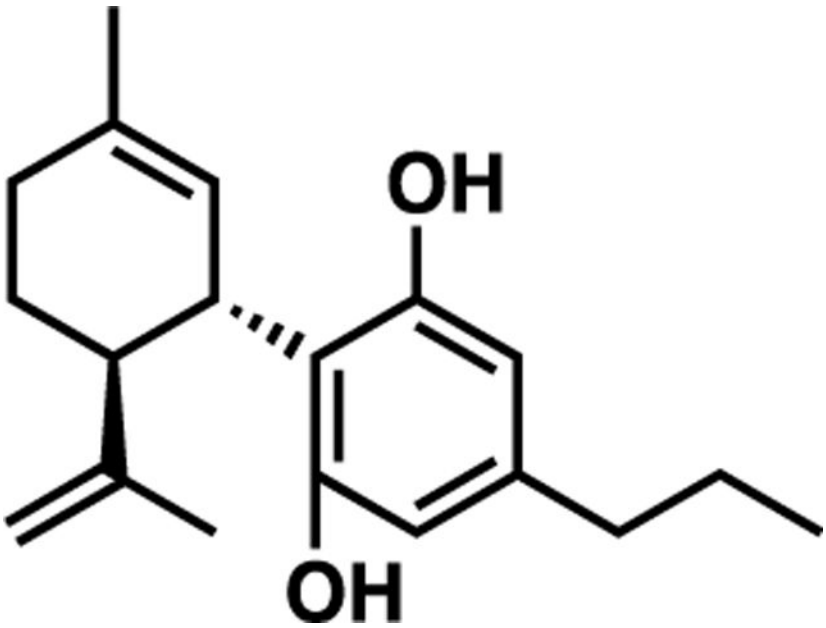

The general procedure above was followed using (1′*S*,2′*S*)-5′-methyl-2′-(prop-1-en-2-yl)-4-propyl-1′,2′,3′,4′-tetrahydro-[1,1′-biphenyl]-2,6-diyl bis(2,2-dimethylpropanoate) (150 mg, 0.330 mmol), which upon purification via flash column chromatography [hexanes:Et_2O (7:1)] produced a clear, colorless oil (90 mg, 0.314 mmol, 96%).

R_f = 0.429 [hexanes:Et_2O (7:1)]; ^{1}H NMR (500 MHz, chloroform-*d*) δ 6.41–6.02 (m, 2H), 5.57 (s, 1H), 4.66 (t, J = 2.0 Hz, 1H), 4.56 (d, J = 2.1 Hz, 1H), 3.86 (ddq, J = 8.6, 4.5, 2.2 Hz, 1H), 2.41 (q, J = 10.8, 9.1 Hz, 3H), 2.31–2.13 (m, 1H), 2.10 (ddt, J = 18.0, 4.9, 2.4 Hz, 1H), 1.86–1.74 (m, 3H), 1.67 (d, J = 10.1 Hz, 3H), 1.58 (h, J = 7.4 Hz, 2H), 1.45–1.22 (m, 2H), 0.90 (t, J = 7.3 Hz, 3H). ^{13}C NMR (126 MHz, chloroform-*d*) δ 154.3, 149.4, 142.9, 140.3, 124.2, 113.9, 111.0, 110.2, 46.3, 37.7, 37.3, 30.5, 28.5, 24.2, 23.8, 20.6, 13.9; TOF-MS (ESI+) *m*/*z* $[M+H]^+$ calculated for $C_{19}H_{27}O_2$ $(M+H)^+$ 287.2006, found 287.2006.

(1′S,2′S)-4-Butyl-5′-methyl-2′-(prop-1-en-2-yl)-1′,2′,3′,4′-tetrahydro-[1,1′-biphenyl]-2,6-diol (JGC39).

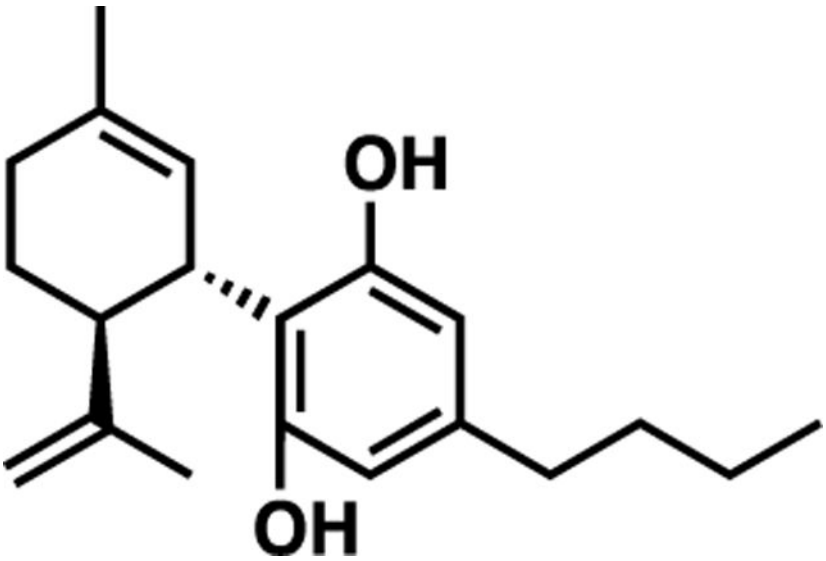

The general procedure above was followed using (1′*S*,2′*S*)-4-butyl-5′-methyl-2′-(prop-1-en-2-yl)-1′,2′,3′,4′-tetrahydro-[1,1′-biphenyl]-2,6-diyl bis(2,2-dimethylpropanoate) (390 mg, 0.832 mmol), which upon purification via flash column chromatography [hexanes:Et_2O (7:1)] produced a clear, colorless oil (91 mg, 0.303 mmol, 78%).

R_f = 0.273 [hexanes:Et_2O (7:1)]; ^{1}H NMR (500 MHz, chloroform-*d*) δ 6.35–6.08 (m, 2H), 5.99 (s, 1H), 5.62–5.52 (m, 1H), 4.66 (t, *J* = 1.8 Hz, 1H), 4.56 (d, *J* = 1.8 Hz, 1H), 3.85 (ddq, *J* = 9.0, 4.7, 2.3 Hz, 1H), 2.48–2.43 (m, 2H), 2.40 (td, *J* = 11.0, 3.4 Hz, 1H), 2.32–2.13 (m, 1H), 2.10 (ddt, *J* = 18.0, 5.1, 2.4 Hz, 1H), 1.87–1.74 (m, 4H), 1.66 (s, 2H), 1.61–1.49 (m, 3H), 1.38–1.23 (m, 3H), 0.90 (t, *J* = 7.4 Hz, 3H). ^{13}C NMR (126 MHz, chloroform-*d*) δ 156.2, 149.5, 143.2, 140.2, 124.2, 113.9, 110.9, 109.9, 46.3, 37.4, 35.3, 33.2, 30.5, 28.6, 23.8, 22.5, 20.7, 14.1; TOF-MS (ESI+) *m*/*z* $[M+Na]^+$ calculated for $C_{20}H_{28}O_2Na$ $(M+Na)^+$ 323.1982, found 323.1981.

(1′S,2′S)-4-Hexyl-5′-methyl-2′-(prop-1-en-2-yl)-1′,2′,3′,4′-tetrahydro-[1,1′-biphenyl]-2,6-diol (JGC40).

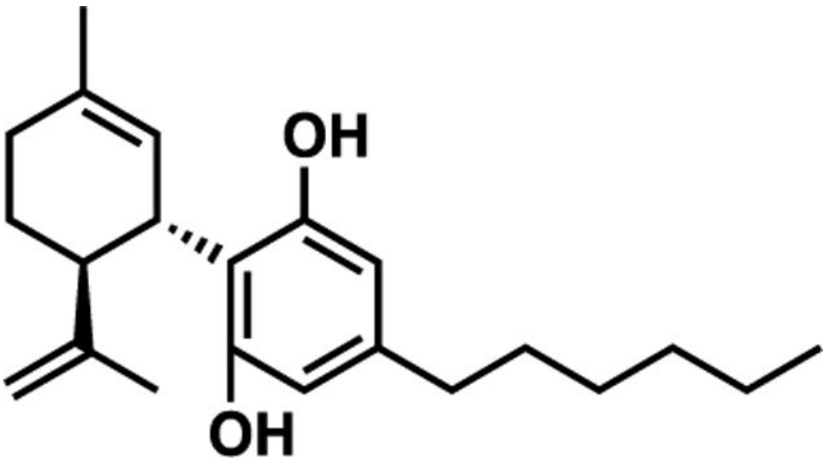

The general procedure above was followed using (1′*S*,2′*S*)-4-hexyl-5′-methyl-2′-(prop-1-en-2-yl)-1′,2′,3′,4′-tetrahydro-[1,1′-biphenyl]-2,6-diyl bis(2,2-dimethylpropanoate) (340 mg, 0.685 mmol), which upon purification via flash column chromatography [hexanes:Et_2O (7:1)] produced a clear, colorless oil (76.5 mg, 0.233 mmol, 34%).

R_f = 0.333 [hexanes:Et_2O (7:1)]; ^{1}H NMR (500 MHz, chloroform-*d*) *δ* 6.37–6.08 (m, 2H), 6.09–5.86 (m, 1H), 5.57 (d, *J* = 2.9 Hz, 1H), 4.66 (t, *J* = 1.8 Hz, 1H), 4.56 (d, *J* = 2.0 Hz, 1H), 3.86 (ddq, *J* = 9.2, 4.7, 2.4 Hz, 1H), 2.54–2.29 (m, 3H), 2.22 (dddd, *J* = 25.4, 15.7, 8.7, 4.1 Hz, 1H), 2.10 (ddt, *J* = 17.9, 5.0, 2.4 Hz, 1H), 1.90–1.72 (m, 5H), 1.66 (s, 2H), 1.62–1.47 (m, 2H), 1.38–1.19 (m, 7H), 0.94–0.79 (m, 3H). ^{13}C NMR (126 MHz, chloroform-*d*) *δ* 156.2, 149.5, 143.2, 140.2, 124.3, 113.9, 110.9, 110.2, 46.3, 37.4, 35.7, 31.9, 31.1, 30.5, 29.1, 28.5, 23.8, 22.7, 20.6, 14.2; TOF-MS (ESI+) *m*/*z* $[M+H]^+$ calculated for $C_{22}H_{33}O_2$ $(M+H)^+$ 329.2475, found 329.2476.

(1′S,2′S)-4-Heptyl-5′-methyl-2′-(prop-1-en-2-yl)-1′,2′,3′,4′-tetrahydro-[1,1′-biphenyl]-2,6-diol (JGC41).

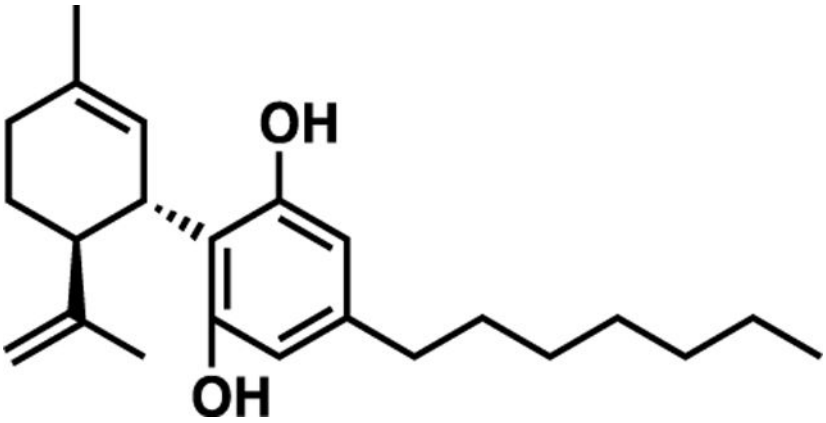

The general procedure above was followed using (1′*S*,2′*S*)-4-heptyl-5′-methyl-2′-(prop-1-en-2-yl)-1′,2′,3′,4′-tetrahydro-[1,1′-biphenyl]-2,6-diyl bis(2,2-dimethylpropanoate) (300

mg, 0.588 mmol), which upon purification via flash column chromatography [hexanes:Et_2O (7:1)] produced a clear, colorless oil (99.2 mg, 0.290 mmol, 49%).

R_f = 0.371 [hexanes:Et_2O (7:1)]; ^{1}H NMR (500 MHz, chloroform-*d*) δ 6.40–5.80 (m, 3H), 5.57 (d, J = 2.9 Hz, 1H), 4.66 (t, J = 1.8 Hz, 1H), 4.56 (d, J = 2.0 Hz, 1H), 3.86 (ddt, J = 10.8, 4.5, 2.2 Hz, 1H), 2.49–2.42 (m, 2H), 2.39 (dd, J = 10.8, 3.4 Hz, 1H), 2.23 (dtd, J = 15.7, 9.6, 4.5 Hz, 1H), 2.10 (ddt, J = 17.8, 5.0, 2.4 Hz, 1H), 1.93–1.72 (m, 5H), 1.66 (s, 2H), 1.56 (h, J = 7.1, 6.1 Hz, 2H), 1.28 (dt, J = 12.5, 3.7 Hz, 9H), 0.88 (t, J = 6.9 Hz, 3H). ^{13}C NMR (126 MHz, chloroform-*d*) δ 154.0, 149.4, 143.2, 140.2, 124.3, 113.9, 110.9, 109.9, 46.3, 37.4, 35.7, 31.9, 31.1, 30.5, 29.4, 29.3, 28.5, 23.8, 22.8, 20.6, 14.2; TOF-MS (ESI+) m/z $[M+H]^+$ calculated for $C_{23}H_{35}O_2$ $(M+H)^+$ 343.2632; found 343.2632.

(1′S,2′S)-5′-Methyl-4-octyl-2′-(prop-1-en-2-yl)-1′,2′,3′,4′-tetrahydro-[1,1′-biphenyl]-2,6-diol (JGC42).

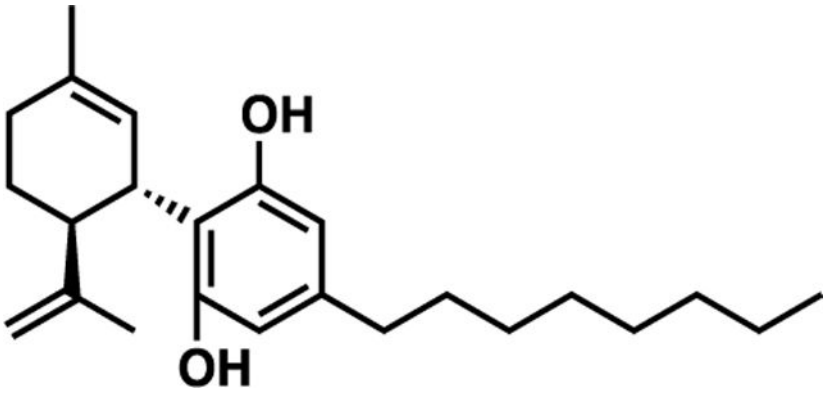

The general procedure above was followed using (1′*S*,2′*S*)-5′-methyl-4-octyl-2′-(prop-1-en-2-yl)-1′,2′,3′,4′-tetrahydro-[1,1′-biphenyl]-2,6-diyl bis(2,2-dimethylpropanoate) (360 mg, 0.687 mmol), which upon purification via flash column chromatography [hexanes:Et_2O (7:1)] produced a clear, colorless oil (77 mg, 0.216 mmol, 31%).

R_f = 0.536 [hexanes:Et_2O (7:1)]; ^{1}H NMR (500 MHz, chloroform-*d*) δ 6.37–6.07 (m, 2H), 5.98 (s, 1H), 5.57 (d, J = 2.7 Hz, 1H), 4.66 (t, J = 1.8 Hz, 1H), 4.56 (d, J = 2.0 Hz, 1H), 3.96–3.65 (m, 1H), 2.47–2.41 (m, 2H), 2.39 (dd, J = 10.8, 3.4 Hz, 1H), 2.23 (dtd, J = 24.5, 9.5, 8.7, 5.1 Hz, 1H), 2.10 (ddt, J = 17.8, 4.9, 2.3 Hz, 1H), 1.91–1.72 (m, 5H), 1.66 (s, 2H), 1.55 (t, J = 7.6 Hz, 2H), 1.27 (dd, J = 10.2, 3.6 Hz, 11H), 0.88 (t, J = 6.8 Hz, 3H). ^{13}C NMR (126 MHz, chloroform-*d*) δ 156.2, 149.5, 143.2, 140.2, 124.3, 113.9, 110.9, 109.9, 46.3, 37.4, 35.7, 32.0, 31.1, 30.5, 29.6, 29.4, 29.4, 28.5, 23.8, 22.8, 20.7, 14.3; TOF-MS (ESI+) m/z $[M+H]^+$ calculated for $C_{24}H_{37}O_2$ $(M+H)^+$ 357.2788, found 357.2788.

(1′S,2′S)-4-Isobutyl-5′-methyl-2′-(prop-1-en-2-yl)-1′,2′,3′,4′-tetrahydro-[1,1′-biphenyl]-2,6-diol (JGC45).

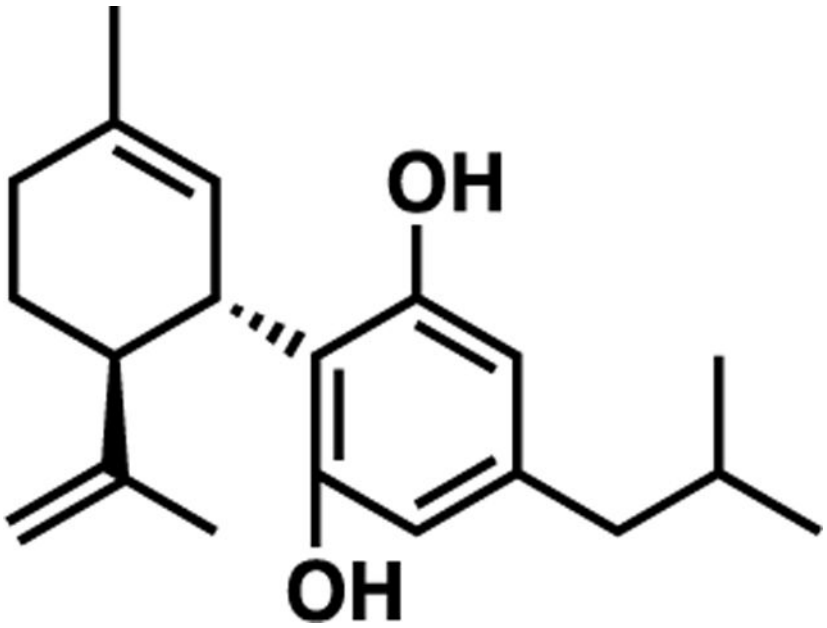

The general procedure above was followed using (1′*S*,2′*S*)-4-isobutyl-5′-methyl-2′-(prop-1-en-2-yl)-1′,2′,3′,4′-tetrahydro-[1,1′-biphenyl]-2,6-diyl bis(2,2-dimethylpropanoate) (244 mg, 0.520 mmol), which upon purification via flash column chromatography [hexanes:Et_2O (7:1)] produced a clear, colorless oil (42 mg, 0.140 mmol, 57%).

R_f = 0.306 [hexanes:Et_2O (7:1)]; ^{1}H NMR (500 MHz, chloroform-*d*) δ 6.10 (s, 1H), 6.09 (s, 1H), 5.88 (s, 1H), 5.48 (d, J = 2.5 Hz, 1H), 4.67–4.34 (m, 2H), 3.74 (ddq, J = 10.8, 4.5, 2.4 Hz, 1H), 2.35–2.08 (m, 4H), 2.00 (ddt, J = 17.8, 4.9, 2.4 Hz, 1H), 1.84–1.63 (m, 6H), 1.55 (s, 2H), 0.77 (d, J = 6.6 Hz, 6H). ^{13}C NMR (126 MHz, chloroform-*d*) δ 154.1, 149.6, 142.0, 140.3, 124.2, 113.9, 110.9, 108.9, 46.3, 45.2, 37.5, 30.6, 30.0, 28.5, 23.8, 22.6, 22.6, 20.8; TOF-MS (APCI+) *m*/*z* $[M+H]^+$ calculated for $C_{20}H_{29}O_2$ $(M+H)^+$ 301.2162, found 301.2165.

(1′S,2′S)-4-(3,7-Dimethyloctyl)-5′-methyl-2′-(prop-1-en-2-yl)-1′,2′,3′,4′-tetrahydro-[1,1′-biphenyl]-2,6-diol (JGC46).

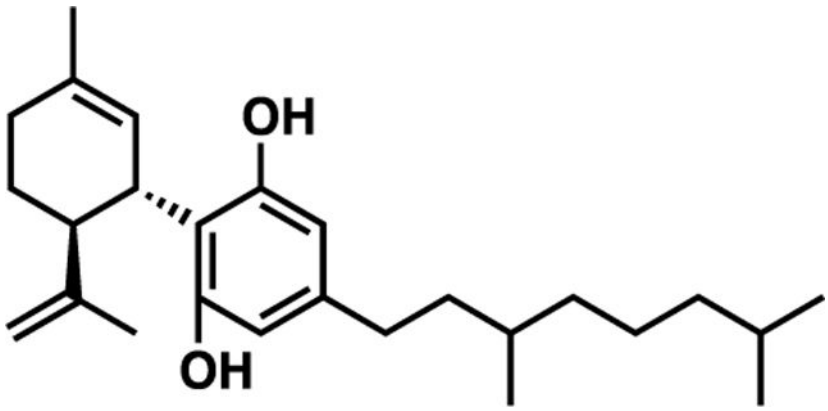

The general procedure above was followed using (1′*S*,2′*S*)-4-(3,7-dimethyloctyl)-5′-methyl-2′-(prop-1-en-2-yl)-1′,2′,3′,4′-tetrahydro-[1,1′-biphenyl]-2,6-diyl bis(2,2-dimethylpropanoate) (412 mg, 0.745 mmol), which upon purification via flash column chromatography [hexanes:Et_2O (7:1)] produced a clear, colorless oil (40.2 mg, 0.105 mmol, 25%).

R_f = 0.457 [hexanes:Et_2O (7:1)]; ^{1}H NMR (500 MHz, chloroform-*d*) δ 6.39–6.07 (m, 2H), 5.96 (s, 1H), 5.57 (s, 1H), 4.67 (t, *J* = 2.1 Hz, 1H), 4.56 (s, 1H), 3.91–3.72 (m, 1H), 2.57–2.30 (m, 3H), 2.23 (t, *J* = 15.2 Hz, 1H), 2.10 (ddd, *J* = 17.8, 5.4, 2.6 Hz, 1H), 1.88–1.72 (m, 5H), 1.65 (s, 3H), 1.53 (ddt, *J* = 22.1, 8.7, 4.8 Hz, 1H), 1.40 (dt, *J* = 15.2, 9.4 Hz, 1H), 1.34–1.18 (m, 5H), 1.18–1.04 (m, 3H), 0.95–0.74 (m, 9H). ^{13}C NMR (126 MHz, chloroform-*d*) δ 149.6, 143.5, 140.2, 124.2, 113.8, 110.9, 46.3, 39.5, 38.5, 37.5, 37.3, 33.2, 32.6, 30.6, 29.9, 28.6, 28.1, 24.8, 23.8, 22.9, 22.8, 20.7, 19.8; TOF-MS (ESI+) *m*/*z* $[M+H]^+$ calculated for $C_{26}H_{41}O_2$ $(M+H)^+$ 385.3101, found 385.3101.

(1′S,2′S)-4-Isopropyl-5′-methyl-2′-(prop-1-en-2-yl)-1′,2′,3′,4′-tetrahydro-[1,1′-biphenyl]-2,6-diol (JGC47).

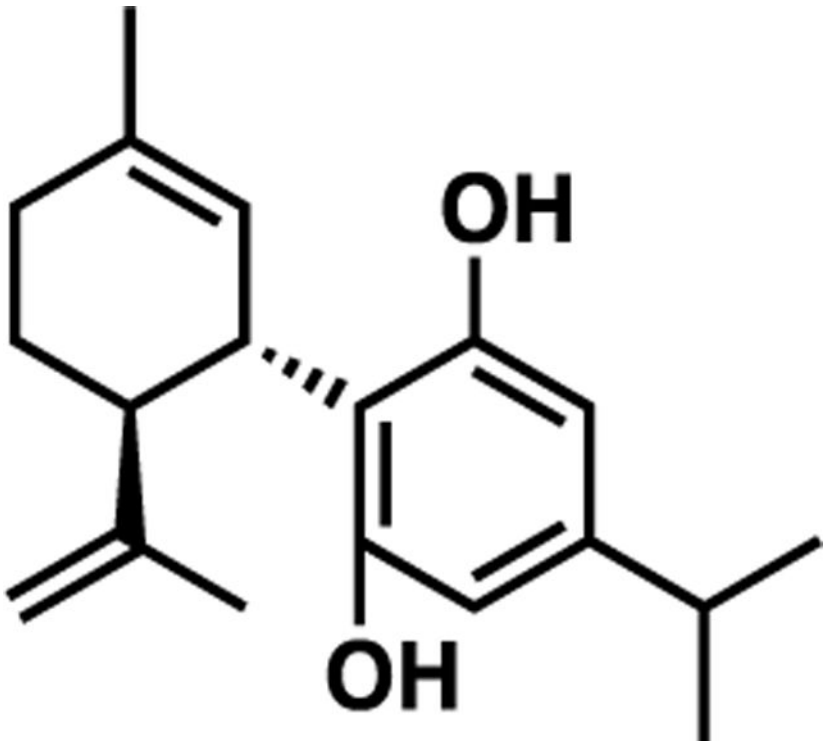

The general procedure above was followed using (1′*S*,2′*S*)-4-(3,7-dimethyloctyl)-5′-methyl-2′-(prop-1-en-2-yl)-1′,2′,3′,4′-tetrahydro-[1,1′-biphenyl]-2,6-diyl bis(2,2-dimethylpropanoate) (398 mg, 0.877 mmol), which upon purification via flash column chromatography [hexanes:Et_2O (7:1)] produced a clear, colorless oil (140 mg, 0.489 mmol, 56%).

R_f = 0.357 [hexanes:Et_2O (7:1)]; ^{1}H NMR (500 MHz, chloroform-*d*) δ 6.27 (s, 1H), 6.26 (s, 1H), 5.98 (s, 1H), 5.65–5.49 (m, 1H), 4.63 (dd, *J* = 50.0, 1.8 Hz, 2H), 3.84 (ddt, *J* = 11.0, 4.3, 2.4 Hz, 1H), 2.74 (p, *J* = 6.9 Hz, 1H), 2.49–2.32 (m, 1H), 2.32–2.17 (m, 1H), 2.10 (ddt, *J* = 17.9, 5.0, 2.3 Hz, 1H), 1.81 (dd, *J* = 15.1, 2.8 Hz, 5H), 1.66 (s, 3H), 1.18 (d, *J* = 6.8 Hz, 6H). ^{13}C NMR (126 MHz, chloroform-*d*) δ 149.7, 149.3, 140.3, 124.2, 113.9, 110.9, 106.3, 46.2, 37.5, 33.8, 30.5, 28.6, 23.9, 23.8, 23.8, 20.8; TOF-MS (APCI+) *m*/*z* $[M+H]^+$ calculated for $C_{19}H_{27}O_2$ $(M+H)^+$ 287.2006, found 287.2008.

(1′S,2′S)-5′-Methyl-2′-(prop-1-en-2-yl)-4-vinyl-1′,2′,3′,4′-tetrahydro-[1,1′-biphenyl]-2,6-diol (JGC43).

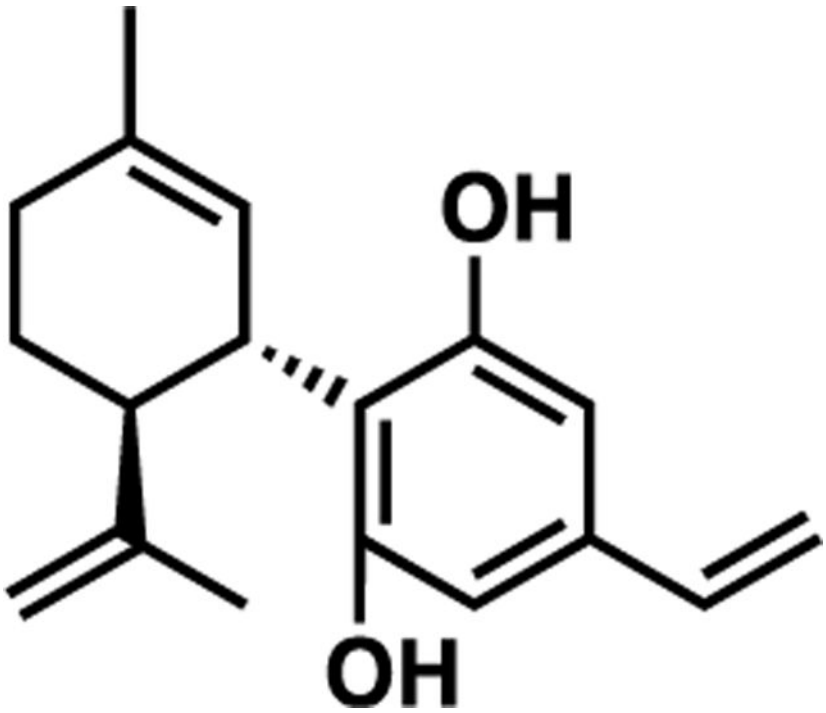

The general procedure above was followed using (1′*S*,2′*S*)-5′-methyl-2′-(prop-1-en-2-yl)-4-vinyl-1′,2′,3′,4′-tetrahydro-[1,1′-biphenyl]-2,6-diyl bis(2,2-dimethylpropanoate) (40 mg, 0.091 mmol), which upon purification via flash column chromatography [hexanes:Et_2O (7:1)] produced a clear, colorless oil (10.1 mg, 0.037 mmol, 41%).

R_f = 0.154 [hexanes:Et_2O (7:1)]; ^{1}H NMR (500 MHz, chloroform-*d*) δ 6.60–6.19 (m, 2H), 5.65 (dd, *J* = 17.6, 0.9 Hz, 1H), 5.60–5.50 (m, 1H), 5.18 (dd, *J* = 10.8, 0.9 Hz, 1H), 4.66 (h, *J* = 1.7 Hz, 1H), 4.57 (dd, *J* = 5.3, 1.7 Hz, 1H), 3.86 (tdd, *J* = 10.4, 4.6, 2.1 Hz, 1H), 2.50 (q, *J* = 7.6 Hz, 1H), 2.41 (tdd, *J* = 10.6, 7.2, 3.4 Hz, 1H), 2.30–2.15 (m, 1H), 2.11 (ddd, *J* = 18.1, 5.4, 2.7 Hz, 1H), 1.80 (t, *J* = 3.5 Hz, 5H), 1.67 (t, *J* = 1.1 Hz, 3H). ^{13}C NMR (126 MHz, chloroform-*d*) δ 149.3, 140.6, 137.5, 136.4, 124.2, 123.8, 116.6, 113.9, 111.2, 111.0, 46.2, 37.5, 30.6, 29.9, 28.5, 23.9; TOF-MS (ESI−) *m*/*z* $[M-H]^-$ calculated for $C_{18}H_{21}O_2$ $[M-H]^-$ 269.1547, found 269.1542.

(1′S,2′S)-4-Allyl-5′-methyl-2′-(prop-1-en-2-yl)-1′,2′,3′,4′-tetrahydro-[1,1′-biphenyl]-2,6-diol (JGC44).

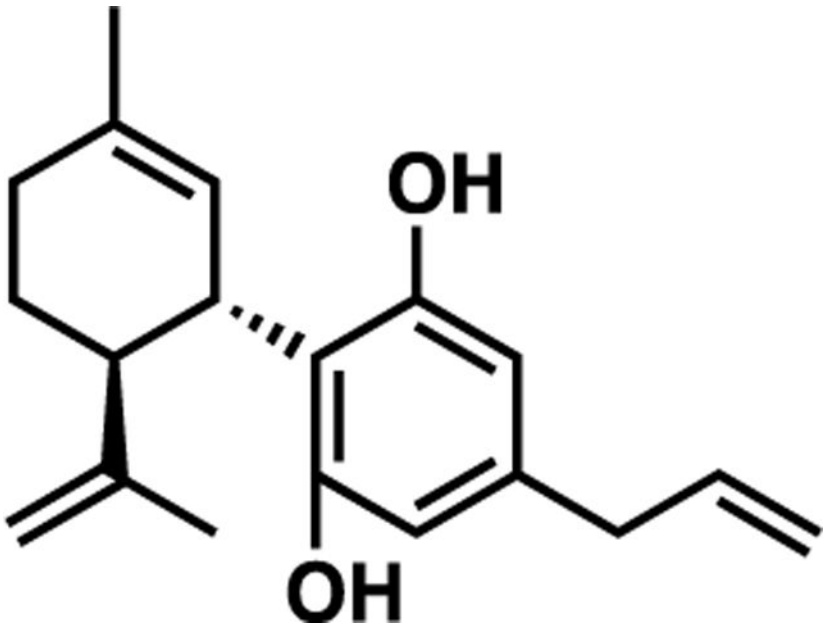

The general procedure above was followed using (1′*S*,2′*S*)-4-allyl-5′-methyl-2′-(prop-1-en-2-yl)-1′,2′,3′,4′-tetrahydro-[1,1′-biphenyl]-2,6-diyl bis(2,2-dimethylpropanoate) (60 mg, 0.133 mmol), which upon purification via flash column chromatography [hexanes:Et_2O (7:1)] produced a clear, colorless oil (17.1 mg, 0.060 mmol, 45%).

R_f = 0.194 [hexanes:Et_2O (7:1)]; ^{1}H NMR (500 MHz, chloroform-*d*) δ 6.40–6.09 (m, 2H), 6.08–5.84 (m, 2H), 5.56 (d, J = 2.8 Hz, 1H), 5.16–4.91 (m, 2H), 4.79–4.39 (m, 2H), 3.86 (ddq, J = 10.9, 4.6, 2.4 Hz, 1H), 3.23 (d, J = 6.7 Hz, 2H), 2.40 (td, J = 11.0, 3.4 Hz, 1H), 2.31–2.14 (m, 1H), 2.10 (ddt, J = 17.8, 4.9, 2.3 Hz, 1H), 1.91–1.62 (m, 5H), 1.66 (s, 2H). ^{13}C NMR (126 MHz, chloroform-*d*) δ 156.5, 149.4, 140.3, 140.3, 137.2, 124.1, 116.0, 114.4, 111.1, 110.2, 46.3, 39.9, 37.3, 30.5, 28.5, 23.8, 20.6; TOF-MS (ESI−) m/z $[M-H]^-$ calculated for $C_{19}H_{23}O_2$ $[M-H]^-$ 283.1704, found 283.1699.

Pink Flamindo cAMP Assay Cell Culture and Transfection.

HEK293 cells were cultured in high-glucose Dulbecco's Modified Eagle Medium (Thermo Fisher Scientific) supplemented with 10% fetal bovine serum and a 1% Pen/Strep solution. Cultures were maintained at 37 °C with an atmosphere of 5% CO_2. For the imaging experiments, the cells were dissociated using trypsin–EDTA (0.05%) and cultured on poly-D-lysine precoated 18 mm glass coverslips in 12-well plates. One day post-plating, the cells were transfected with the human-derived μOR (hμOR), the fluorescent protein EYFP, and the red fluorescent cAMP indicator, Pink Flamindo,[62] using Lipofectamine 2000 Transfection Reagent (Thermo Fisher Scientific). After 3.5 h, the transfection reagent was replaced with cell culture media and the cells used for experiments within two days of transfection.

Cell Imaging and cAMP Binding Assay.

Transfected HEK293 cells were imaged in an extracellular solution containing (mM) NaCl 119, KCl 5, $CaCl_2$ 2, $MgCl_2$ 1, glucose 30, and HEPES 20, pH 7.4, using a Nikon inverted microscope fitted with a Hamamatsu Flash 4 camera and Nikon Elements AR acquisition software. Drugs were initially prepared as a stock in DMSO or ethanol, diluted using extracellular solution to their final concentration, and then used on the same day. For experiments using the HEK293 cells, the test compounds were coapplied with μOR agonists [D-Ala,[2] N-MePhe,[4] Gly-ol]-enkephalin (DAMGO; EC_{100}: 250 nM[38]) or fentanyl (EC_{95}; 500pM), followed several minutes later by the adenylyl cyclase activator, forskolin (Fsk; 100 μM). Images were acquired every 30 s for 15 min and then analyzed using FIJI software (https://imagej.net/software/fiji/downloads) with the 1-click ROI manager plugin,[63] to measure changes in fluorescence intensity. Target cells were chosen by taking the first image in the series, increasing the brightness, and marking cells that exhibited a baseline Pink Flamindo fluorescence. Occasional (<5%) cells exhibited a high-baseline fluorescence relative to the general transfected cell population. These cells were excluded from analysis since they were close to saturation. This mask of identified cells (typically 15–25 per experiment) was then applied to the image series. Baseline fluorescence intensity was normalized to 100 based on the first 2 min of the time series. Each plotted point on a time series represents the average fluorescent intensity (AFI) +/− SEM of 3 independent experiments, at a specific time point.

DAMGO-Activation Experiments.

For our DAMGO-activation experiments, a drug concentration series for (–)-CBD (5 nM-5 μM) was coadministered with DAMGO (250 nM) in hμOR-HEK293 cells. From this, an IC_{50} value was calculated using area under the curve (AUC) analysis and nonlinear regression for time points from 0 to 15 min. Following this, each synthetic CBD analog (JGC*x*) in the library was screened at a concentration of 500 nM and compared to that of (–)-CBD.

Fentanyl-Activation Experiments.

Following the DAMGO activation experiments, (–)-CBD and 15 CBD analogs (JGC*x*) were chosen to be tested in fentanyl-activation experiments. An EC_{95} for fentanyl was calculated by testing a fentanyl drug concentration series (60 pM–650 nM) in hμOR-HEK293 cells. The fentanyl EC_{95} (500pM) was then tested against a drug concentration series of (–)-CBD/JGC*x*/naloxone (1 nM-10 μM), to determine an IC_{50} for each compound against fentanyl.

Competitive vs Noncompetitive μOR Antagonism Experiments.

In a separate set of experiments, hμOR-transfected HEK293 cells were pretreated with the EC_{95} for fentanyl (500pM), followed several minutes later by Fsk (100 μM), plus either one of the two most potent CBD analogs (JGC*x*; 1 μM), (–)-CBD (1 μM), or naloxone (1 μM), or both (JGC*x*/(–)-CBD (1 μM) + naloxone (1 μM)). Data were acquired and analyzed using the same methodology as described above.

Statistics.

Statistically significant differences in these responses were taken as nonoverlapping 95% confidence intervals. For a given experimental treatment, a same-day Fsk-only experimental control was included, and the experimental results were compared to their respective same-day controls using an unpaired *t*-test. Calculations of the EC_{95} for fentanyl, and the IC_{50}'s for naloxone, (–)-CBD, and the 15 CBD analogs (JGC*x*) tested in this assay, were done using GraphPad Prism 9.

Materials.

Drugs: fentanyl citrate was purchased from BioSupply (Temecula, CA). Forskolin and naloxone were purchased from Cayman Chemical (Ann Arbor, MI). Stocks (10 mM) of DAMGO (in DMSO), naloxone (in DMSO), and (–)-CBD (in ethanol) were stored at −80 °C and diluted shortly before use. Our CBD (JGC*x*) compounds were initially prepared as a stock in DMSO and then diluted using extracellular solution to their final concentration shortly before use.

Molecular Modeling.

The putative (–)-CBD binding sites was identified within the X-ray crystal structures of the μOR bound to a morphinan agonist (BU72, PDB 5C1ML)[41] and an irreversible antagonist (β-FNA, PDB 4DKL)[40] using AutoSite.[39] Autodock Vina[42] was used to identify favorable binding interactions formed by (–)-CBD within the extracellular vestibule. For the active structure, docking was carried out using a modified model based on PDB 5C1ML in which the first 58 residues of the N-terminal loop were deleted to prevent occlusion of the putative allosteric pocket. Protein models were prepared for docking by selecting flexible residues and adding Gasteiger-Marsili charges to the protein and saving coordinates for flexible residues and rigid residues in Autodock's PDBQT format. Docking box sizes around the target sites were defined in Autodock Tools. Initial three-dimensional coordinates for 14 ligand models for compounds for which IC_{50} measurements were available were built using Avogadro, followed by 10,000 steps of steepest-descent energy minimization using the MMFF94 force field in Avogadro. MOL2 files from Avogadro were converted to PDBQT-format models with Gasteiger-Marsili charges and rotatable torsions using Autodock Tools. Autodock Vina docking was performed with exhaustiveness parameter set to 25. After obtaining docking results, poses were evaluated by estimating binding free energies using an artificial neural network trained on known binding affinities associated with known structures of ligand-protein complexes, K_{DEEP}.[43] KDEEP predictions allow us to rank the binding poses and predict the binding affinity of CBD analogs to guide further efforts to optimize for the ability to displace fentanyl. A total of 9 docking solutions (poses) were obtained per compound, per mu-opioid receptor conformation. Poses for post-processing were selected by visual examination of all 14 × 9 = 126 possible poses. Docked ligand conformations within the receptors were variable, especially for poses within the active-state conformation. Therefore, a consensus pose with the limonene moiety situated within a pocket between transmembrane helices 1, 2, and 3 and with the alkyl chain below extracellular loop 2 near transmembrane helices 4 and 5 was chosen. In cases where this pose was not attained, the pose with the closest similarity was chosen. From this process, 14

poses were selected for post-processing with K_{DEEP}. Flexible residues were reincorporated into the receptor structure, and PDBQT files were converted to PDB structures using a custom Python script. Ligands were converted from PDBQT to MOL2 format using Avogadro.[64]

Supplementary Material

Refer to Web version on PubMed Central for supplementary material.

ACKNOWLEDGMENTS

This work was supported by the National Institutes of Health National Institute on Drug Abuse [Grant DA024628] and by the Indiana University Grand Challenge Award.

ABBREVIATIONS USED

AFI	average fluorescence intensity
aq	aqueous
AUC	area under the curve
BINOL	1,1′-bi-2-naphthol
cAMP	cyclic AMP
cat	catalytic
(–)-CBD/CBD	cannabidiol
DAMGO	H-Tyr-D-Ala-Gly-*N*-MePhe-Gly-OH
EYFP	enhanced yellow fluorescent protein
Fsk	forskolin
GCMS	gas chromatography–mass spectrometry
h	hours
HPLC	high-pressure liquid chromatography
HRMS	high-resolution mass spectra
hμOR	human mu opioid receptor
LRMS	low-resolution mass spectrometry
L-selectride	lithium tri-*sec*-butylborohydride
min	minutes
NAM	negative allosteric modulator
nM	nanomolar

NMR	nuclear magnetic resonance
piv	pivaloyl
R_f	retention factor
SAR	structure–activity relationship
sat	saturated
SEM	standard error of the mean
TLC	thin-layer chromatography
TOF-MS	time-of-flight mass spectrometry
9-I-9-BBN	9-iodo-9-borabicyclo[3.3.1]nonane
°C	Celsius
β-FNA	β-funaltnexamine
μOR	mu opioid receptor

REFERENCES

(1). Feng Y; He X; Yang Y; Chao D; Lazarus LH; Xia Y. Current research on opioid receptor function. Curr. Drug Targets 2012, 13, 230–246.

(2). Kandasamy R; Hillhouse TM; Livingston KE; Kochan KE; Meurice C; Eans SO; Li MH; White AD; Roques BP; McLaughlin JP; Ingram SL; Burford NT; Alt A; Traynor JR Positive allosteric modulation of the mu-opioid receptor produces analgesia with reduced side effects. Proc. Nat. Acad. Sci 2021, 118, 16.

(3). Williams JT; Ingram SL; Henderson G; Chavkin CC; von Zastrow M; Schulz S; Koch T; Evans CJ; Christie MJ Regulation of mu-opioid receptors: Desensitization, phosphorylation, internalization, and tolerance. Pharmacol. Rev 2013, 65, 223–254.

(4). Pathan H; Williams JT Basic opioid pharmacology: an update. British J. Pain 2012, 6.

(5). CDC Opioid Data Analysis and Resources, < https://www.cdc.gov/opioids/data/analysis-resources.html> (2021).

(6). Hug CC Jr.; Murphy MR Fentanyl disposition in cerebrospinal fluid and plasma and its relationship to ventilatory depression in the dog. Anesthesiology 1979, 50, 342–349.

(7). Peng PWH; Sandler AN A Review of the Use of Fentanyl Analgesia in the Management of Acute Pain in Adults. Anesthesiology 1999, 90, 577–599.

(8). Suzuki J; El-Haddad S. A review: Fentanyl and nonpharmaceutical fentanyls. Drug Alcohol Depend 2017, 171, 107–116.

(9). Stanley TH The fentanyl story. J. Pain 2014, 15, 1215–1226.

(10). Poklis A. Fentanyl: a review for clinical and analytical toxicologists. J. Toxicol. Clin. Toxicol 1995, 33, 439–447.

(11). George AV; Lu JJ; Pisano MV; Metz J; Erickson TB Carfentanil—an ultra potent opioid. Am. J. Emerg. Med 2010, 28, 530–532.

(12). Volpe DA; McMahon Tobin GA; Mellon RD; Katki AG; Parker RJ; Colatsky T; Ja KT; Verbois SL Uniform assessment and ranking of opioid μ receptor binding constants for selected opioid drugs. Regul. Toxicol. Pharmacol 2011, 59, 385–390.

(13). Maguire P; Tsai N; Kamal J; Cometta-Morini C; Upton C; Loew G. Pharmacological profiles of fentanyl analogs at mu, delta and kappa opiate receptors. Eur. J. Pharmacol 1992, 213, 215–225.

(14). Blumberg H; Dayton HB; Wolf PS Counteraction of narcotic antagonist analgesics by the narcotic antagonist naloxone. Proc. Soc. Exp. Biol. Med 1966, 123, 755–758.

(15). Moss RB; Carlo DJ Higher doses of naloxone are needed in the synthetic opioid era. Subst. Abuse Treat. Prev. Policy 2019, 14, 6.

(16). CDC Lifesaving Naloxone, <https://www.cdc.gov/stopoverdose/naloxone/index.html> (2022).

(17). Changeux JP; Christopoulos A. Allosteric modulation as a unifying mechanism for receptor function and regulation. Cell 2016, 166, 1084–1102.

(18). Kenakin T; Miller LJ Seven transmembrane receptors as shapeshifting proteins: the impact of allosteric modulation and functional selectivity on new drug discovery. Pharmacol. Rev 2010, 62, 265–304.

(19). Wootten D; Christopoulos A; Sexton P. Emerging paradigms in GPCR allostery: implications for drug discovery. Nat. Rev. Drug Discov. 2013, 12, 630–644.

(20). Nickols HH; Conn PJ Development of allosteric modulators of GPCRs for treatment of CNS disorders. Neurobiol. Disease 2014, 61, 55–71.

(21). Livingston KE; Stanczyk MA; Burford NT; Alt A; Canals M; Traynor JR Pharmacologic evidence for a putative conserved allosteric site on opioid receptors. Mol. Pharmacol 2018, 93, 157–167.

(22). Vaysse PJJ; Gardener EL; Zukin RS Modulation of rat brain opioid receptors by cannabinoids. J Pharm Exp Ther 1987, 241, 534–539.

(23). Kathmann M; Flau K; Redmer A; Tränkle C; Schlicker E. Cannabidiol is an allosteric modulator at mu- and delta-opioid receptors. Naunyn-Schmiedeberg's Arch. Pharmacol 2006, 372, 354–361.

(24). Laprairie RB; Bagher AM; Kelly ME; Denovan-Write EM Cannabidiol is a negative allosteric modulator of the cannabinoid CB1 receptoor. Br. J. Pharmacol 2015, 172, 4790–4805.

(25). Straiker A; Dvorakava M; Zimmowitch A; Mackie K. Cannabidiol inhibits endocannabinoid signaling in autaptic hippocampal neurons. Mol. Pharmacol 2018, 94, 743–748.

(26). Ibeas CB; Chen T; Nunn AV; Bazelot M; Dallas M; Whalley BJ Molecular targets of cannabidiol in neurological disorders. Neurotherapeutics 2015, 12, 699–730.

(27). Labadie GR; Viswanathan R; Poulter DC Farnesyl Diphosphate Analogues with ω-Bioorthogonal Azide and Alkyne Functional Groups for Protein Farnesyl Transferase-Catalyzed Ligation Reactions. J. Org. Chem 2007, 72, 9291–9297.

(28). Kozela E; Haj C; Hanus L; Chourasia M; Shurki A; Juknat A; Kaushansky N; Mechoulam R; Vogel Z. HU-446 and HU-465, Derivatives of the Non-psychoactive Cannabinoid Cannabidiol, Decrease the Activation of Encephalitogenic T Cells. Chem. Biol. Drug Des. 2016, 87, 143–153.

(29). Breuer A; Haj CG; Fogaca MV; Gomes FV; Rodrigues Silva N; Francisco Pedrazzi J; Del Bel EA; Hallak JC; Crippa JA; Zuardi AW; Mechoulam R; Guimaraes FS Fluorinated Cannabidiol Derivatives: Enhancement of Activity in Mice Models Predictive of Anxiolytic, Antidepressant and Antipsychotic Effects. PLoS One 2016, 11, No. e0162087.

(30). Gong X; Sun C; Abame MA; Shi W; Xie Y; Xu W; Zhu F; Zhang Y; Shen J; Aisa HA Synthesis of CBD and Its Derivatives Bearing Various C4′-Side Chains with a Late-Stage Diversification Method. J. Org. Chem 2020, 85, 2704–2715.

(31). Fehr C; Ochloff G. Patent: Process for the preparation of (+)-p-mentha-2,8-dien-1-ol. US4,433,183A (1981).

(32). Reich HJ; Wollowitz S. Preparation of α, β-unsaturated carbonyl compounds and nitriles by selenoxide elimination. Org. React 2004, 44, 1–296.

(33). Sharpless KB; Lauer RF Mild procedure for the conversion of epoxides to allylic alcohols, First organoselenium reagent. J. Am. Chem. Soc 1973, 95, 2697–2699.

(34). Clive DLJ Fragmentation of selenoxides: a new method for dehydrogenation of ketones. J. Chem. Soc., Chem. Commun 1973, 695–696, 695.

(35). Schafroth MAZ; Krautwald SG; Sarlah D; Carreira EM Stereodivergent total synthesis of Δ9-tetrahydrocannabinols. Angew. Chem., Int. Ed 2014, 53, 13898–13901.

(36). Chen Y; Mestek A; Liu J; Hurley JA; Yu L. Molecular cloning and functional expression of a mu-opioid receptor from rat brain. Mol. Pharmacol 1993, 44, 8–12.

(37). Al-Hasani R; Bruchas MR Molecular mechanisms of opioid receptor-dependent signaling and behavior. Anesthesiology 2011, 115, 1363–1381.

(38). Kaserer T; Lantero A; Schmidhammer H; Spetea M; Schuster D. μOpioid receptor: novel antagonists and structural modeling. Sci. Rep 2016, 6, 21548.

(39). Ravindranath PA; Sanner MF AutoSite: an automated approach for pseudo-ligands prediction—from ligand-binding sites identification to predicting key ligand atoms. Bioinformatics 2016, 32, 3142–3149.

(40). Manglik A; Kruse A; Kobilka T; Thian F; Mathiesen J; Sunahara R; Pardo L; Weis W; Kobilka B; Granier S. Crystal structure of the μ-opioid receptor bound to a morphinan antagonist. Nature 2012, 485, 321–326.

(41). Huang W; Manglik A; Venkatakrishnan A; Laeremans T; Feinberg E; Sanborn A; Kato H; Livingston K; Thorsen T; Kling R; Granier S; Gmeiner P; Husbands S; Traynor J; Weis W; Steyaer J; Dror R; Kobilka B. Structural insights into μ-opioid receptor activation. Nature 2015, 524.

(42). Trott O; Olson A. AutoDock Vina: Improving the speed and accuracy of docking with a new scoring function, efficient optimization, and multithreading. J. Comput. Chem 2009, 31, 455–461.

(43). Jiménez J; Škalič M; Martínez-Rosell G; De Fabritiis G. KDEEP: Protein–Ligand Absolute Binding Affinity Prediction via 3D-Convolutional Neural Networks. J. Chem. Inf. Model 2018, 58, 287–296.

(44). CDC Provisional Drug Overdose Death Counts, <https://www.cdc.gov/nchs/nvss/vsrr/drug-overdose-data.htm > (2020).

(45). Mascal M; Hafezi N; Wang D; Hu Y; Serra G; Dallas ML; Spencer JPE Synthetic, non-intoxicating 8,9-dihydrocannabidiol for the mitigation of seizures. Sci. Rep 2019, 9, 7778.

(46). Rosenberg EC; Chamberland S; Bazelot M; Nebet ER; Wang X; McKenzie S; Jain S; Greenhill S; Wilson M; Marley N; Alejandro S; Bailey S; Patra PH; Rose R; Chenouard N; Sun SED; Jones D; Buzsáki G; Devinsky O; Woodhall G; Scharfman HE; Whalley BJ; Tsien RW Cannabidiol modulates excitatory-inhibitory ratio to counter hippocampal hyperactivity. Neuron 2023, 111, 1282–1300.e8.

(47). Sait LG; Sula A; Ghovanloo MR; Hollingworth D; Ruben PC; Wallance BA Cannabidiol interactions with voltage-gated sodium channels. eLife 2020, 9, No. e58593.

(48). Zhuang Y; Wang Y; He B; He X; Zhou XE; Guo S; Rao Q; Yang J; Liu J; Zhou Q; Wang X; Liu M; Liu W; Jiang X; Yang D; Jiang H; Shen J; Melcher K; Chen H; Jiang Y; Cheng X; Wang MW; Xie X; Xu HE Molecular recognition of morphine and fentanyl by the human μ-opioid receptor. Cell 2022, 185, 4361–4375.e19.

(49). Qu Q; Huang W; Aydin D; Paggi PM; Seven AB; Wang H; Chakroborty S; Che T; DiBerto JF; Robertson MJ; Inoue A; Suoomivuori CM; Roth BL; Majumdar S; Dror RO; Kobilka BK; Skinoitis G. Insights into distinct signaling profiles of the μOR activated by diverse agonists. Nat. Chem. Biol 2022, 423.

(50). Anand R; Cham PS; Gannedi V; Sharma S; Kumar M; Singh R; Vishwakarma RA; Singh PP Stereoselective Synthesis of Nonpsychotic Natural Cannabidiol and Its Unnatural/Terpenyl/Tail-Modified Analogues. J. Org. Chem 2022, 87, 4489–4498.

(51). Seccamani P; Franco C; Protti S; Porta A; Profumo A; Caprioglio D; Salamone S; Mannucci B; Merli D. Photochemistry of cannabidiol (CBD) revised. A combined preparative and spectrometric investigation. J. Nat. Prod 2021, 84, 2858–2865.

(52). Focella A; Teitel S; Brossi A. A simple and practical synthesis of olivetol. J. Org. Chem 1977, 42, 3456–3457.

(53). Shultz ZP; Lawrence GA; Jacobson JM; Cruz EJ; Leahy JW Enantioselective Total Synthesis of Cannabinoids—A Route for Analogue Development. Org. Lett 2018, 20, 381–384.

(54). Krautwald S; Schafroth MA; Sarlah D; Carreira EM Stereodivergent α-Allylation of Linear Aldehydes with Dual Iridium and Amine Catalysis. J. Am. Chem. Soc 2014, 136, 3020–3023.

(55). Habrant D; Rauhala V; Koskinen AMP Conversion of carbonyl compounds to alkynes: general overview and recent developments. Chem. Soc. Rev 2010, 39, 2007–2017.

(56). Buffet MF; Dixon DJ; Edwards GL; Procter DJ The synthesis of thiols, selenols, sulfides, selenides, sulfoxides, selenoxides, sulfones and selenones. Chem. Soc. Perkin Trans. 2000, 1, 835–871.

(57). Golliher AE; Tenorio AJ; Dimauro NO; Mairata NR; Holguin FO; Maio W. Using (+)-carvone to access novel derivatives of (+)-ent-cannabidiol: The first asymmetric syntheses of (+)-ent-CBDP and (+)-ent-CBDV. Tetrahedron Lett. 2021, 67, No. 152891.

(58). Reich HJ; Wollowitz S. Preparation of α, β-unsaturated carbonyl compounds and nitriles by selenoxide elimination. S. Org. React 2004, 1–296.

(59). Trost BM; Salzmann TN New synthetic reactions. Sulfenylation-dehydrosulfenylation as a method for introduction of unsaturation. J. Am. Chem. Soc 1973, 95, 6840–6842.

(60). Parsons DE; Frontier A. Noncanonical Cation–π Cyclizations of Alkylidene β-Ketoesters: Synthesis of Spiro-fused and Bridged Bicyclic Ring Systems. Org. Lett 2019, 21, 2008–2012.

(61). Tuyet TMT; Harada T; Hashimoto K; Hatsuda M; Oku A. Asymmetric synthesis of axially chiral biaryls via desymmetrization of 2,2′,6,6′-tetrahydroxybiphenyl using 1,4-Di-O-benzyl-l-threitol as a chiral template. J. Org. Chem 2000, 65, 1335–1343.

(62). Harada K; Ito M; Wang X; Tanaka M; Wongso D; Konno A; Hirai H; Tsuboi T; Kitaguchi T. Red fluorescent protein-based cAMP indicator applicable to optogenetics and in vivo imaging. Sci. Rep 2017, 7, 1–9.

(63). Thomas LS.; Gehrig J. (eds Thomas LS.; Gehrig J.) (*ImageJ/Fiji*; microPublication Biology, 2020).

(64). Hanwell M; Curtis D; Lonie D; Vandermeersch T; Zurke E; Hutchison G. Avogadro: an advanced semantic chemical editor, visualization, and analysis platform. Aust. J. Chem 2012, 4.

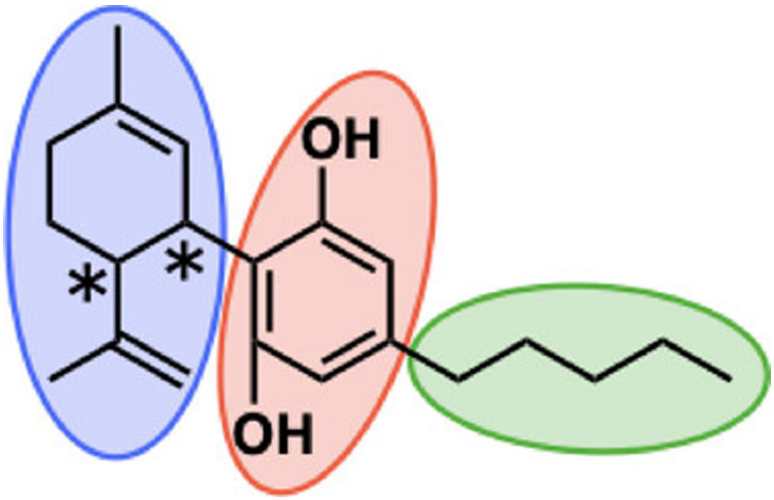

Figure 1.
Cannabidiol scaffold broken down into four distinct regions: blue—limonene, red—resorcinol, green—lipid tail, and asterisks—diastereomers.

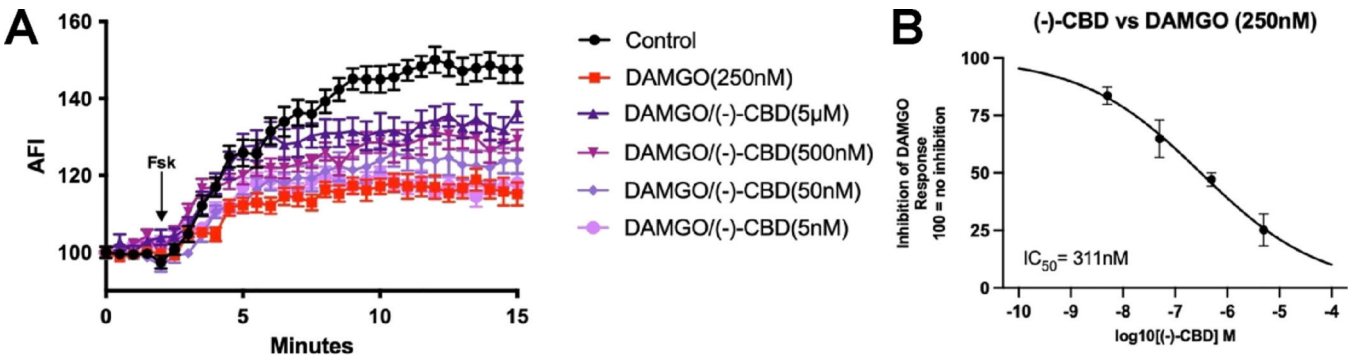

Figure 2.

Summary of the (–)-CBD effect on DAMGO-induced signaling. (A) Sample time courses show (–)-CBD concentration-dependently (5 nM–5 μM) interferes with μOR inhibition of cAMP in transfected hμOR-HEK293 cells. (B) Summarized data from multiple experiments and AUC analysis revealed an IC_{50} for (–)-CBD (IC_{50}: (95% CI): 311 nM (186 nM–531 nM)) in reversing the inhibition of cAMP by DAMGO (n = 3). Data presented as mean ± SEM.

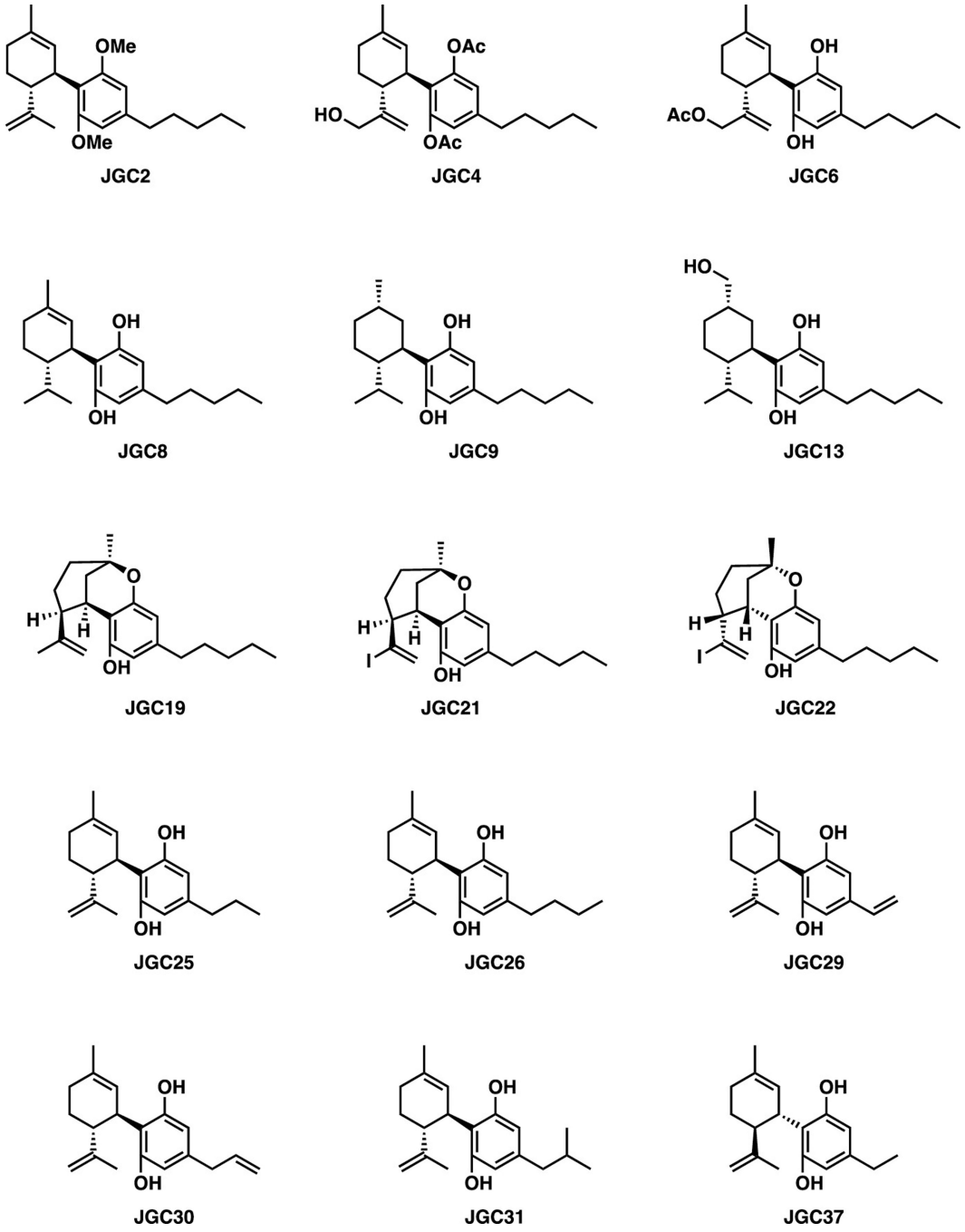

Figure 3.

Name and chemical structure of 15 synthetic cannabidiol analogs that were investigated against fentanyl-induced cAMP inhibition.

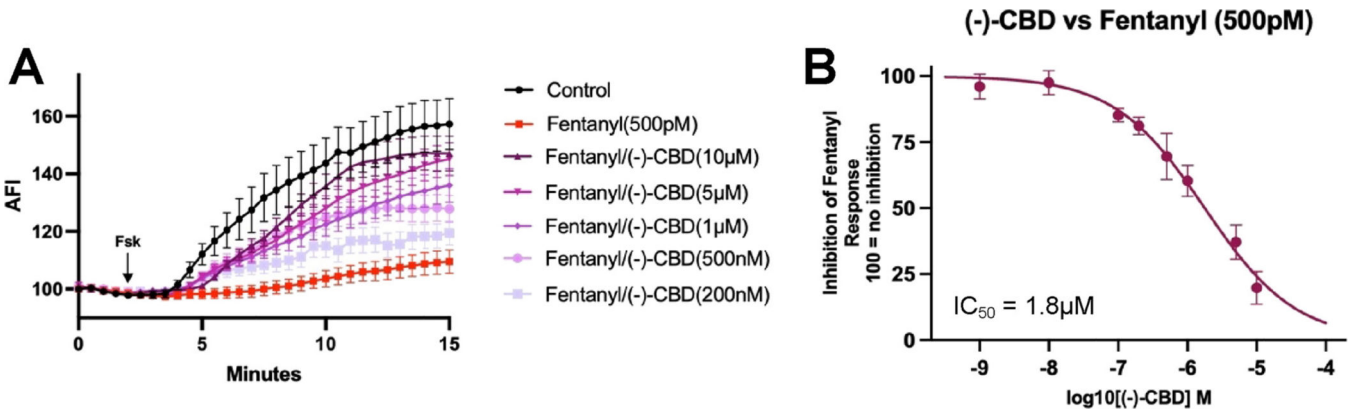

Figure 4.

Summary of (–)-CBD on fentanyl-induced μOR signaling. (A) Sample time courses in hμOR-expressing HEK293 cells show (–)-CBD concentration-dependent (200 nM–10 μM) reversal of fentanyl-induced cAMP inhibition (n = 3). (B) AUC analysis and summarized data (1 nM–10uM; n = 3) reveal an IC_{50} for (–)-CBD (IC_{50}: (95% CI): 1.8 μM (1.4 μM–2.2 μM)) in reversing fentanyl-induced inhibition of cAMP accumulation in our transfected HEK293 cells. Data presented as mean ± SEM. Refer to Figure SI–2 for fentanyl EC_{95} data.

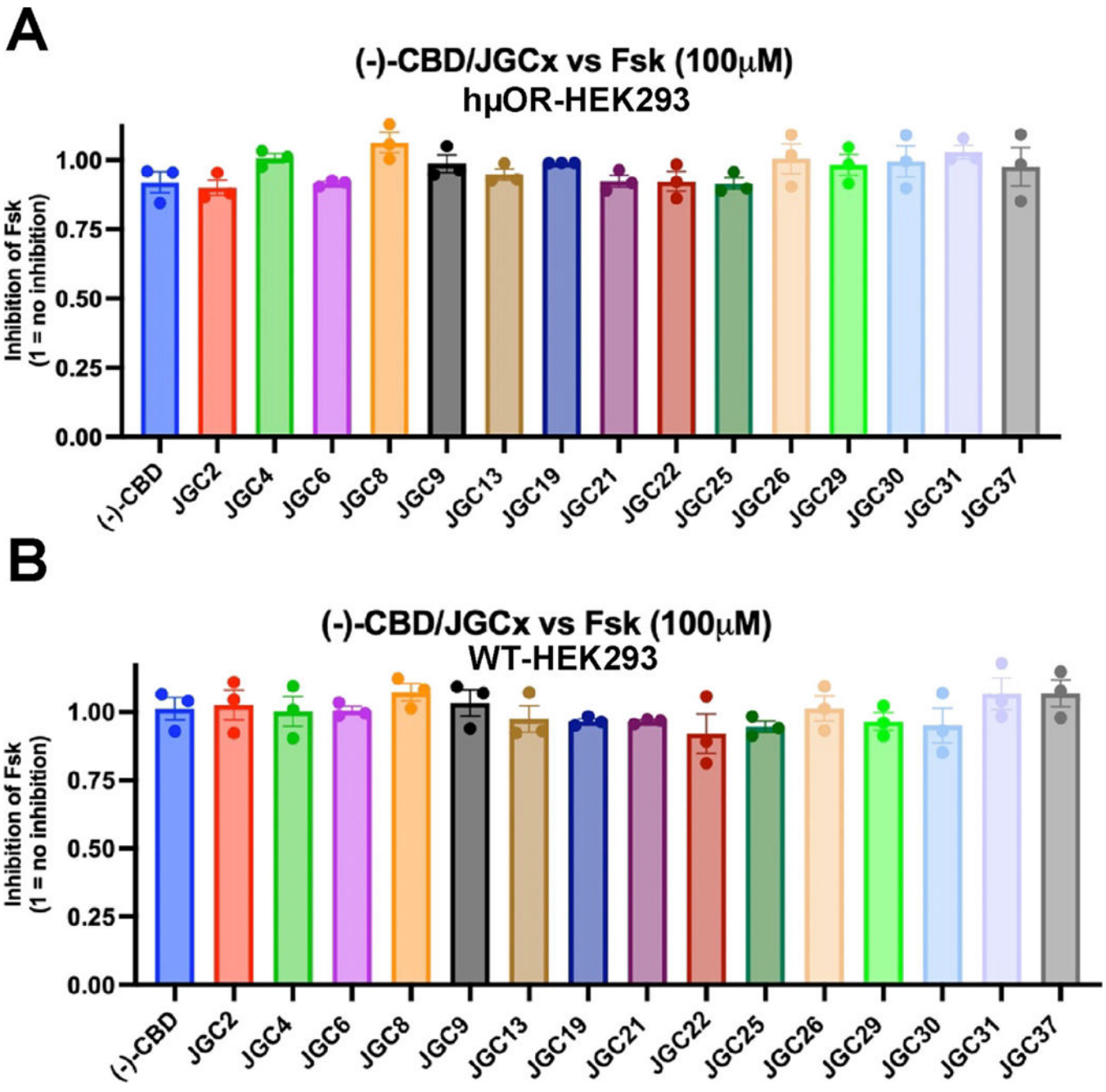

Figure 5.

(–)-CBD and CBD analog (JGC*x*) signaling in HEK293 cells. (A) AUC analyses show (–)-CBD and our CBD analogs (1 μM) do not impact cAMP accumulation in the absence of fentanyl, in hμOR-HEK293 cells (n = 3). (B) AUC analyses show (–)-CBD and our CBD analogs (1 μM) do not impact cAMP accumulation in the absence of the hμOR in the wild-type (WT) HEK293 cells (n = 3). Refer to Tables SI–3 and SI–4 for data analysis.

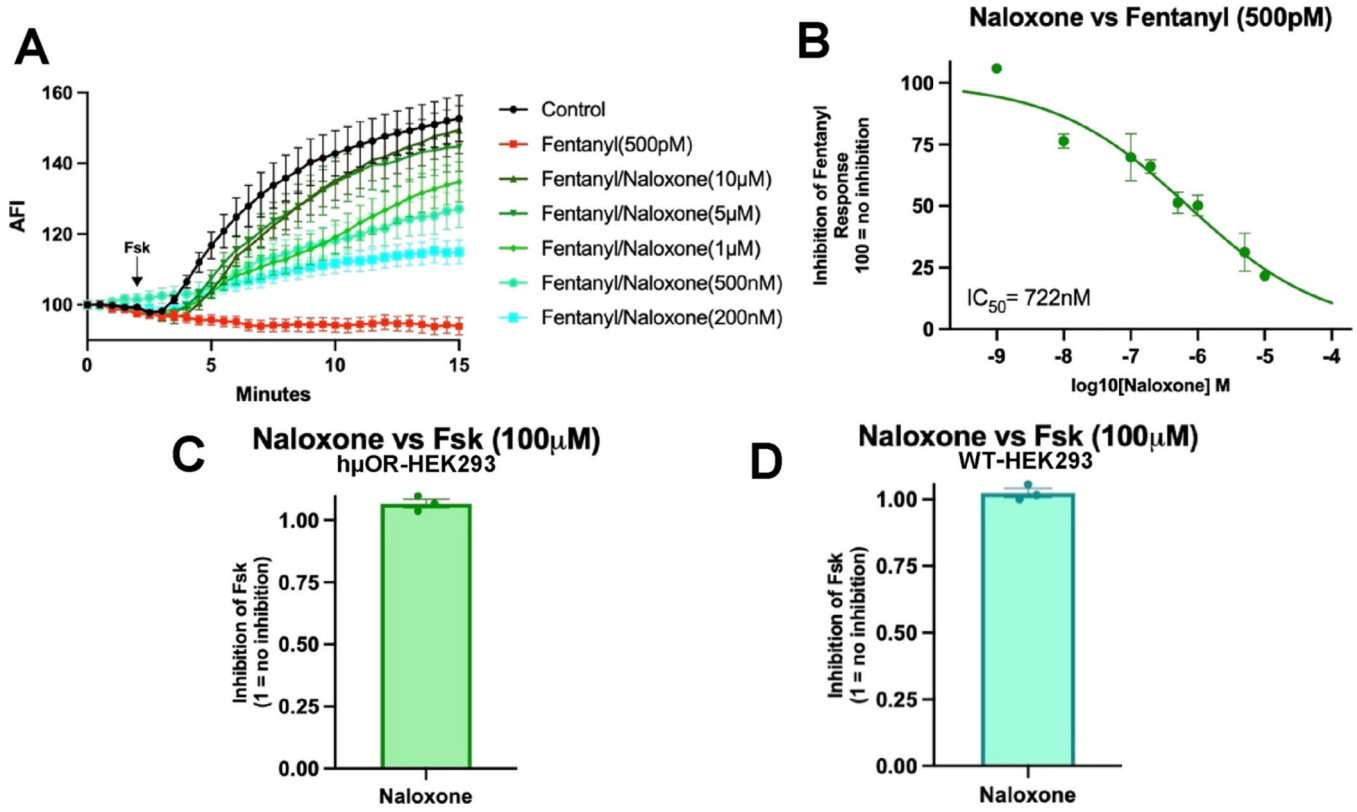

Figure 6.

Summary of naloxone on fentanyl-induced μOR signaling. (A) Sample time course in hμOR-HEK293 cells show concentration-dependent reversal of fentanyl-induced cAMP inhibition by naloxone ($n = 3$). (B) AUC analysis and summarized data ($n = 3$) reveal an IC_{50} for naloxone (IC50 (95% CI): 722 nM (367 nM–1.5 μM) in attenuating fentanyl-induced inhibition of cAMP accumulation in our transfected HEK293 cells. (C) AUC analyses show naloxone (1 μM) does not impact cAMP accumulation in the absence of fentanyl, in hμOR-HEK293 cells ($n = 3$). (D) AUC analyses show naloxone (1 μM) does not impact cAMP accumulation in the absence of the hμOR in wild-type HEK293 cells ($n = 3$). Data presented as mean ± SEM.

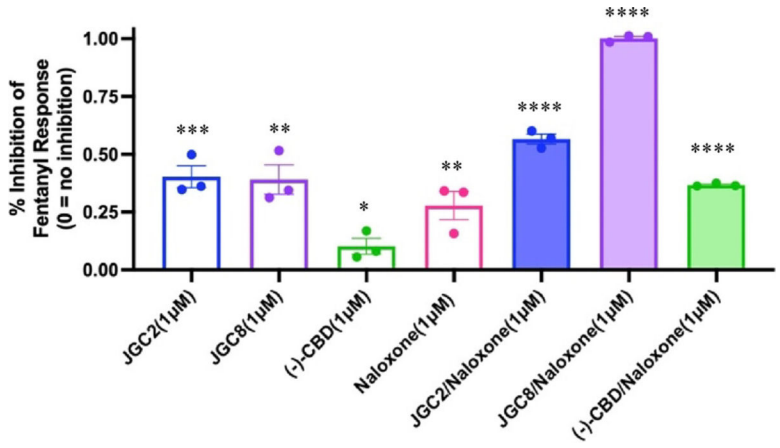

Figure 7.

Summary of fentanyl signaling followed by (–)-CBD, JGC2, JGC8, and naloxone application. Summarized data ($n = 3$) shows augmented cAMP accumulation following the coapplication of (–)-CBD, JGC2, or JGC8 with naloxone, when compared to singular application, following fentanyl preapplication. Data presented as mean ± SEM. (–)-CBD: 0.10 ± 0.034; JGC2: 0.40 ± 0.048; JGC8: 0.39 ± 0.063; naloxone: 0.28 ± 0.061; $n = 3$ for each; unpaired *t*-test, *p*-value < 0.05, (–)-CBD, $p = 0.041$; JGC2, $p = 0.001$; JGC8, $p = 0.004$; naloxone, $p = 0.010$; (–)-CBD + naloxone: 0.37 ± 0.004; JGC2 + naloxone: 0.57 ± 0.021; JGC8 + naloxone: 1.002 ± 0.008; $n = 3$ for each; unpaired *t*-test, *p*-value < 0.05, (–)-CBD, $p < 0.0001$; JGC2, $p < 0.0001$; JGC8, $p < 0.0001$; *, $p < 0.05$, ** $p < 0.01$, ***, $p < 0.001$, ****, $p < 0.0001$. Refer to Figure SI–7 for time courses for the individual and coapplication data.

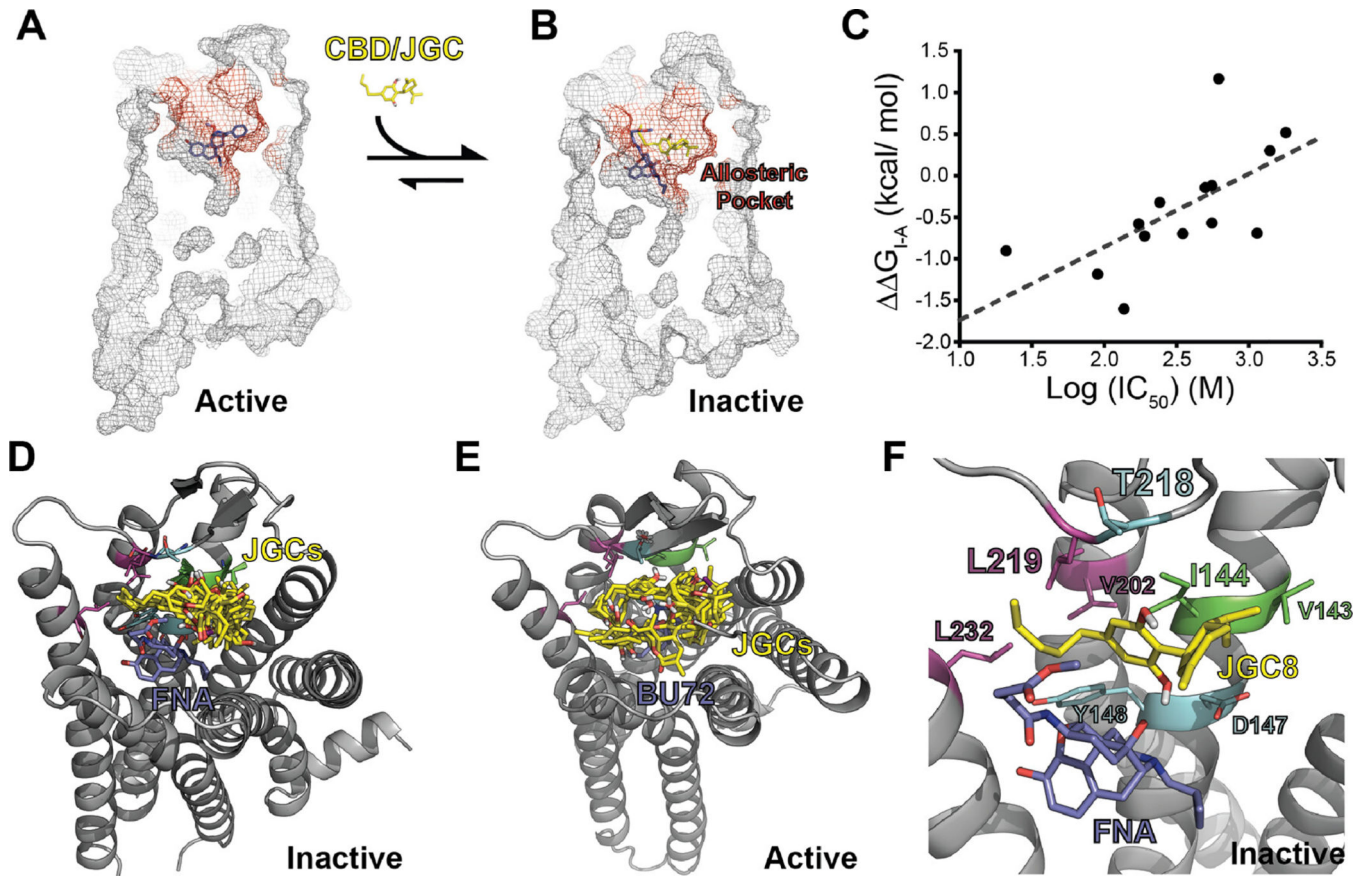

Figure 8.

Comparative docking of CBD analogs into the active and inactive conformations of the μ opioid receptor. Structural models of docked compounds are shown in the context of a proposed thermodynamic mechanism for the allosteric inhibition of the μOR. An allosteric pocket within the extracellular vestibule is constricted in the context of (A) the active-state conformation (PDB 5C1ML) relative to (B) the inactive-state conformation (PDB 4DKL). Selective binding of CBD analogs to the allosteric pocket within the inactive conformation may drive the equilibrium toward the inactive state potentially without displacing the agonist. (C) The difference in the free energy of binding for the inactive and active conformations ($\Delta\Delta G_{I-A}$) was estimated from the docked conformations of each compound using K_{DEEP} and plotted against the logarithm of the IC_{50} value for 15 experimentally characterized CBD analogs. Negative $\Delta\Delta G_{I-A}$ values indicate preferential binding to the inactive conformation. A linear fit (dashes) is shown for reference (Pearson's $R = 0.64$). (D) Consensus-docked poses of the 15 experimentally characterized CBD analogs are overlaid in the context of the β-FNA-bound inactive conformation (PDB 4DKL). (E) Consensus-docked poses of the 15 experimentally characterized CBD analogs are overlaid in the context of the BU72-bound active conformation (PDB 4DKL). (F) The consensus pose of JGC8 in the context of the inactive conformation is shown for reference.

Table 1.

IC_{50} Values of (–)-CBD (JGC1) and 15 Synthetic CBD Analogs when Tested against Fentanyl (500 pM)[a]

compound	IC_{50} (nM)	compound	IC_{50} (nM)
JGC1	1800	JGC21	499
JGC2	90	JGC22	556
JGC4	1170	JGC25	556
JGC6	619	JGC26	173
JGC8	21	JGC29	190
JGC9	1400	JGC30	1400
JGC13	137	JGC31	242
JGC19	349	JGC37	6500

[a]Reference Figures SI–5 and SI–6 for data analysis.